Influence of different methods of bed compression on protein separation in process chromatography

by

Darryl Yung Chiu Kong

A thesis submitted for the degree of
Doctor of Engineering
of
University College London

Department of Biochemical Engineering
University College London

July 2019

Declaration

I hereby declare that except where specific reference is made to the work of others, the contents of this dissertation are original and have not been submitted in whole or in part for consideration for any other degree or qualification in this, or any other University. This dissertation is the result of my own work and includes nothing which is the outcome of work done in collaboration, except where specifically indicated in the text.

Darryl Yung Chiu Kong

London, July 2019

Acknowledgement

The EngD process is a fortunate experience that entails a combination of frustration and joy. Many people have helped me throughout my time at UCL. The following people are friends and colleagues whom I would like to personally thank for their contribution to the success of my research.

Firstly, I would like to express my deepest gratitude to my supervisor, Professor Nigel J. Titchener-Hooker, who has been truly inspirational. His extensive knowledge and encouragement have guided me through challenging setbacks encountered during my research. I am very grateful for his support and encouragement. I would also like to acknowledge David Gruber and Ross McCluckie, my industrial supervisors at Ipsen Bioinnovation Ltd. for their invaluable discussions and hospitality. Along with Prof. Titchener-Hooker, they were heavily involved in publication efforts and provided valuable feedback. I also thank Ipsen Bioinnovation Ltd. for financial sponsorship of this research.

For technical and moral support, I wish to thank the following from the department: Spyridon Gerontas, Sheun Oshinbolu, Charnett Chau, Michael Martinez, Lara Fernandez Cerezo, Roman Zakrzewski, Neha Patel, Chika Nweke and Alice Pearce. Special thanks to Paula Thomas and Derrick Abraham for organising numerous meetings and notably with financing travel and other expenses.

Special mention must be made to Bertie Watkins for his support and patience throughout these years.

My list would not be complete without thanking my parents and family for their continued support. All would not have been possible without them. I love you, always and forever and words will never be enough to show my gratitude.

Abstract

This thesis examines the effects of hydrodynamic and mechanical compression on process chromatography. Poorly packed columns can have serious consequences on the performance of chromatography and efforts to understand the impact of different methods of compression on protein separation is limited in the literature. By understanding this impact, there is significant potential for facilitating better decisions in chromatographic operations, minimising batch failures while achieving high chromatographic performance.

Conventional methods were used to quantify five different structural properties of chromatographic resins; the column efficiency was used to assess the quality of packing and porosity tests was used to determine the interparticle and intraparticle porosity of the packed bed. The influence of bed length, column diameter, and average particle size on the extent of bed compression were examined. The results showed better asymmetry and reduced plate height with both increasing levels of hydrodynamic and mechanical compression.

There were practical limitations in using the conventional approaches to investigate the quality of packing; column efficiency and porosity tests only provide an overall indication of the whole column. The reverse-flow technique using an acetone tracer was therefore developed as a novel technique in this field to quantify the microscopic dispersion effects due to bed compression on defined axial sections within a packed bed. This technique allows reversible macroscopic factors to be separated from irreversible microscopic factors. The results showed higher levels of compression towards the bottom of the column with hydrodynamic compression and higher levels of compression towards the top of the column with mechanical compression. This technique has shown to be a simple, non-intrusive method for investigating microscopic factors along the different sections of the column.

The breakthrough curves were used to determine the dynamic binding capacities for three different anion exchange resins using BSA as a model protein. Q Sepharose Fast Flow, Q Sepharose High Performance and Capto Q were selected to cover a range of bead rigidity and particles sizes. The shape and position of the breakthrough curves

were used to assess quantitatively the impact of bed compression on binding capacity and mass transfer properties. In particular, a range of rigidity and particle sizes of AEX chromatography resins were examined. The results showed the overall impact of compression on breakthrough performance depended heavily on the method of compression applied to the bed. For both hydrodynamic and mechanical compression, the dynamic binding capacity (DBC) increased by 60% for Capto Q. However, when Q Sepharose FF, a softer resin was hydrodynamically compressed the DBC decreased by 10% at 0.15 CF. By contrast, when Q Sepharose HP (2 – 3 times smaller than Q Sepharose FF) was hydrodynamically compressed to the equivalent compression factor, the DBC increased by 20%. This suggests that the particle size distribution (PSD) also influenced changes in breakthrough behaviour when compressed. For all three resins tested, mechanical compression produced the largest increases in DBC.

Finally, purification factor vs. yield (PFY) diagrams were used to relate directly the effects of bed compression to the maximum purity and yield at each compression factor. In this study, fractionation diagrams were adapted to describe the elution profiles of the product and its various impurities to show the relationships between bed compression and overall chromatographic performance. A protein mixture was used to challenge three AEX resins (Q Sepharose Fast Flow, Q Sepharose High Performance, and Capto Q) and subsequently a gel filtration resin (Sepharose CL-6B). In particular, the effects of one-step vs. multiple incremental step compression were also examined. The results showed one-step hydrodynamic compression caused flow instability, due to the formation of regions of higher compaction towards the bottom of the packed bed which together resulted in poor protein separation. With mechanical compression via multiple incremental steps, an even distribution of pressure was applied from the top column diameter which gave greater levels of product purity and yield for all resins.

Impact statement

Poor packing of chromatography columns is known to reduce drastically both the column efficiency and to produce broader peaks. These each have implications for productivity and separation performance. Controlled bed compression has been suggested as a useful approach for solving these problems and forms the basis for this largely experimental study.

The relationship between column efficiency and resolution of protein separation were examined when preparative chromatography media were compressed using mechanical and hydrodynamic methods, to varying levels of compression and by application of compression in single or multiple steps. Five different resins; DEAE Sephacel, Q Sepharose Fast Flow, Q Sepharose High Performance, Capto Q and Sepharose CL-6B were selected to cover a broad range of bead rigidity and particle size.

Bed asymmetry and height equivalent of a theoretical plate (HETP) for all beds, uncompressed and compressed, were determined by using 2% v/v acetone. The void volume and intraparticle porosity ($\boldsymbol{\varepsilon}_p$) were estimated by using blue dextran. Furthermore, microscopic dispersion was evaluated along bed axial length using a reverse flow pulse technique. All of these metrics were correlated with the method and extent of compression and as a function of the media employed.

Compression resulted in more homogeneous packing, as voidage decreased. For Q Sepharose FF and Q Sepharose HP, hydrodynamic compression gave lower levels of improvement than for Capto Q. For Capto Q, both hydrodynamic and mechanical compression showed up to a 60% increase in DBC and an increased purification factor (PF) of BSA by over 15%. The trends demonstrate the potential of bed compression to enhance both column resolution and productivity and the data explore the complex interactions between mode and rate of compression as well as matrix type.

Table of Contents

Table of Figures

Table of Tables

Symbols and Abbreviations

AEX	Anion exchange
BSA	Bovine serum albumin
CIP	Clean-in-place
C.I.	Confidence interval
CPP	Critical process parameter
CQA	Critical quality attribute
D	Diffusivity
DNA	Deoxyribonucleic acid
DSP	Downstream processing
FDA	Food and Drug Administration
GMP	Good manufacturing practice
MHRA	Medicines and Healthcare Products Regulatory Agency
MW	Molecular weight
N	Number of theoretical plates
NMR	Nuclear magnetic resonance
NaCl	Sodium chloride
NaOH	Sodium hydroxide
PAT	Process analytical technology
PF	Purification factor
QbD	Quality by design
QTPP	Quality target product profile

SEM Scanning electron microscope

UCL University College London

Parameters

A_s Asymmetry factor

C Concentration of solute in fluid phase (mg mL^{-1})

CV Column volume (mL)

D Column diameter (cm)

DBC Dynamic binding capacity (mg mL^{-1})

De Diffusivity (cm^2 s^{-1})

d_p Effective particle diameter (µm)

$HETP$ Height-equivalent-to-a-theoretical-plate (cm)

L Bed height (cm)

L_o Gravity settled bed height (cm)

MPa Mega Pascal

ΔP Packed bed hydrodynamic pressure drop (MPa)

Re Reynolds Number

t_R Retention time (s)

V_e Elution volume (mL)

V_h Peak width at half height (mL)

u Superficial linear flow velocity (cm h^{-1})

U_{crit} Critical velocity (cm/h)

V_{co} Gravity settled bed volume (cm^3)

V_c Packed bed volume (cm^3)

ε_p Intraparticle porosity

ε Voidage space in bed

List of publications

Kong DYC, Gerontas S, McCluckie RA, Mewies M, Gruber D, Titchener-Hooker NJ (2018) Effects of Bed Compression on Protein Separation on Gel Filtration Chromatography at Bench and Pilot Scale. *Journal of Chemical Technology & Biotechnology*: doi:10.1002/jctb.5411

Conference presentation

International Symposium on Chromatography (ISC), Cork Ireland held 28th August – 1st September 2016: Poster presentation - The effect of bed compression on the quality of column packing for protein separation

American Chemical Society (Kiss *et al.*) National Meeting, New Orleans USA held 18th – 22nd March 2018: Oral presentation - Effects of bed compression on protein separation on gel filtration chromatography at bench and pilot scale

Recovery of Biological Products XVIII Conference, Asheville, USA held 7th – 12th October 2018: Poster presentation - The effect of bed compression on the degree of separating proteins in ion exchange resins

Introduction

Process chromatography is an important technique commonly used in the purification of bio-molecules for human diagnostic or therapeutic purposes. To meet the stringent and exact purification specifications required by regulatory agencies, it is therefore essential that the chromatography performance is efficient, reliable and scalable. Such requirements place increasing demand on biochemical engineers who are often relied on for their experience when optimising or trouble shooting chromatographic processes to limit batch failures. These may include scenarios concerning poorly packed columns that subsequently lead to low yields and/or purity. Understanding the effects of column packing is hence a high priority, in order to meet the stringent purification requirements and to maintain high levels of separation consistently.

This thesis, completed in collaboration with Ipsen Bioinnovation Ltd., aims to understand the effect of bed compression on column efficiency and protein separation when using different resins varying in size and rigidity. By understanding this, there is significant potential for facilitating timely and improved decisions in chromatographic operation. This will potentially facilitate higher protein separation by achieving improved column efficiency whist reducing the chances of batch failures.

A range of resins (see Table 2-1) with different rigidities and average particle sizes were selected and kindly supplied by the sponsoring company, Ipsen Bioinnovation ltd. and readily available in-house. The expected output is a structural understanding when different methods of compression are applied to the chromatographic bed; achieved by studying a range of research objectives.

Objectives

- To apply innovative methods of bed compression for improving the column efficiency for a selection of resins at bench and pilot scale.
- Quantification of the overall column efficiency and bed porosity of the chromatographic bed in order to determine relevant structural changes that occurs during compression and to link these to the methods of packing.

To achieve these objectives, the use of mechanical and hydrodynamic compression via one-step and/or multiple incremental step compression will be applied to five commercially available chromatography media - Sepharose CL-6B, DEAE Sephacel,

Q Sepharose Fast Flow, Q Sepharose High Performance and Capto Q. A range of compression factors (λ = 0.0, 0.02, 0.05, 0.10, 0.15) will be used. The three properties used for characterisation purpose are average particle size, matrix type, and bead rigidity. The traditionally used methods - acetone and blue dextran injections will be used to determine the overall column efficiency and porosity of the beds formed under a range of conditions and for each of the five resins.

- Quantification of microscopic dispersive effects in defined axial sections within a packed bed.

A reverse-flow technique will be used to investigate band broadening and microscopic dispersion effects along different axial sections of the chromatographic column observed in resins exposed to two different methods of compression (hydrodynamic and mechanical compression). In this procedure, an XK16 column at 10 cm bed height is used. Under a low Reynolds number, a pulse of tracer will be introduced into the system until it has reached the desired section of the bed, the flow can then be reversed and the distribution of the resultant tracer peak measured. This will provide an indication of the heterogeneity within the volume of the bed for each resin examined. Statistical analysis will also be employed to determine the significance of these results and to determine whether reverse-flow technique can be used to measure heterogeneity within chromatography beds and hence provide insights as to the bed structure developed during packing.

- The use of maximum Purification Factor vs. Yield (PFY) diagrams to investigate as the effect of bed compression on protein separation.

PFY diagrams will be used to assess the effects of different methods of compression (hydrodynamic and mechanical) and modes of compression (one-step and multiple incremental step) on protein separation observed across a range of commercially available chromatography resins. A selection of two types of chromatography (anion exchange and gel filtration) will be compressed and each challenged with a fixed mixture of proteins (ovalbumin, BSA and β-Lactoglobulin). The eluate will be collected and analysed and the results plotted on PFY diagrams.

The use of PFY diagrams provides a rapid and early interpretable method by which to compare the effects of the different methods of compression on the overall column performance and productivity.

Scope of thesis

This research aims to understand and characterise the structural differences of chromatographic beds that results when different methods of compression are applied to a range of resins. Ultimately, such analysis provides a means of establishing a set of methods to improve column packing. Investigation of bed compression is a challenging task – publications describing an understanding of the impact of different methods of compression on protein separation are scarce. In this thesis, investigations were performed to understand better bed stability by applying compression to a variety of chromatography resins. This will potentially facilitate improved decisions in chromatographic operations, minimising batch failures whilst achieving better column performance.

The quality of packing has a direct impact on the chromatographic process, which in turn would affect the process throughput. It is therefore hoped that the knowledge gained in this thesis could lead to better decisions of column packing that can potentially contribute to higher levels of protein separation. The expected output is an increasing detail of understanding of how different methods of bed compression impact column behaviours, achieved by studying a range of research objectives as noted earlier.

The main objectives were organised by chapters, as follows:

Chapter 1 – this chapter reviews literature to highlight the role of chromatography and the different techniques used to pack chromatographic columns. An overview on the materials, equipment, analytical techniques and experimental methods used in this thesis is provided. Subsequently, the challenges faced by industry when validating the chromatographic process are briefly discussed.

Chapter 2 – examines the effect of hydrodynamic and mechanical compression on the quality of packing. The column efficiency is measured to investigate the effects of bed compression on five commercially available chromatography media (Q Sepharose FF, Q Sepharose HP, DEAE Sephacel, Capto Q, and Sepharose CL-6B). Also in this

chapter, the influence of column diameter, and the effect of one-step vs. multiple incremental step compression are examined.

Chapter 3 – examines the effect of hydrodynamic and mechanical compression on voidage space and intraparticle porosity by using blue dextran and acetone as inert tracers.

Chapter 4 – introduces a reverse-flow technique to quantify the microscopic dispersive effect of bed compression in defined axial sections within a packed bed. This technique allows the band broadening effects due to reversible macroscopic factors to be separated from irreversible microscopic factors. It is used reveal the influence of packing method and extent of compression on bed structure, and to characterise the extent of bed heterogeneity.

Chapter 5 – examines the effects of bed compression on dynamic binding capacity. The change in capacity and breakthrough characteristics for a model test protein, BSA, were examined. Breakthrough curve analysis was also used to describe the mass transfer properties of compressed beds.

Chapter 6 – explores the use of purification factor vs. yield diagrams as the basis for characterising chromatographic separations using a fixed mixture of proteins. PFY diagrams reduce chromatograms to a simple curve that can show the trade-off between purity and yield and as a function of the level of compression factor.

Chapter 7 – will draw overall conclusions from the work reported in this thesis.

Finally, Chapter 8 discusses future work that could be undertaken based on the results obtained.

Overall, the results from this thesis should provide valuable insights to the likely mechanisms of hydrodynamic and mechanical compression. The methods developed are practical and can be automated for easy implementation to evaluate the impacts of chromatographic bed compression typically found in industrial separations.

1 Literature review

This literature review was configured to address the underlying principles that are covered in this research. An understanding of chromatography first requires understanding of the components that make the column and the different factors that influence overall performance.

In this literature review, the various modes of bed compression in chromatography operations are highlighted briefly, the importance and factors that influence packing quality. The main components that make up a column and the different types of chromatography resins are highlighted. A description of the role of resins and the different stationary base materials available provide a basis for understanding the structural characteristics of the resins used in this thesis. The section on packing and heterogeneity is intended to take the reader through the different factors influenced by bed compression and the consequences for column efficiency. Subsequently, the relationship between band broadening effects and poor column packing are discussed as a means of demonstrating the various influences the column is exposed to during operation. This section concludes with the impact of bed compression on the overall pressure drop across the column.

The chapter then leads on to the importance of process validation to meet both economic and regulatory requirements, with particular significance on the characterisation of bed compression on protein separation. Current techniques used to quantify the impact of compression on column efficiency in research are subsequently discussed. This section is split into validating the column packing process by examining the critical quality attributes and measuring process characteristics (yield and purity).

1.1 Process chromatography

1.1.1. Introduction to chromatography

Chromatography is one of the most widely used separation processes in bioprocessing. Chromatography is a separation technique for biological molecules to identify, quantify and/or remove impurities in substances. Mikhail Tsvet was the first scientist

to separate plant pigments using chromatography based on colour disparity in 1900. In the 1940s, Richard Laurence Millington Synge and Archer John Porter pioneered chromatography further to develop gas and high performance liquid chromatography (Giddings and Keller, 2014). Now there are many modes of operation employed in the bioprocessing industry (Table 1-1).

Table 1-1 Mode of chromatography adapted from (Nweke, 2017)

Type of chromatography	Separation principle
Ion exchange	Net charge
Hydrophobic interaction/ reverse phase	Hydrophobicity
Size exclusion/ Gel filtration	Size and shape
Affinity	Biological function
Chromatofocusing	Isoelectric point
Immunosorption	Antigenicity
Lectin affinity	Carbohydrate content
Immobilised metal affinity	Metal binding
Chemisorption	Chemical reactions
Hydroxyapatite, dye affinity	Miscellaneous

Chromatography can be used as a means of quality control throughout various industries; in the food industry, chromatography can separate and analyse vitamins, preservatives and additives (Rathore *et al.* 2018), to environmental testing of contaminants in drinking water, DDT in groundwater, and air quality (Rathore *et al.* 2018).

Throughout the many different industries (food, pharmaceutical, nutraceuticals and biotech/biopharma), the biopharmaceutical markets account for the largest share, with global revenues estimated at US$160 billion per year and predicted to expand (Gassmann *et al.* 2018). The chromatography market is expected to reach US$ 8 billion by 2021. In large-scale chromatography processes, 70% of the costs are attributed to resins and solvents (Turner *et al.* 2017). The reason for the growing demand of chromatography resins is due to their ability to purify key biological products used for medical and therapeutic drugs, such as monoclonal antibodies,

insulin, growth hormone etc. These are hugely costly drugs and for this reason, there is a need to drive the processing costs down.

1.1.2. Role of DSP in bioprocessing

Downstream processing (DSP) describes the process used for the recovery and purification of products from biochemical processes (Titchener-Hooker *et al.* 2007). Chromatography in DSP is used to separate the product from its impurities. Regulatory agencies, such as the Food and Drug Administration (FDA) in the US and the Medicines and Healthcare Products Regulatory Agency (MHRA) in the UK require that biopharmaceutical products be manufactured with a consistent purity and quality that excludes any harmful impurities (Hentschel 2013; Rathore 2009; Rathore and Kapoor 2017). For most biologics, chromatography is the only unit operation that is able to meet these strict requirements at scale (Steinebach *et al.* 2016). Consequently, most downstream processes typically utilise three chromatographic stages to achieve the purity required (Johnson *et al.* 2017).

1.1.3. Components of chromatography column

The physical chromatography system consist of the column, stationary phase (see Section 1.1.4), mobile phase, the pumping and detector system, sample injection, and fraction collector Figure 1-1. Figure 1-2 illustrates an XK chromatography column from GE Healthcare (Uppsala, Sweden) used in this study.

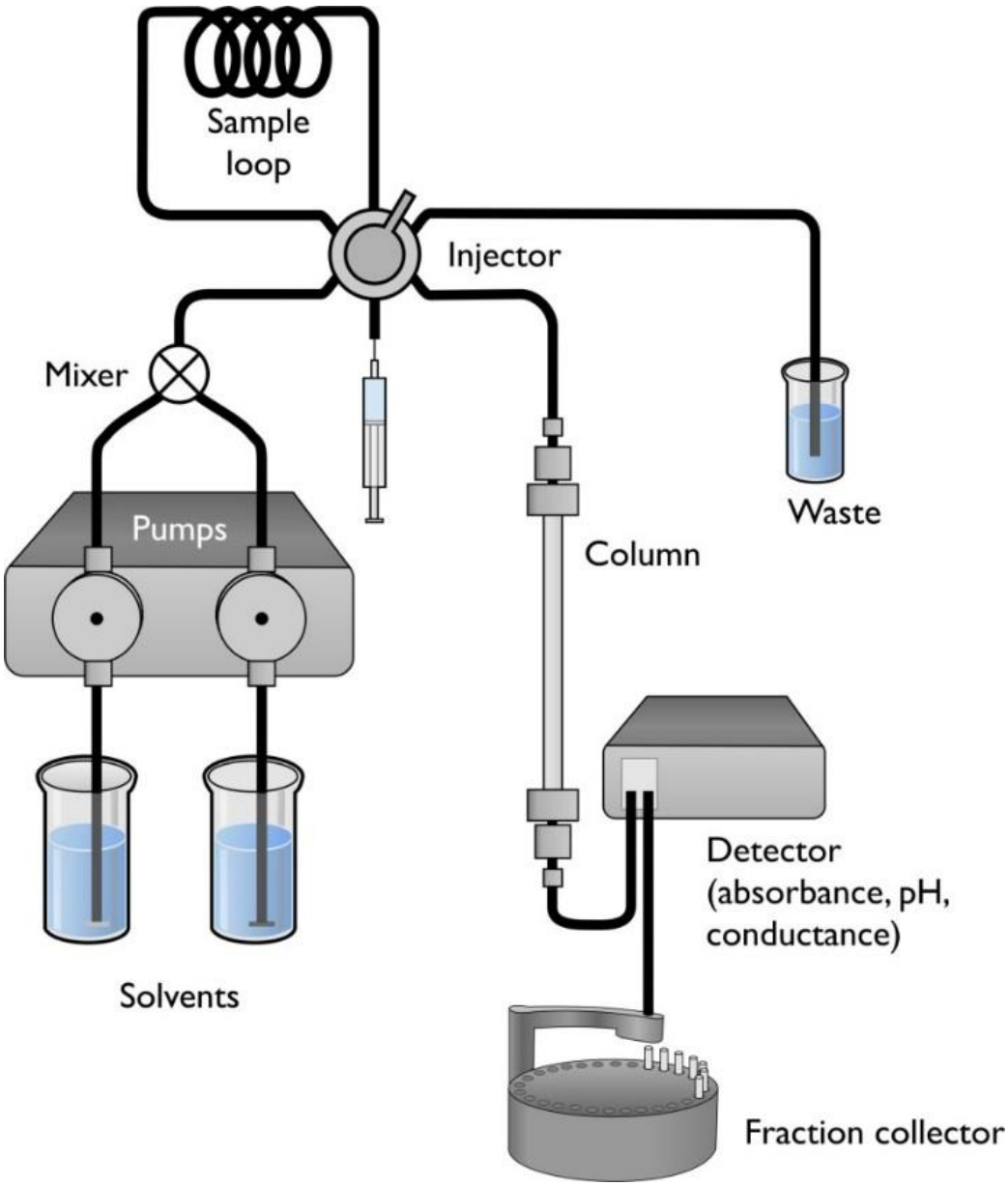

Figure 1-1 Illustrates a schematic chromatographic diagram adapted from (Rao and Goyal 2016).

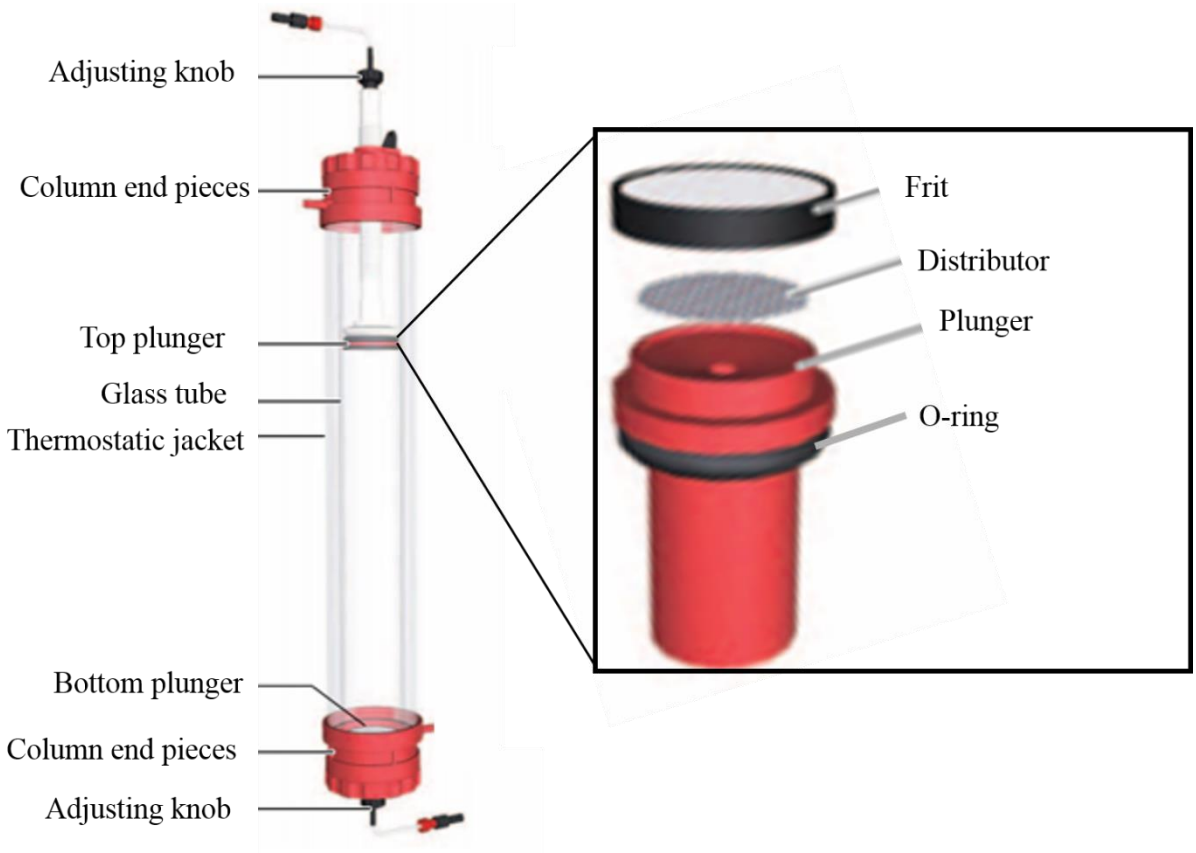

Figure 1-2 Illustrates the components of an XK GE chromatography column adapted from (Healthcare 2000)

The chromatographic column tube consists of the glass tube, thermostatic jacket and respective column end pieces. In small-scale experiments, the columns are of borosilicate glass whereas at large-scale the columns are made of stainless steel (Dileo *et al.* 2010). At small scale, the end pieces hold the glass tube and jacket in place. The top and bottom adapters are supported by a flow distributor, which is placed on top of a plunger and is fixed in place by the frit. Once the top and bottom adapters are set in place, O-rings seal it within the column tube.

The mobile phase is also referred to as the eluent and is largely the buffer system. Typical processes include an equilibration buffer, an elution buffer, a wash buffer, a Clean-in-place (CIP) buffer and in some cases a regeneration buffer. The selection of buffers are based on the separation method and the ability to separate compounds effectively (Carta and Jungbauer 2010).

1.1.4. Types of stationary phases

The stationary phase plays a vital role in chromatographic operation. They can also be referred to as the resin, the bead, the matrix, or the adsorbent. In bioprocessing the resins are typically 20 - 100 µm in size and assumed spherical prior to bed compression Figure 1-3.

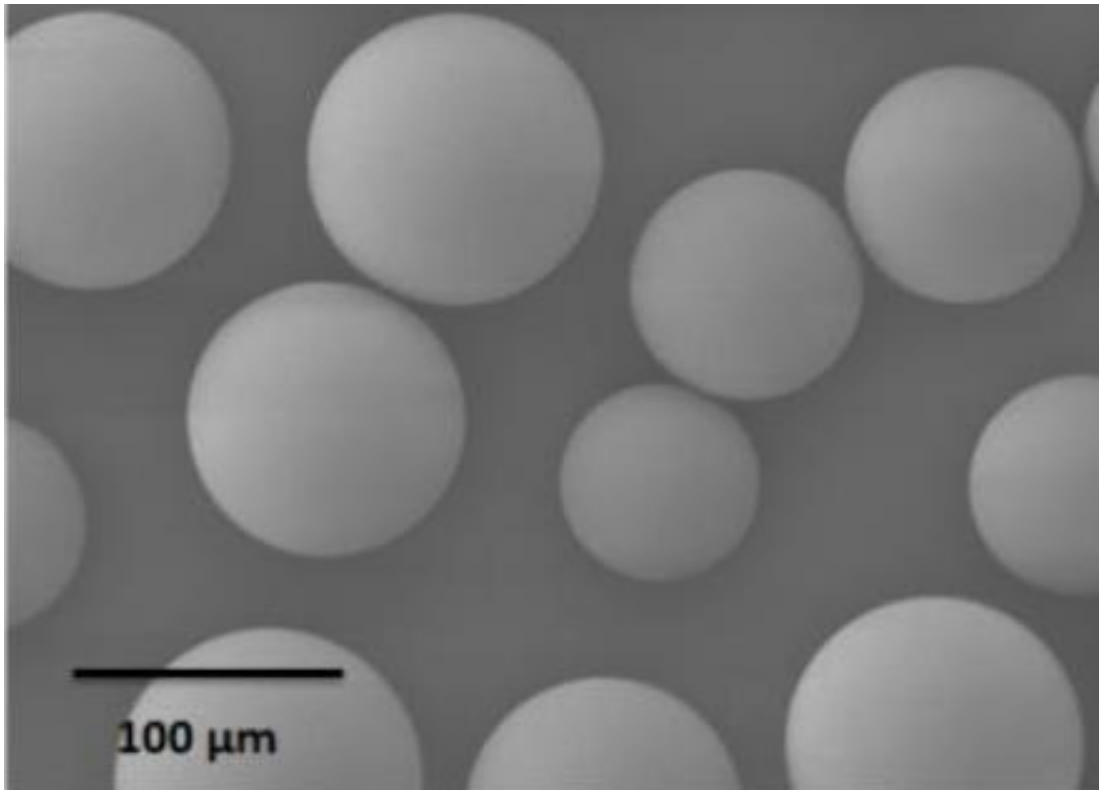

Figure 1-3 Image using scanning electron micrograph showing fresh Sepharose CL-6B post-air drying. Accelerating voltage 2.0 kV, x220 magnification, 3cm = 100 µm.

Many different base materials can be used in the formation of stationary phases. Typical base materials for chromatographic media include agarose, cellulose, ceramics, dextran, silica, polystyrene, and polyacrylamide (Nweke *et al.* 2017). Depending on the level of separation required the base materials is chosen depending on a number of factors. These factors include the cost of resins, safety considerations (leachables and toxicology), susceptibility to fouling (longevity and number of reuses), performance (binding capacities and throughput), and stability (chemical and mechanical) (Ioannidis *et al.* 2012). The chemical resistance of resins is dependent on the coupling chemistry and choice of spacer and ligand chemistry. Mechanical resistance of resins is dependent on the composition of the base material (Nweke *et al.*

2017). The number of properties that are considered ideal for base matrices and are listed in Table 1-2.

Table 1-2 Ideal base matrix compositional properties adapted from (Nweke *et al.* 2017)

Ideal base matrix compositional properties
Hydrophilic
Large pore size/ surface area
Spherical (mono-sized) particle
Low level of unspecific adsorption
Easy to functionalise
Reusability and low cost
Chemically stable
Mechanically stable

The different modes of chromatography each display different interactions between the stationary phase and the mobile phase Table 1-1. The types of chromatography can be categorised into two groups; adsorption chromatography and non-adsorption chromatography.

Adsorption chromatography include the chemical interactions between the molecules in the stationary phase, the mobile phase, and the solute. The strength of the interactions will vary depending on each component in the solute (Jungbauer 2005). This difference in interaction will cause each component to migrate through the stationary phases at different velocities. Molecules with weaker interactions will migrate through first and then those with the stronger levels of interaction later. For this reason, a mixture of components in a solute will elute through the column at different times allowing a mixture to be resolved into separate components (Dorsey *et al.* 1998). However, the presence of biological impurities such as host-cell proteins (HCPs), nucleic acids, and oligomers require multiple chromatography steps be employed in order to reach high levels of purity (often > 99%) dictated for each use (Albanese *et al.* 2011).

The types of adsorptive chromatography include (Jagschies *et al.* 2007):

Ion exchange chromatography – Electrostatic interaction between the sample molecule and the ion exchange matrix

Affinity chromatography – Interaction between the matrix and specific groups on the molecule of the sample

Hydrophobic interaction chromatography – Interaction between hydrophobic regions of the sample molecules and a hydrophobic stationary phase

Mixed mode chromatography – combined types of adsorptive chromatography to increase selectivity

Non-adsorptive chromatography consists of gel filtration, also referred to as size exclusion chromatography. Size exclusion chromatography separates the components based on the size of the molecules and no chemical interaction between the molecule and stationary phase is exploited (Jagschies *et al.* 2007; Ioannidis *et al.* 2012).

1.2 Chromatographic operations

1.1.5. Column packing and bed compression

Efficient packing of a column is an important factor for the successful separation of biopharmaceutical products. Typically higher column efficiency is achieved with taller bed heights and a smaller particle size. A well-packed column will also provide a stable bed that will be slow to deteriorate over time (Jagschies *et al.* 2007).

Prior to packing, it is typical for the resins to be suspended in a slurry and poured into the column. The slurry is allowed to settle by gravity and the pre-packed bed height is measured. To achieve a homogenously packed column, the column undergoes two additional steps: flow packing and bed compression. Flow packing is accomplished by applying a constant liquid flow (hydrodynamic) through the bed; this is low enough to prevent particle deformation. In general, the more rigid the resin, the higher the flow rate it can withstand (Billen *et al.* 2005).

After flow packing, the second step is bed compression; where the bed is compressed further to create a stable bed that will not deform if operated within a set of pre-defined process operation limits. During bed compression, interparticle friction prevents the bed from becoming closely packed but at the same time friction is required to keep the bed in place; also referred to as bed consolidation. As a result, different methods of packing lead to different packing behaviour of the packed bed and hence differing distribution of stress (Dorn *et al.* 2017). Figure 1-4 illustrates a well-packed column that has controlled interstitial volume (space between the particles) and where the density of the packed resin is homogeneous.

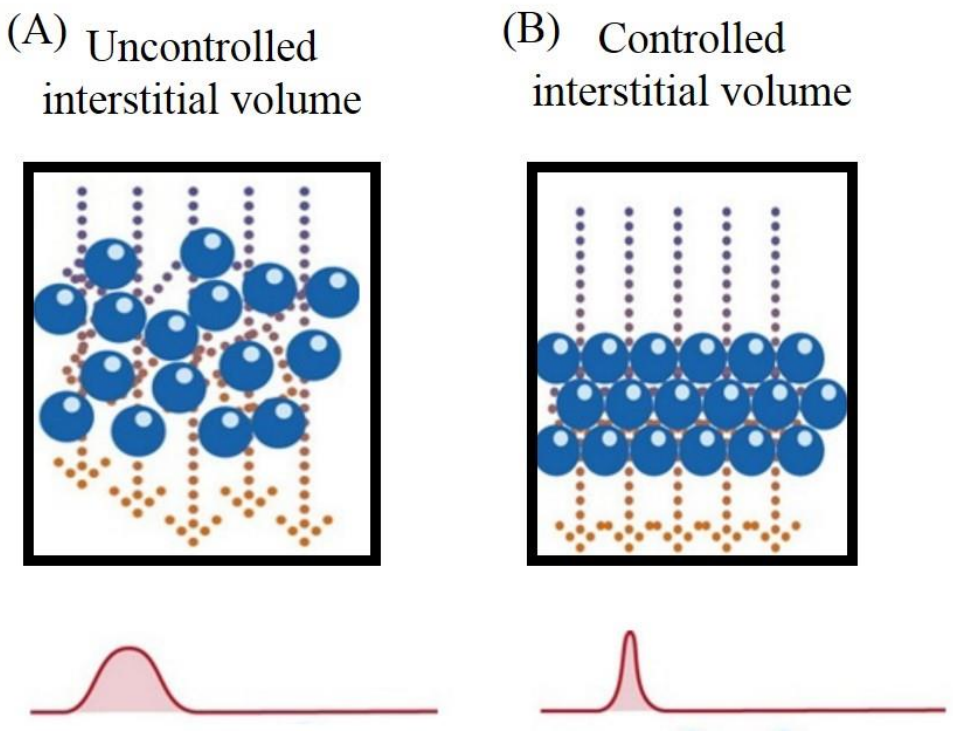

Figure 1-4 Schematic cross-section diagram of chromatography resins arrangement: (A) poorly packed column (B) well-packed column adapted from (Healthcare 2000)

Bed compression is applied to reach the final bed height and can be achieved by (Cherrak *et al.* 2002; Dorn and Hekmat 2016):

- Hydrodynamic compression (Flow packing) – Uses constant pressure or flow rate

- Mechanical compression (Dynamic axial compression) – Achieving by axially compressing the media slurry
- Stall packing – Packing by pumping media into the column via nozzles.

1.1.6. Quantifying packing quality

The preparation and quantification of packed columns both for purification process and for final product preparation is to ensure robustness and safety. In order to characterise the chromatography column without interference, a non-binding tracer is made to flow through the column, and being inert this refrains from chemical interactions with the medium. Efficiency testing is through the analysis of the Residence Time (RT) distribution for a tracer substance passing through the column. A typical test signal is a pulse. A small volume of tracer substance flows into the column inlet and the broadening of this pulse as it exits the column is analysed.

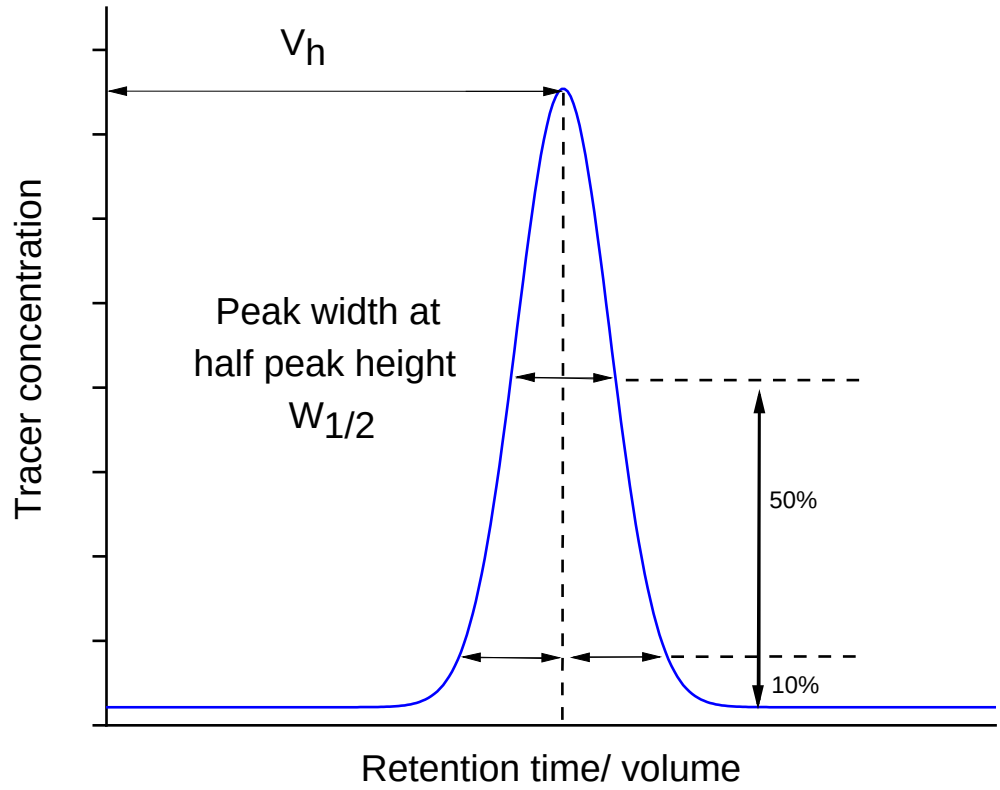

Figure 1-5 shows a typical chromatogram peak, the pulse response is plotted against time or volume and the peak width at half peak height is measured.

In industry, the quality of packed columns is often expressed in terms of two parameters; the number of theoretical plates (N) and asymmetry factor (As). Both values are experimentally determined via a column efficiency test.

The number of theoretical plates (N) can also be expressed in height equivalent of a theoretical plate (HETP) or reduced plate height (h). The retention time or retention volume is measured at the maximum peak height corresponding to the symmetric (Gaussian) peak shape. A dimensionless and thus convenient parameter for efficiency characterisation is the reduced plate height (h). This parameter facilitates the comparison of column efficiency irrespective of column length and particle diameter of the media. Manufacturers in the biopharmaceutical industry often apply reduced plate height and asymmetry factor to quantify and monitor the performance of a packed bed (GE Healthcare, 2000). The theoretical equations are described below.

$$N = \frac{{\mu_f}^2}{\sigma^2} \approx 5.54 \left(\frac{V_R}{W_{1/2}}\right)^2 \qquad \textbf{Eq. 1-1}$$

where N is the number of theoretical plates, V_R is the retention volume of probe molecule, $W_{1/2}$ is the width of peak at half the maximum height.

$$HETP = \frac{L}{N} \qquad \textbf{Eq. 1-2}$$

where L is the total length of the column. A relative method is the use of the reduced plate height (h), this normalises HETP for particle diameter and is useful when comparing HETPs for columns with different particles sizes.

$$h = \frac{HETP}{d_p} \approx \frac{L}{d_p} \frac{1}{5.54} \left(\frac{W_{1/2}}{V_R}\right)^2 \qquad \textbf{Eq. 1-3}$$

The asymmetry factor (As) describes the deviation from an ideal Gaussian peak shape and is calculated from the peak width at 10% of peak height:

$$A_s = \frac{b}{a} \qquad \textbf{Eq. 1-4}$$

Where a is the distance from leading edge of peak to midpoint of peak at 10% peak height, b is the distance from midpoint of peak to tailing edge of peak at 10% peak height.

In addition, by measuring the HETP and asymmetry the integrity of the bed can be quickly quantified before starting the purification process. Although this method does not directly predict the purity of any separation, this method can indicate crucial parameters that facilitate a robust operation protocol.

To ensure a well-packed column, manufacturers have suggested ideal ranges for these parameters. A reduced plate height of $h \leq 3$ for porous media employed in bioprocess chromatography is considered optimal. An asymmetry factor close to As = 1 is ideal. A typical acceptable range could be $0.8 < A_S < 1.8$ when working towards a reduced plate height of $h \leq 3$ (GE Healthcare, 2000).

Operating under high velocity may increase productivity however; under the same conditions, efficiency may be unfavourable. Peak broadening and therefore chromatographic efficiency is strongly dependent on the liquid velocity applied during the test. The relationship between peak broadening and liquid velocity is described theoretically by the Van Deemter equation (Eq. 1-5).

$$HETP = A + \frac{B}{u} + C.u \qquad \textbf{Eq. 1-5}$$

Where A is eddy dispersion, B is molecular diffusion, C is mass transfer resistance, and u is liquid velocity (cm h^{-1}). A, B, and C are factors which contribute to band broadening (Ioannidis, 2009).

A - Eddy diffusion

As the mobile phase moves through the column, solute molecules will take different paths through the stationary phase at random. This will bring about broadening of the solute band, as different paths are of different lengths.

B - Longitudinal diffusion

Analyte concentration is reduced at the edges of the band relative to that at the centre. Analyte diffuses out from the centre to the edges. This brings about band broadening. High mobile phase velocity means that the analytes spends less time on the column, which decreases the effects of longitudinal diffusion.

C - Resistance to mass transfer

The analyte spends a certain amount of time equilibrating between the stationary and mobile phase. High mobile phase velocity will result in the analyte having a stronger affinity for the stationary phase. The result of this is that an analyte in the mobile phase will move ahead of an analyte in the stationary phase, resulting in broadening of the analyte band. The higher the velocity of the mobile phase, the greater the band broadening becomes.

At lower velocities, the efficiency is reduced by means of molecular diffusion corresponding to the term B in the Van Deemter equation. At high test velocities, and thus shorter residence time over the column, peak broadening increases as a result of the limiting intraparticle diffusion as represented by the term C in the Van Deemter equation (Eq. 1-5). By plotting mobile phase velocity vs. plate height (Van Deemter curve) the optimal linear velocity can be determined. For the column efficiency tests, a linear velocity of 30 cm h^{-1} was chosen (refer to Figure 1-6).

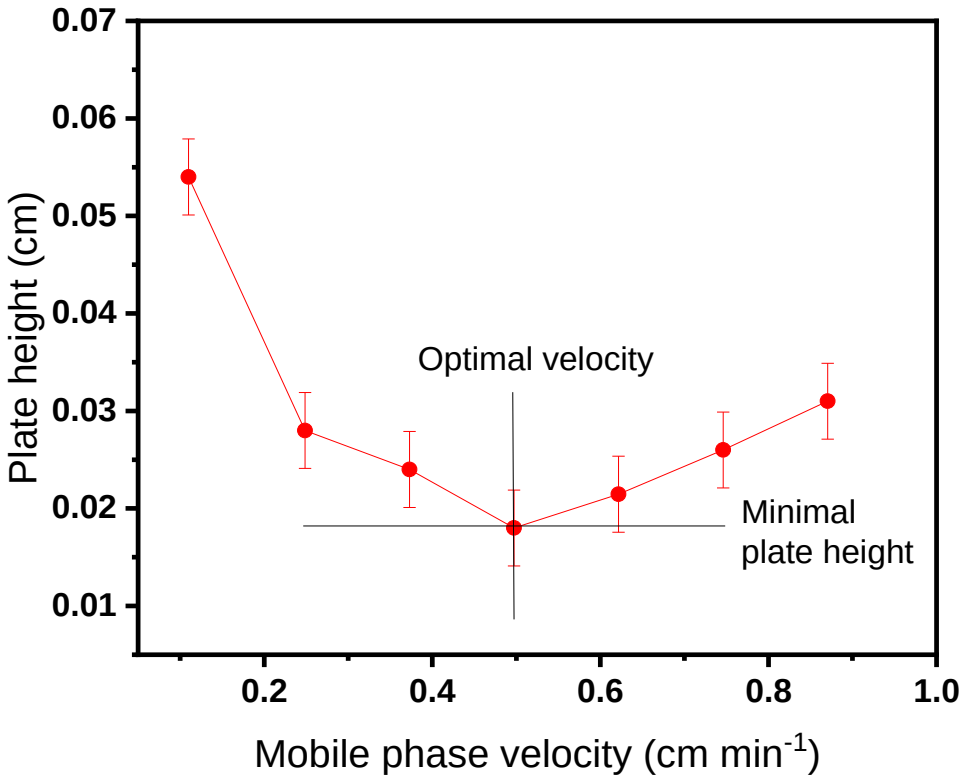

Figure 1-6 Van Deemter curve under hydrodynamic compression. Columns packed with Sepharose CL-6B, 0.016 m I.D., 20 cm bed height. Measurements were repeated three times with a relative standard deviation of less than 5% in all measurements.

1.1.7. Impact of bed compression on packing quality

Packing and flow heterogeneity

It is well recorded that poor column packing and flow heterogeneity cause reduced column performance and band broadening (Guiochon and Sarker 1995; Grushka 1972). Table 1-3 illustrates the different causes of band broadening. A number of studies have investigated the impact of bed compression and flow heterogeneity on chromatography resins using a variety of experimental techniques that measure band broadening effects (Farkas *et al.* 1994; Ergun 1952; Cramers *et al.* 1981; Fishman and Barford 1970; Eon 1978), including interparticle and intraparticle porosity (Guan and Guiochon 1996; De Smet *et al.* 2005), magnetic resonance imaging (Keener *et al.* 2002; Yuan *et al.* 1999), reverse flow technique (Freitag *et al.* 1994; Dorn *et al.* 2017; Davies and Bellhouse 1989), and computer fluid dynamic modelling (Dorn *et al.* 2017; Teepakorn *et al.* 2016; Dorn and Hekmat 2016).

Table 1-3 Causes of band broadening effects

Band Broadening Factors
Uneven packing
Uneven flow distribution
Mass transfer resistances
Slow binding kinetics
Viscosity
Extra-column effects

The packing of industrial-scale columns is achieved by keeping the residence time constant (Fang 2010), however there is much evidence that increasingly heterogeneous packing across the radial distribution of the column is likely to occur due to the "wall effect" (Farkas *et al.* 1994; Guiochon and Sarker 1995; Sarker *et al.* 1996). In addition, the increased pressure and bed compression are important factors upon scaling-up because increasing the aspect ratio will result in the loss of wall support. Various reports have investigated the impact of scale-up on the pressure drop of chromatography resins (Fang 2010; Mohammad *et al.* 1992a; Moscariello *et al.* 2001).

The level of bed compression is an essential precursor in forming a well-packed bed; however, excessive compression of the matrix can cause detrimental effects on the column efficiency, resulting in extreme flow instability (Mohammad *et al.* 1992b; Mohammad *et al.* 1992a; Soriano *et al.* 1997; Stickel and Fotopoulos 2001).

The Blake-Kozeny equation describes the pressure drop as a function of flow rate for laminar flow through a packed bed of incompressible beads and of a single size (MacDonald *et al.* 1991).

$$\frac{dP}{dL} = \frac{150\,\mu}{{d_p}^2}\,\frac{(1-\varepsilon)^2}{\varepsilon^3}\,.\,v \qquad \textbf{Eq. 1-6}$$

The pressure drop is largely influenced by bed porosity and particle size; these two factors are known to cause a sharp increase in pressure drop. For a well-packed bed the porosity range is between 0.3 – 0.55. Most chromatographic beads are compressible to varying degrees; agarose-based supports are commonly used but are relatively soft compared to more rigid resins (e.g. ceramic-based, silica-based, and glass-based supports). The compressibility of the beads reduces the porosity of the bed and that in turn can cause the pressure across the column to rise. This may have detrimental effects on the separation efficiency. Several articles have dealt with the pressure drops of chromatographic columns; in particular identifying the critical velocity, the point at which the rate of change in pressure drop with velocity becomes infinite upon compression (Mohammad *et al.* 1992b; Mohammad *et al.* 1992a; Stickel and Fotopoulos 2001; Tran *et al.* 2007).

Most reports investigating the impact of bed compression tend to focus on quantifying the column efficiency across the whole bed by measuring certain parameters, such as reduced plate height, asymmetry, porosity etc. (Freitag *et al.* 1994; Guiochon and Sarker 1995; Koh and Guiochon 1998). A few literature reports have shown improvements in resolution with hydrodynamic compression for gel filtration chromatography (De Smet *et al.* 2005; Edwards and Helft 1970; Fishman and Barford 1970).

Some reports have alluded to the differences in bed structure along the different sections of the column predicted by computer fluid dynamics (Dorn *et al.* 2017), or observed via magnetic resonance imaging (Dorn and Hekmat 2016), and scanning electron microscopy (Nweke *et al.* 2017). These methods are expensive and can be intrusive; an alternative easier and faster method is needed. This provided a huge motivation of this study.

In addition, the reports do not focus on the influence of different methods of compression on performance parameters such as yield, purity, and throughput, which may vary depending on the method of compression used. Further effects of bed compression applied to the top of the column include differences in packing densities and hydrodynamic stresses caused by high fluid flow and poor liquid distribution from the top adapter (Kong *et al.* 2018; Yuan *et al.* 1999). These issues lead to poorly packed beds that can cause channelling and band broadening effects, all contributing to packed bed failure. There is a need to understand the effects of different methods of compression to achieve optimal packing and protein separation.

1.3 Validating column packing process

Biopharmaceutical process development involves producing and then optimising well-characterised processes for production of potential therapeutic bio-molecules. However, in recent years increased product titres has created heavier burdens on downstream processing, this subsequently led the regulatory agencies such as the FDA to request for better defined processes from manufacturers (Hernandez 2015). The Chemistry Manufacturing Controls (CMC) refers to data describing the components, manufacture, and specification of a drug product and its ingredients. CMC plays a critical role in ensuring an adequate and safe supply of the drug product. In 2004, the Quality by Design (QbD) initiative was followed by that of Process Analytical Technology (PAT), both introduced into the CMC review process (Read *et al.* 2010). QbD has been defined in the International Conference on Harmonization (ICH) Q8 guideline as;

> "a systematic approach to development that begins with predefined objectives and emphasizes product and process understanding and process control, based on sound science and quality risk management"

Regulatory bodies now require a QbD approach to process development and involves the identification of the critical quality attributes (CQA) and quality target product profile (QTPP). The CQA and QTPP relates to the product characteristics such as the purity and efficacy, outlined by Rathore & Kapoor 2016. Critical process parameters (CPP) are process parameters that have an impact on the CQAs and can be identified through risk assessment followed by experimental verification (Gibson 2018).

Column packing is validated by analysing the column efficiency in regards to the height-equivalent-to-theoretical-plate (HETP), asymmetry factor (As), and reduced plate height (h). The FDA emphasises that validation of chromatography processes should measure packing heterogeneity, process characterisation, lifetime of resin, among other see Table 1-4.

Table 1-4 Parameters associated with the quantification of resin lifetime adapted from (Nweke *et al.* 2018)

Measurable parameters for determining chromatography resin lifetime	
Bed height	Purity of product
Column efficiency (HETP, Asymmetry)	Product yield
Peak Integrity	Dynamic binding capacity
Voidage (inter/intra particle porosity)	Impurities (e.g. DNA)
Elution/Load profile	Adsorption isotherms
Bed height	Productivity

Quality by Design (QbD)

Whilst in-depth research has been put into the characterisation and validation of chromatographic media through determining the dynamic binding capacity, purity, yield, etc. little research has gone into investigating the effects of different modes of compression on purity and yields, as a means of fulfilling regulatory requirements.

The CQAs are the attributes of the final product that are critical to its quality. For the chromatography step, the CQA that is affected most is the purity of the drug. Under the QbD approach, a multidimensional design space is defined through understanding the interactions between the CPPs and the CQAs. Before the introduction of QbD, any deviations from the set point could result in a batch failure, this can have a great effect on the feasibility of the manufacturing process. Through the multidimensional design, changes within the defined specifications in the CPPs will not have an adverse effect on the CQAs (Rathore and Velayudhan 2002).

Purification factor vs. yield diagram

Design of Experiments (DoE) is used to provide a systematic approach to reducing the number of experiments that are required for validating the chromatographic process. The purification factor vs. yield diagram (PFY) provides a method of characterising the chromatographic performance as a function of its purity and yield (Ngiam *et al.* 2003). Ngiam and co-workers adapted the PFY method for chromatography in order

to analyse the trade-offs between purity and yields. This method was developed to identify the optimal chromatographic condition within the operating window of the process (Tengliden 2008). The PFY diagram is derived from the fractionation diagrams plots that are calculated from analysing the fractions collected from the eluate (refer to Figure 1-7).

Summary

The sections above have highlighted the different methods of bed compression for packing chromatographic columns as well as the different causes of packing heterogeneity. The relationship between bed compression and factors relating to packing quality, especially with biological molecules are often complex and varied.

Bed compression is known to produce changes in the column efficiency, column resolution, capacity and increased compression factor. These are critical parameters when designing multidimensional experiments for a chromatographic step, as these parameters may have implications for the purity and economy of the overall step. Thus, it is important to evaluate a number of conditions so as to select the optimal level of bed compression required to minimise flow heterogeneity while ensuring a well-packed bed to ensure highest purity and yields.

Regulatory authorities are aware the impact of poorly packed columns can ultimately effect the consistency and purity of the product. However, little research have been done to comprehend the impact of different methods of compression on protein separation in adsorptive and non-adsorptive chromatography. Therefore, a challenge for bioprocess engineers is to design chromatographic processes that relate bed compression to a number of CQAs. The effect of bed compression on both the product purity and the economics of the process will be of great importance in better understanding the ways to improving chromatographic performance at scale.

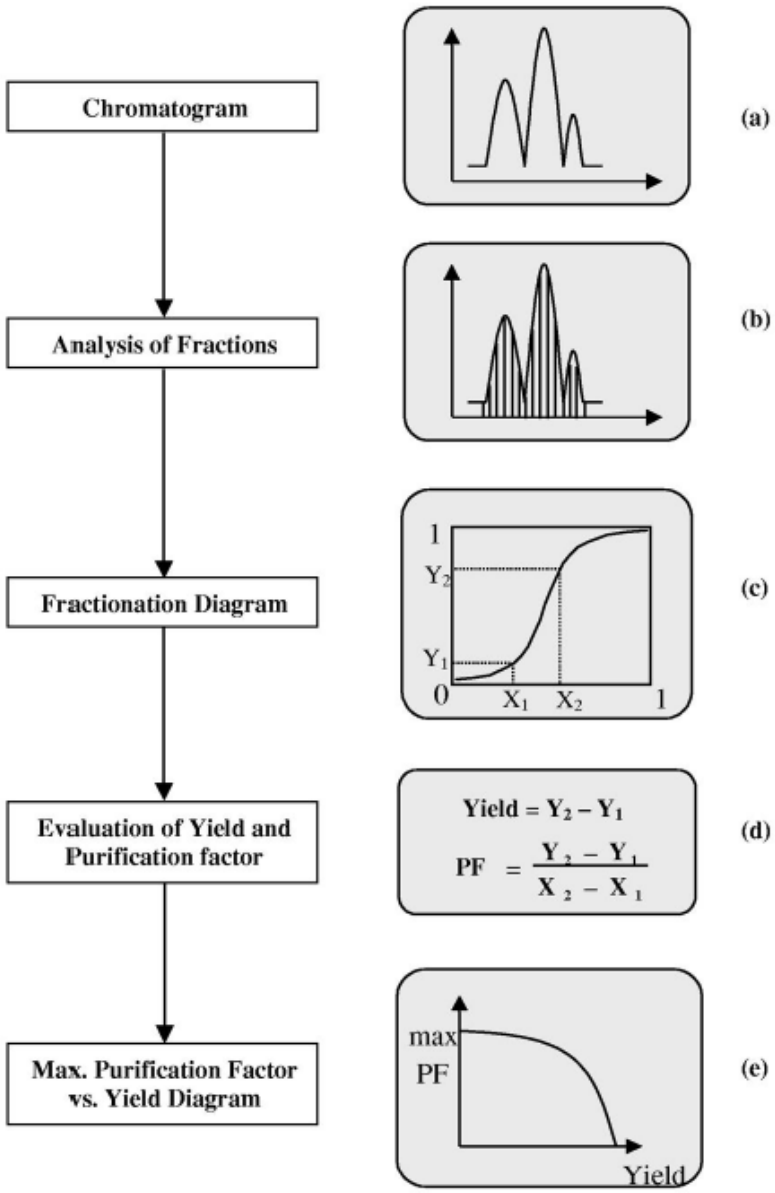

Figure 1-7 Schematic illustration of the procedure to generate the fractionation diagram and the corresponding maximum purification vs. yield diagram from an elution chromatogram. X and Y represent the cumulative fraction of total material and target product respectively, adapted from (Ngiam *et al.*, 2001).

2 Effect of hydrodynamic and mechanical compression on column efficiency

2.1 Abstract

Analysis of column efficiency as a function of different packing methods were examined for a range of chromatography resins: Sepharose CL-6B, DEAE Sephacel, Q Sepharose FF, Q Sepharose HP and Capto Q. Two methods of compression were applied; hydrodynamic and mechanical compression. Hydrodynamic compression used high liquid velocities to compress the column; in contrast, under mechanical compression physical compression of the bed via the top adapter was employed. One-step and multiple incremental step compression revealed the differences produced by adaptation of the two column packing strategies. A pulse injection method using acetone validated the packing quality of the column in terms of the reduced plate height and asymmetry.

Mechanical compression led to a significant improvement in asymmetry and reduced plate height for both one-step and multiple step compression. Hydrodynamic compression showed earlier signs of over-compression via one-step compression at high liquid flow velocities.

Four anion exchange resins were studied with different base matrix rigidities. Capto Q showed significant improvements under both hydrodynamic and mechanical compression, whereas Q Sepharose FF and HP showed poor packing quality above 0.05 CF. The addition of the dextran surface extender on Capto Q inferred greatest benefit compared to all other resins. Five different batches of DEAE Sephacel were studied to validate the reproducibility of the packing behaviour at both bench and pilot scale. Overall, the factors affecting column efficiency is resin and packing strategy dependent.

2.2 Materials and Methods

2.2.1 Bench scale setup

Bench-scale experiments (up to 40 mL column volume) were carried out using the ÄKTA Avant 25 (GE Healthcare, Little Chalfont, Buckinghamshire, UK) fast protein

liquid chromatography system equipped with pump unit P-903, UV cell (280 nm, 2 mm path length), conductivity cell, and auto sampler A-900. The control software UNICORN 6.0 (GE Healthcare, Little Chalfont, Buckinghamshire, UK) was used. The extra column dead volume was kept to a minimum by using an inner diameter (I.D.) of 0.12 mm capillary tube to connect the column to the injector. An XK16 column (GE Healthcare, Uppsala, Sweden) was used with an I.D. of 0.016 m (XK16, with adjustable column lengths). All chromatography experiments were performed in triplicate and at room temperature 20 ± 5 ℃.

2.2.2 Pilot-scale setup

Pilot-scale experiments (up to 1.6 L column volume) were carried out using the ÄKTA Pilot system (GE Healthcare, Little Chalfont, Buckinghamshire, UK) equipped with pump unit P-907, UV cell (280 nm), conductivity cell, and auto sampler A-950 supplied with the UNICORN 5.11 control software. A BPG-100/500 (GE Healthcare Uppsala, Sweden) was used with an I.D. of 0.1m with adjustable column lengths. All chromatography experiments were performed in triplicate and at room temperature 20 ± 5 ℃.

2.2.3 Stationary phases

All reagents were from a single supplier (Sigma–Aldrich, Poole, Dorset, UK) unless stated otherwise. Studies were carried out using a gel filtration resin: Sepharose CL-6B (GE Healthcare Uppsala, Sweden). Sepharose CL-6B is a 6% cross-linked agarose gel filtration base matrix which may be used to separate samples of diverse molecular weight; $1 \times 10^4 - 1 \times 10^6$ Da. The resin is available in both Sepharose and Sepharose CL forms where the cross linked form is chemically and physically more resistant, allowing identical selectivity but at increased flow conditions. The spherical resins had a size distribution of 45 – 165 µm (quoted by the manufacturer). The average bead diameter was determined to be d_p = 98 µm ± 5 µm (Malvern Mastersizer 3000 laser sizer; Malvern Instruments, Worcestershire, UK).

In addition to studying gel filtration resins, three strong anion exchangers (quaternary amine) were investigated; Q Sepharose Fast Flow, Q Sepharose High Performance and Capto Q (GE Healthcare Uppsala, Sweden). Both Q Sepharose resins are highly cross-

linked agarose beads, whereas Capto Q has an additional dextran surface extender. Both Q Sepharose FF and Capto Q have a particle size, d_p of ~ 90 µm, whilst Q Sepharose HP has a size distribution of average particle size, d_p of 34 µm (quoted by the manufacturer).

Studies were also carried out on a weak anion exchanger; DEAE Sephacel (GE Healthcare Uppsala, Sweden). The resin has a cross-linked cellulose structure with a diethylaminoethyl functional group. The average bead diameter was determined to be, d_p = 96 µm $\pm$ 5 µm using a Malvern 3000E Particle Sizer with Mastersizer^{TM} 2000 control software (Malvern Mastersizer 3000 laser sizer; Malvern Instruments, Worcestershire, UK). Five different lot batches of DEAE Sephacel were examined to investigate the consistency and reliability of the experiments. Table 2-1 summarises the resins used.

Table 2-1 Specification of chromatography resins

	Q Sepharose CL-6B	Q Sepharose FF	Q Sepharose HP	Q Capto	DEAE Sephacel
Matrix	6% cross-linked agarose	6% cross-linked agarose	6% cross-linked agarose	Highly cross-linked agarose with dextran surface extender	Cross-linked cellulose
Avg. particle size (µm)	98	90	34	90	96
Type	Gel filtration	Strong anion	Strong anion	Strong anion	Weak anion
pH stability range	3-14	2-12	2-12	2-12	2-9
Max. pressure drop (MPa)	0.045	0.3	0.3	0.3	0.03

2.2.4 Mobile phases

For Sepharose CL-6B, all reagents were from a single supplier (Sigma–Aldrich, Poole, Dorset, UK) unless stated otherwise. The packing buffer used was a 20 mmol L^{-1} sodium phosphate buffered saline (PBS) with 130 mmol L^{-1} NaCl at pH 7.2. The mobile phase was filtered using 0.22 µm Stericup filter units (Merck & Co., Darmstadt, Germany).

For anion exchange resins, all reagents were from a single supplier (Sigma–Aldrich, Poole, Dorset, UK) unless stated otherwise. The equilibration buffer used was a 50 mM Tris-HCl at pH 8.5. The elution buffer was 50 mM Tris-HCL 1 M NaCl pH 8.5. The mobile phases was filtered using 0.22 µm Stericup filter units (Merck & Co., Darmstadt, Germany).

Columns were stored in 20% v/v ethanol solution, as per the manufacturer's recommendations. Columns stored in 20% v/v ethanol were washed with 5 CV of packing buffer prior to the equilibration step.

2.2.5 Determining dead volume

To achieve accurate data in any chromatographic system it is necessary to determine the dead volume. This was achieved by attaching a piece of tubing of known volume from the system to the top of the column. An acetone tracer was then applied to the system at a flow rate of 0.5 mL min^{-1}. The dead column volume of the system was determined by subtracting the known volume of the connecting tubing from the retention volume of the eluted acetone pulse.

2.2.6 Bed compression factor

As a consequence of the application of each incremental increase in compression the bed height reduced. This was captured through the bed compression factor (λ) defined as:

$$\boldsymbol{\lambda = \frac{V_{CO} - V_C}{V_{CO}}} \qquad \textbf{Eq. 2-1}$$

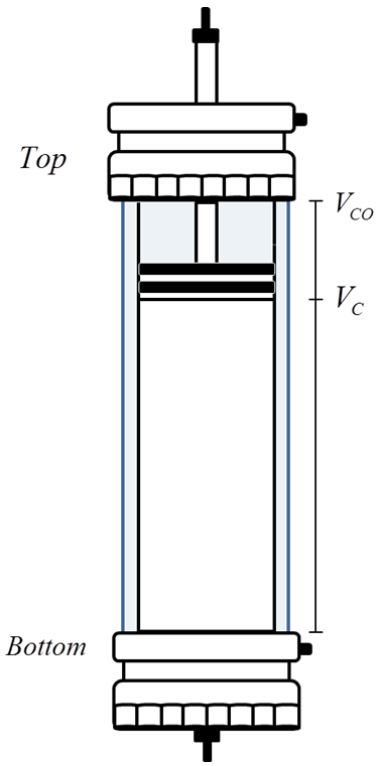

Figure 2-1 Diagram of a bench-scale chromatography column with adjustable column length and inner diameter of 1.6 cm (XK16 model, GE Healthcare, Uppsala, Sweden).

where V_c is the packed bed volume and V_{co} is the initial settled bed volume. A maximum level of bed compression factor (λ) of 0.15 was used, as this was determined to be the maximum pressure drop of the resins, provided by the manufacturer. For both methods of compression, three repeats were conducted.

Table 2-2 Experimental velocities used for hydrodynamic compression.

	Sepharose CL-6B	Q Sepharose FF	Q Sepharose HP	Q Capto	DEAE Sephacel
Packing velocity (cm h^{-1})	30	50	50	50	30
Maximum velocity (cm h^{-1})	150	400	150	700	100

2.2.7 Hydrodynamic and mechanical compression

For hydrodynamic compression, packing buffer was pumped through the column at 80% of the maximum flow rate (within the pressure drop limit) for bench and pilot scale column until the desired bed height was achieved (refer to Table 2-2). Once the measured pressure drop remained constant for at least 1 CV, the top column adapter was immediately lowered to the matrix bed surface to retain the level of compression.

For mechanical compression, the top adapter was physically pushed down until the desired bed compression had been achieved. When lowering the top adapter, the O-ring was loosened and the column inlet connector disconnected from the ÄKTA. This allowed buffer to escape at the top of the column during compression. Once compressed, the column adapter was secured and connected back to the ÄKTA. Care was taken to ensure no air was trapped in the tubing or column.

2.2.8 Modes of Compression

When no compression was applied (compression factor of 0.00), the column was flow packed at the appropriate packing linear velocity for 5 CV for both bench and pilot scale experiments (refer to Table 2-2).

Two modes of resin compression were investigated. The first method applied compression in a single step by taking the column from the original flow packed bed state to the desired compressed state (Kong *et al.* 2018). This is referred to as one-step compression.

1. Compression was applied to the bed in a single step until the desired bed compression factor was achieved by hydrodynamic or mechanical methods, described in the previous subsections (refer to 2.2.7).

2. Compression was applied to four different compression factors (0.02, 0.05, 0.10 and 0.15).

3. Columns were repacked for the next compression factor.

The second method of compression went from the original packed bed to the compressed state by applying a multiple series of steps. This is referred to as multiple incremental step compression.

1. For hydrodynamic compression, the packing flow rate was applied and increased to maximum flow rate (refer to Table 2-2) until the desired bed compression factor was achieved. Mechanical compression was applied as described in the subsection (see 2.2.7).

2. Four different compression factors (0.02, 0.05, 0.10 and 0.15) were applied starting with the lowest compression factor. The next compression factor was reached without repacking of the column.

2.2.9 Acetone test

Column efficiency was measured by asymmetry and reduced plate height using a 2% CV injection of 2% v/v acetone, applied using a V-7 sample injector with a 100 µL loop for the bench scale column and directly injected using the sample pump for the pilot scale column.

2.3 Results and Discussion

Sepharose CL-6B

Figure 2-3 show the impact of two different methods of compression, hydrodynamic and mechanical, on reduced plate height and asymmetry for Sepharose CL-6B. For each method of compression, four different compression factors (0.02–0.15) were achieved by multiple incremental steps or one-step compression as presented in Figure 2-3. At 0.02 CF, both hydrodynamic and mechanical compression using multiple incremental and one-step compression showed improvements in reduced plate height and asymmetry. Mechanical compression yielded higher column efficiency than did hydrodynamic compression – a 3.5 - fold improvement in reduced plate height Figure 2-3. All conditions showed a lower reduced plate height and an asymmetry factor closer to 1.0 except for hydrodynamic compression via multiple incremental step.

Hydrodynamic compression by one-step compression showed the poorest column efficiency. At 0.15 CF, the reduced plate height was above 10 and the asymmetry factor was furthest away from 1.0. The main difference between hydrodynamic and mechanical compression is the radial force applied onto the column. Under mechanical compression an even pressure along the top surface of the column by physically pushing the top adapter to the desired bed height. This method applies an even force to the radial surface area of the bed by pushing the smooth surface of the top adapter. By contrast, hydrodynamic compression forces the bed to the desired compression factor by applying mobile phase through the top adapter, frit and filter. The many parts that make up the adapter can produce irregular distribution of liquid flowing at high velocity that can produce uneven flow patterns. This can result in disruption of the top surface of the bed and overall column homogeneity (Amsterdam *et al.* 1975; Kennedy 2003; Bio-Rad 2014).

Another important factor is the difference between hydrodynamic compression via one-step and multiple incremental step. Multiple incremental steps changes the chromatography bed by undergoing several steps of achieve the desired level of compression. Further interruption of the bed increases the chance of instability and heterogeneity developing within the column. Under hydrodynamic compression, data

suggests that the level of column efficiency is step-dependent. One-step via hydrodynamic compression was shown to produce broader peaks by increasing the reduced plate height by 35%. Mechanical compression showed a higher level of column efficiency. For Sepharose CL-6B efficiency could be improved no matter if the column was compressed mechanically in one or multiple steps.

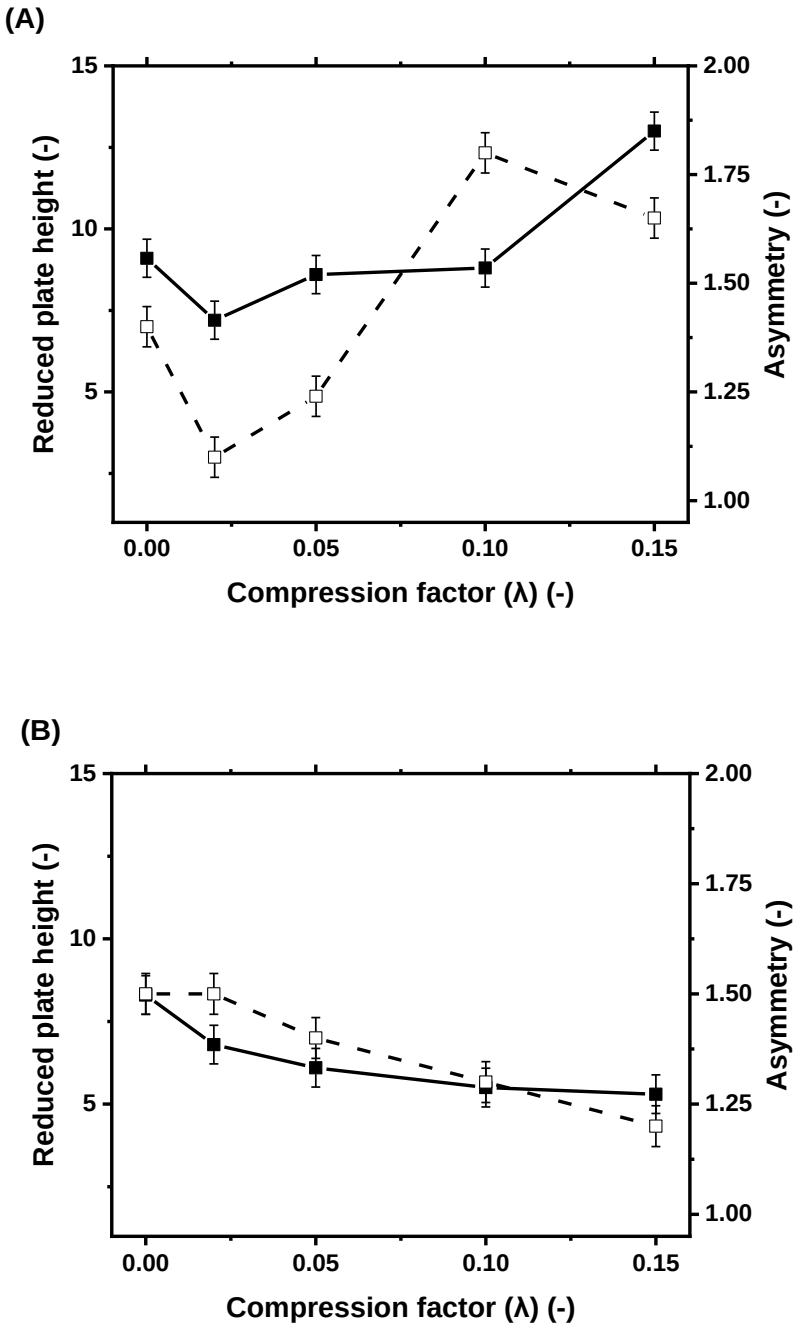

Figure 2-2: Comparison of reduced plate number and asymmetry for compressed beds achieved by hydrodynamic methods. Columns packed with Sepharose CL-6B 0.016 m I.D. 20 cm bed height; a flow rate of 0.5 mL min^{-1} was used. (A) hydrodynamic compression achieved by one-steps (B) hydrodynamic multiple incremental step compression. (■) reduced plate height; (□) asymmetry. Measurements were repeated three times with a relative standard deviation of less than 5% in all measurements.

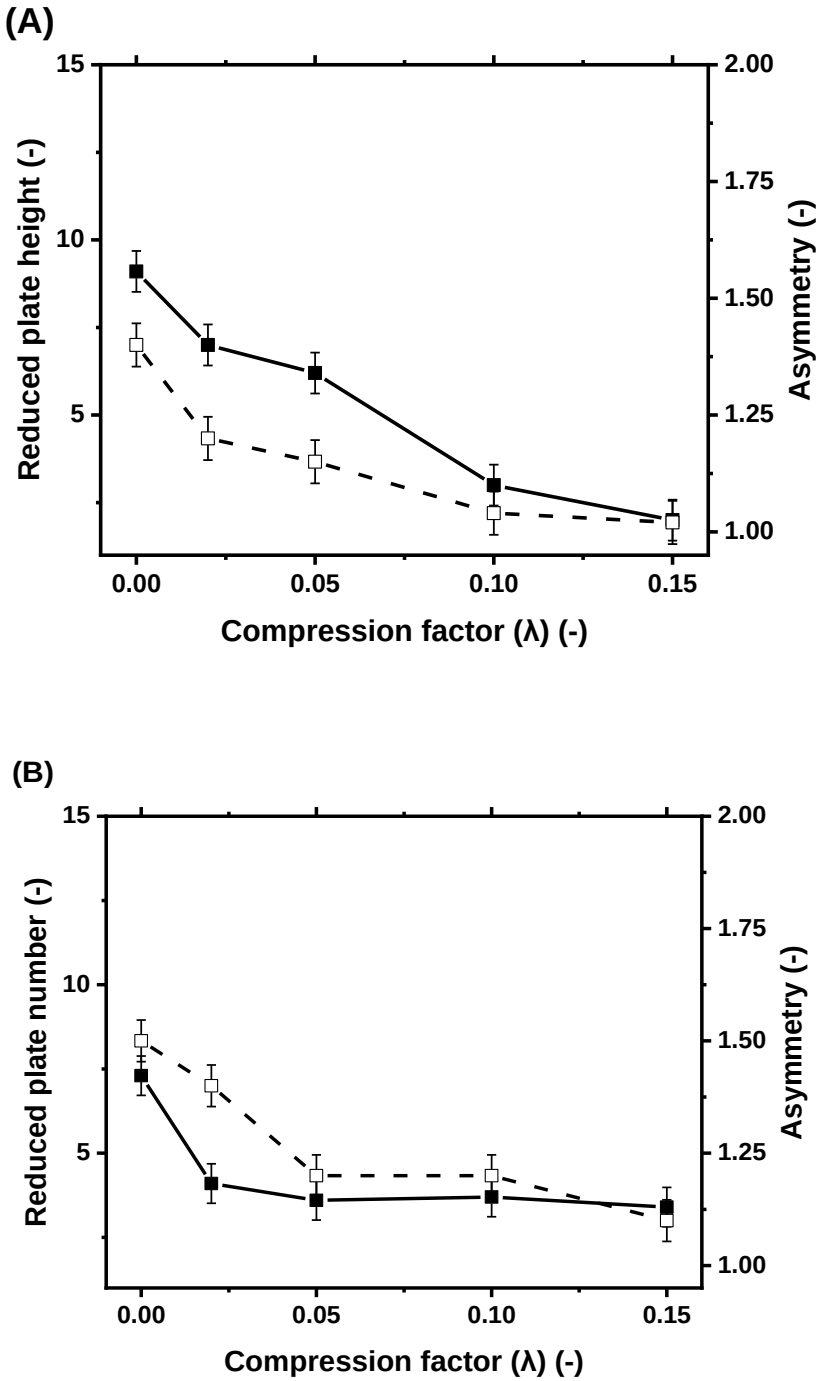

Figure 2-3: Comparison of reduced plate number and asymmetry for compressed beds achieved by mechanical methods. Columns packed with Sepharose CL-6B 0.016 m I.D. 20 cm bed height; a flow rate of 0.5 mL min^{-1} was used. (A) mechanical compression achieved by one-steps (B) mechanical multiple incremental step compression. (■) reduced plate height; (□) asymmetry. Measurements were repeated three times with a relative standard deviation of less than 5% in all measurements.

DEAE Sephacel

The next phase of studies set out to examine a softer resin DEAE Sephacel, a weak anion exchange resin. DEAE Sephacel has a lower maximum pressure limit of 0.03 MPa compared to Sepharose CL-6B, 0.045 MPa. In the studies, the effects of hydrodynamic and mechanical compression via multiple incremental steps on column efficiency on DEAE Sephacel were examined. Since multiple incremental step compression showed greater differences compared to one-step compression, it was decided to examine further these effects for five different batch studies.

Five different batches of DEAE Sephacel were studied. The data was standardised by subtracting the mean and dividing by the standard deviation. In both experiments examining the asymmetry factor and reduced plate height, all trends investigating hydrodynamic and mechanical compression showed high levels of consistency.

Figure 2-4 shows the measured asymmetry factor of DEAE Sephacel when hydrodynamically or mechanically compressed. At high levels of compression, the asymmetry factor for hydrodynamic and mechanical compression was below 1.0 indicating that the column was over compressed. Fronting of the acetone profile is evidence of premature breakthrough as indicated by an asymmetry factor below 1.0. High levels of stress forces resins to deform into another that obstructs the diffusional path along the column. This forms channels within the column resulting in early breakthrough (Eghbali *et al.* 2007; Eghbali *et al.* 2008; Khirevich 2010).

Mechanical compression showed an asymmetry factor closest to 1.0 at 0.10 CF. Both methods showed improvement with compression; however, the optimal levels of asymmetry is reached under mechanical compression (0.10 CF) whereas hydrodynamic compression does not fell an asymmetry of 1.0. Under hydrodynamic compression, the asymmetry factor reached below 1.0 earlier compared with mechanical compression; proving further evidence that the bed was more easily over compressed.

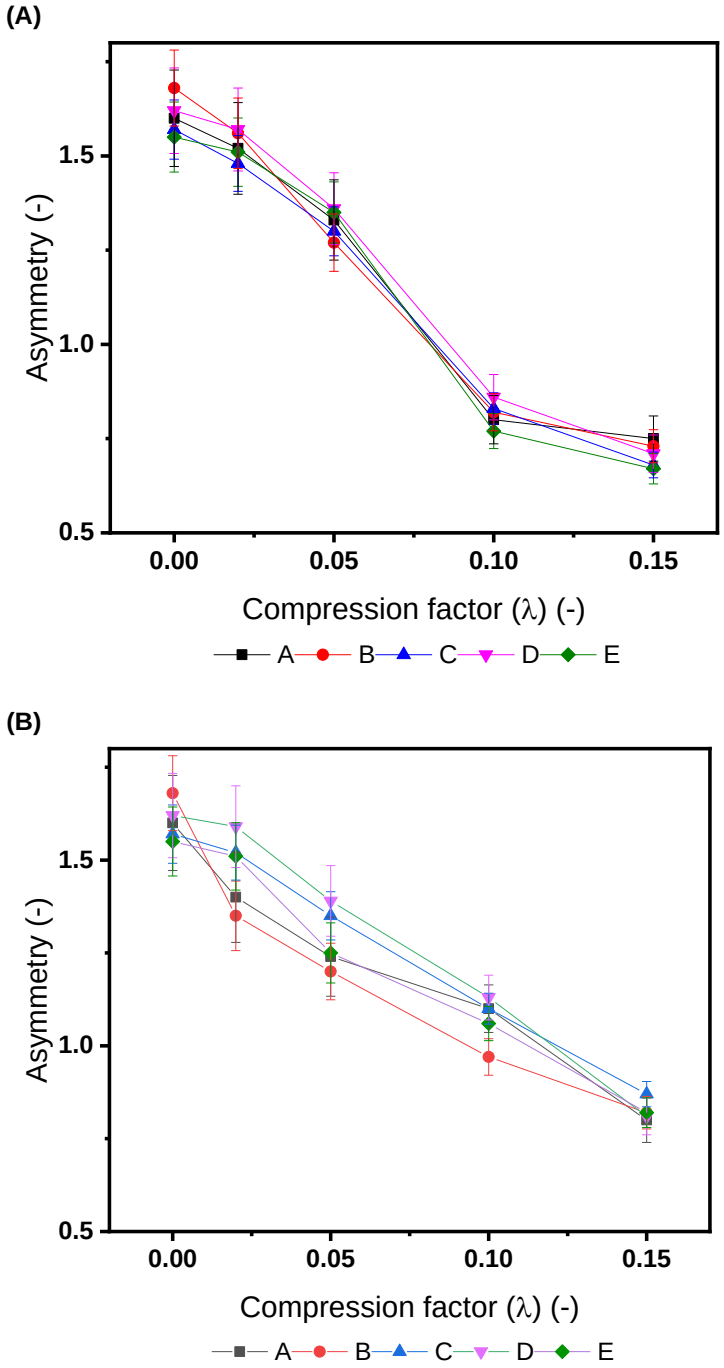

Figure 2-4: Comparison of asymmetry for compressed beds achieved by (A) hydrodynamic and (B) mechanical compression by multiple incremental step methods. Columns packed with DEAE Sephacel 0.016 m I.D. 10 cm bed height. Five different batches of resins were used (A – E). Measurements were repeated three times with a relative standard deviation of less than 5% in all measurements.

Figure 2-5 shows the reduced plate height of DEAE Sephacel under hydrodynamic and mechanical compression. Comparing the greatest change in reduced plate height, mechanical compression showed a higher decrease in reduced plate height (70%) compared to hydrodynamic compression (50%). The lowest reduced plate height achieved was 1.9 under mechanical compression and 4.1 under hydrodynamic compression. This suggests that mechanical compression produces a superior level of packing quality than does hydrodynamic compression. Based on acetone profiles, soft resins, such as DEAE Sephacel are more sensitive to over-compression when the column undergoes flow packing. Especially at 0.15 CF, multiple rounds of compression showed detrimental performance in both mechanical and hydrodynamic compression.

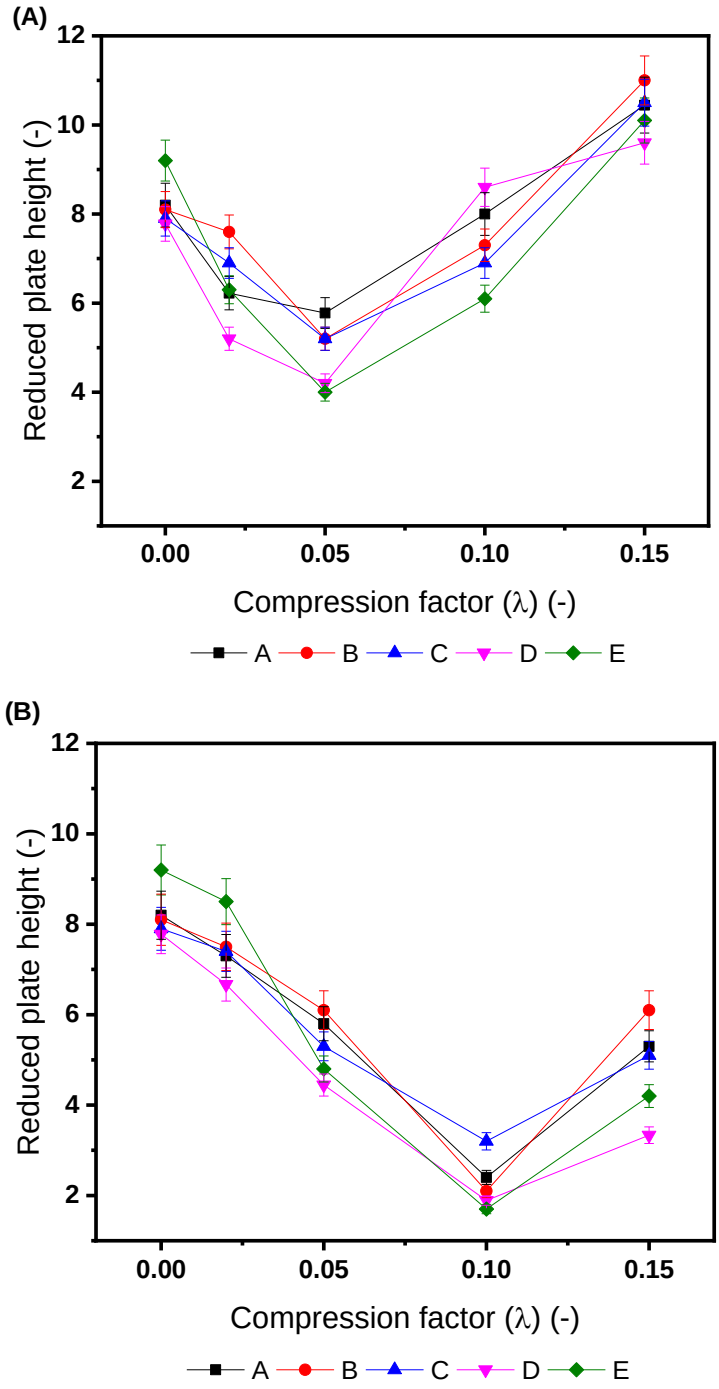

Figure 2-5: Comparison of reduced plate height for compressed beds achieved by (A) hydrodynamic and (B) mechanical compression by multiple incremental step methods. Columns packed with DEAE Sephacel 0.016 m I.D. 10 cm bed height. Five different batches of resins were used (A – E). Measurements were repeated three times with a relative standard deviation of less than 5% in all measurements.

Anion exchange resins

After examining the soft resins, the study turned to look at a wide range of rigidity of strong anion exchange resins: Q Sepharose FF, Q Sepharose HP and Capto Q. Figure 2-6 shows the asymmetry factor data of three strong anion exchange resins when hydrodynamically and mechanically compressed. The base matrix for the three resins is a highly crossed linked agarose; except for Capto Q which has an additional dextran extender on its surface for extra rigidity. Another difference, both Q Sepharose FF and Capto Q have an average particle size of 90 µm, whereas Q Sepharose HP is 34 µm in size.

Q Sepharose FF and HP showed poor asymmetry under hydrodynamic compression above 0.05 CF. Capto Q showed improvements under both hydrodynamic and mechanical compression. The main difference between the resins is the extra rigidity of Capto Q due to the additional dextran surface extender. This allows Capto Q to withstand higher levels of pressure exerted onto the bed without suffering in column efficiency when hydrodynamic compression was applied in multiple incremental steps. Q Sepharose FF and HP showed asymmetry factor out of the acceptable range ($0.8 < As < 1.2$), as with the softer resins (Sepharose CL-6B and DEAE Sephacel).

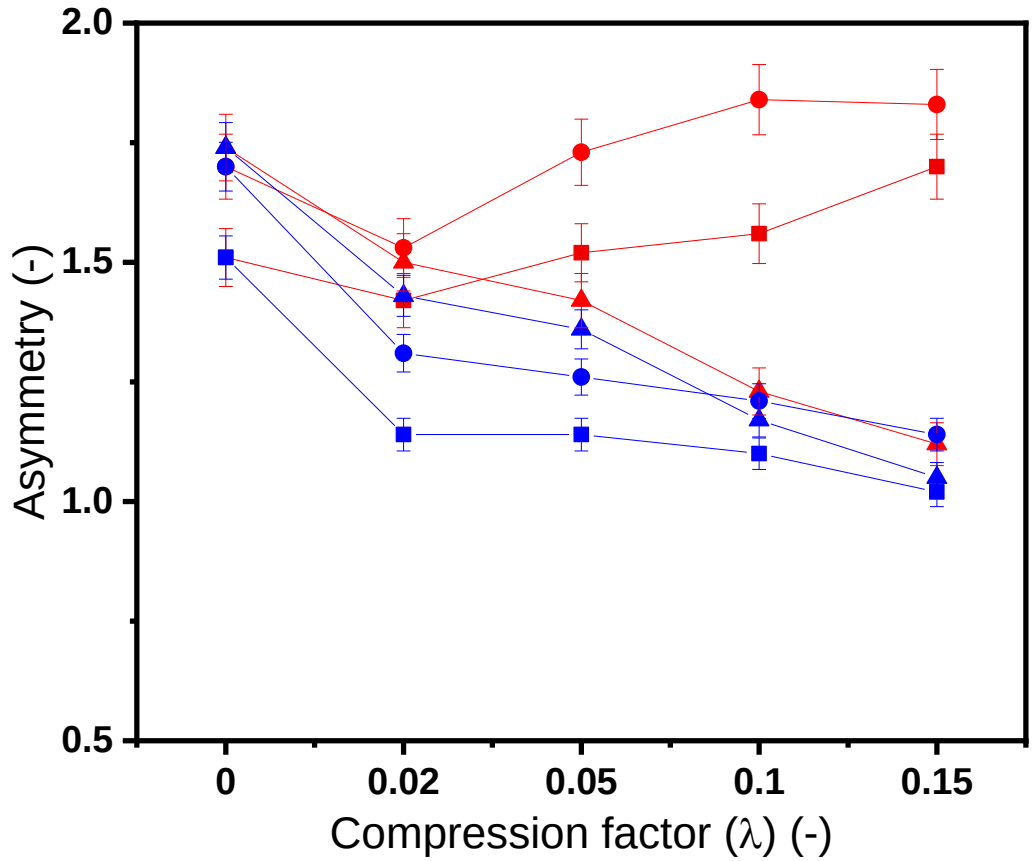

Figure 2-6 Comparison of hydrodynamic (red line) and mechanical (blue line) compression on asymmetry factor. Columns were packed with an internal diameter of 0.016 m and a bed height of 10 ± 0.1 cm with Sepharose FF (▪), Sepharose HP (●) and Capto Q (▲). Five different batches were used (A – E). Measurements were repeated three times with a relative standard deviation of less than 5% in all measurements.

Figure 2-7 shows the reduced plate height results of the three anion exchange resins under hydrodynamic and mechanic compression. The reduced plate height and asymmetry trends were similar characteristics, where Capto Q yet again showed superior column efficiency when compared with the softer resins.

Hydrodynamic compression via multiple incremental steps showed an increase of 50% in reduced plate height when $\lambda > 0.10$ for Q Sepharose FF and HP. It appears that the structures within the column change due to multiple sessions of high liquid flow-packing. This clearly has consequences in flow distribution and packing asymmetry resulting in poor column behaviour. Hydrodynamic compression allowed excess liquid to escape through the bottom end of the column, whereas mechanical compression allowed excess liquid to exit at the top. This leading to the differences in packing density down the column and hence to the destructive column behaviours.

In this next section, experiments were conducted in an attempt to explore the differences in the inner region of the column between the wall friction and interparticle friction which may influence the overall column efficiency of the column. For this reason, the packing behaviour under both hydrodynamic and mechanical compression were evaluated together with the asymmetry and plate height of DEAE Sephacel at pilot scale (BPG100/500). [DEAE Sephacel was kindly supplied by Ipsen Bioinnovation Ltd.] Further studies of the other resins at pilot scale are expensive and labour intensive so were not investigated.

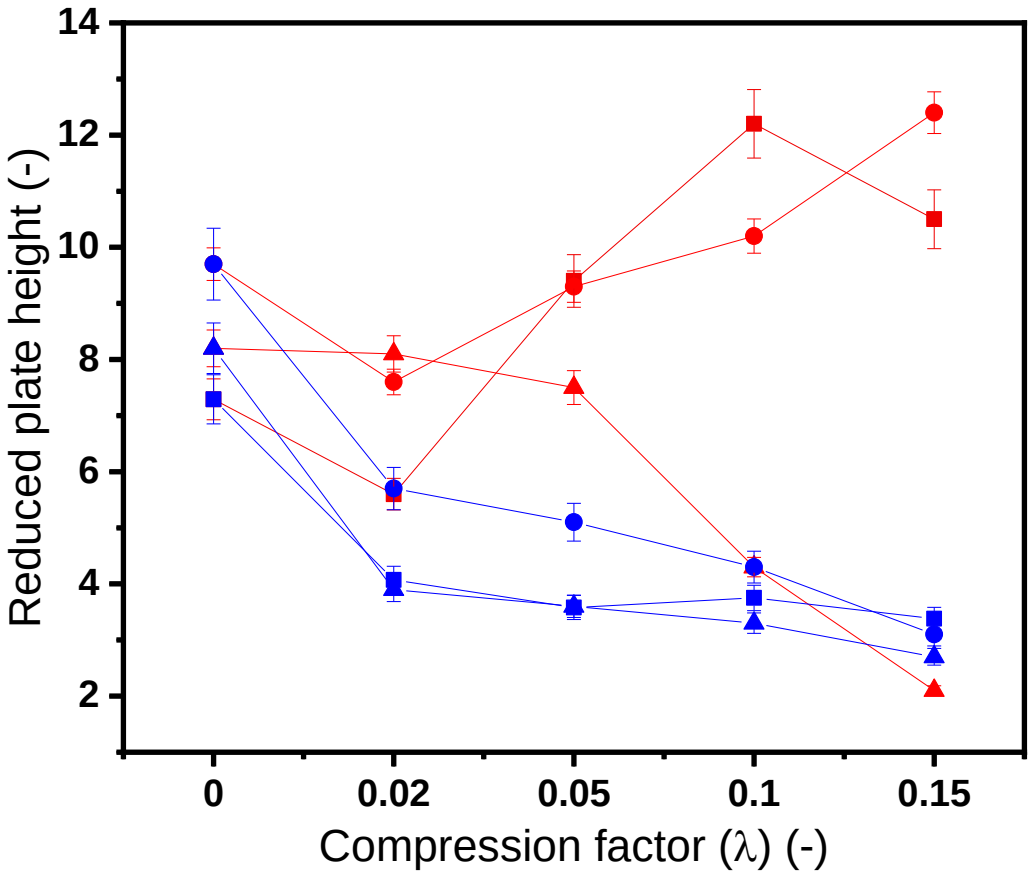

Figure 2-7 Comparison of hydrodynamic (red line) and mechanical (blue line) compression on reduced plate height. Columns were packed with an internal diameter of 0.016 m and a bed height of 10 ± 0.1 cm with Sepharose FF (▪), Sepharose HP (●) and Capto Q (▲). Measurements were repeated three times with a relative standard deviation of less than 5% in all measurements.

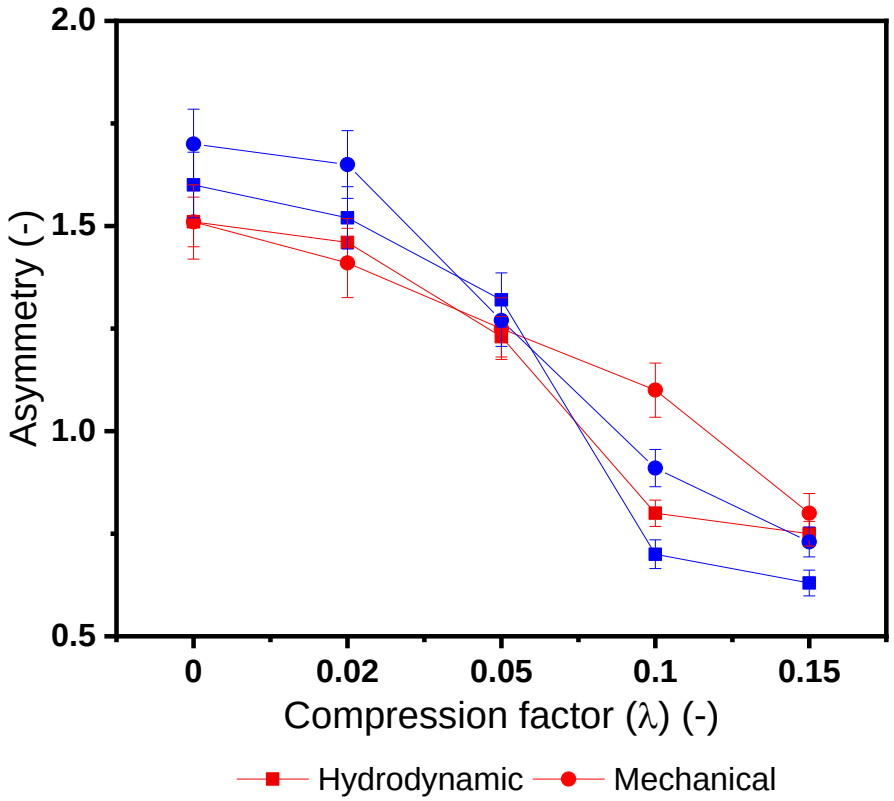

Figure 2-8 Effect of hydrodynamic (▪) and mechanical (●) compression on asymmetry at bench (XK16) and pilot scale (BPG-100/500). Columns were packed with DEAE Sephacel to a bed height of 10 ± 0.1 cm; (red line) XK16 (0.016 m I.D.); (blue line) BPG 100/500 (0.05 m I.D.).

Figure 2-8 shows the results for asymmetry of DEAE Sephacel at bench and pilot scale. Both methods of compression showed a decrease in asymmetry with increasing compression factor. The pilot scale data, indicated by the blue lines, suggested a greater degree of change compared to the bench scale studies for hydrodynamic and mechanical compression. At 0.15 CF, the asymmetry factor was lower at pilot scale (0.66) compared to bench scale (0.75). A lower asymmetry factor, suggests the column was more compressed. The degree of compression at the bottom of the column increases with increasing diameter (Keener *et al.* 2004). Wider columns allow more compaction of the column, by virtue of the diminishing the wall effect (Colby *et al.* 1996b; Fang 2010; Janson and Hedman 1982; Keener *et al.* 2004; Mohammad *et al.* 1992a).

Figure 2-9 shows reduced plate height data from hydrodynamic and mechanical compression at bench and pilot scales. Similar trends are shown for bench and pilot profiles depending on the method of compression. At both scales, optimum reduced plate heights were achieved at 0.05 CF for hydrodynamic compression and at 0.10 CF for mechanical compression. Data shows that bench scale studies achieved lower plate heights compared to pilot scale studies. As the bed diameter increases so the extent to which the column wall supports the bed material falls (Grier and Yakabu 2016; Tran 2011). This allows the impact of longitudinal forces down the column length to increase.

A lower reduced plate height was achieved for mechanically compressed columns at both bench and pilot scales. Mechanical compression provided greater uniformity and column efficiency at both scales. Hydrodynamic compression via multiple steps has repeatedly shown poorer packing quality indicated by broader peaks resulting in larger peak heights and asymmetry factors below 0.8. The negative effects of hydrodynamic compression were shown earlier at pilot scale, this is evident in both asymmetry and reduced plate height results (Figure 2-8 & Figure 2-9).

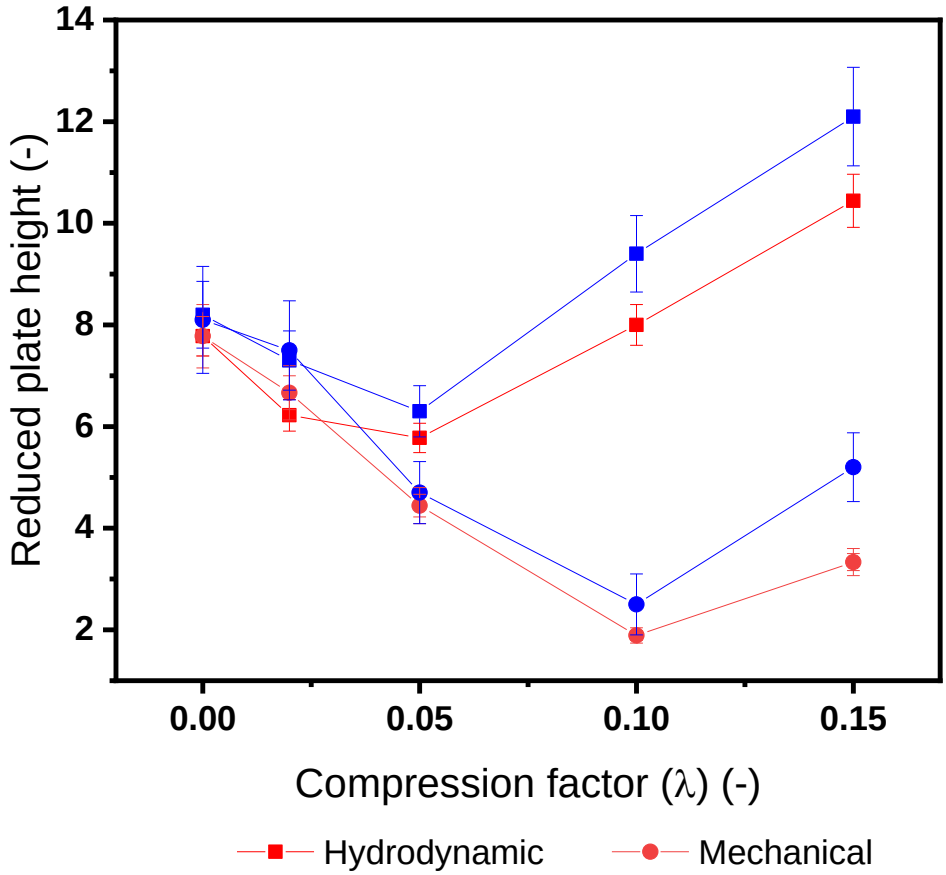

Figure 2-9 Impact of hydrodynamic (▪) and mechanical (●) compression on reduced plate height at bench (XK16) and pilot scale (BPG-100/500). Columns were packed with DEAE Sephacel to a bed height of 10 ± 0.1 cm; (red line) XK16 (0.016 m I.D.); (blue line) BPG 100/500 (0.05 m I.D.).

2.4 Conclusion

A careful and in-depth analysis of column efficiency using different packing methods were examined with a range of chromatography resins: Sepharose CL-6B, DEAE Sephacel, Q Sepharose FF, Q Sepharose HP and Capto Q. Mechanical compression led to a significant improvement in asymmetry and reduced plate height for both one-step and multiple step compression. Whereas hydrodynamic compression showed earlier signs of over-compression via multiple steps of high fluid velocity. Four anion exchange resins were studied with different matrix strengths. Five different batches of DEAE Sephacel were studied and showed the packing behaviour to be reproducible at both bench and pilot scales. Capto Q showed significant improvement under hydrodynamic and mechanical compression, whereas Q Sepharose FF and HP showed poor packing quality above 0.05 CF. The addition of dextran surface extender on Capto Q showed greatest benefit compared to all other resins. The factors affecting column efficiency are resin and packing strategy dependent.

3 Examination of the impact of hydrodynamic and mechanical compression on bed porosity

3.1 Abstract

The bed porosities of five chromatographic resins under hydrodynamic and mechanical compression at a range of compression factors were investigated. A detailed examination of different matrixes was conducted on: DEAE Sephacel, Q Sepharose FF, Q Sepharose HP, Capto Q and Sepharose CL-6B. Hydrodynamic compression gave significant problems at higher compression factors, with greatest changes to the level of intraparticle porosity. Mechanical compression showed less change in external and internal porosity across a greater range of resins. Results showed that larger resins, such as Q Sepharose FF, produced beds with a greater change in voidage space with increasing compression factor compared to smaller resins (Q Sepharose HP). The rigidity of a matrix will depend on a number of factors including the material from which the resin is made, the size and microscopic structure of the matrix particles, and hence the porosity of the beads. Columns packed with Capto Q under both hydrodynamic and mechanical compression had higher external and internal porosities comparable with the other resins due to its extra dextran surface giving additional matrix strength and hence bed support.

3.2 Introduction

Numerous studies of packing materials in analytical columns have been conducted; examining the effect of flow velocity and porosity distribution (Golshan-Shirazi and Guiochon 1989; Guan and Guiochon 1996; Koh and Guiochon 1998). Flow packing is a widely accepted and understood method of packing preparative chromatographic beds (Farkas *et al.* 1994). Efforts to understand pressure drop and flow velocity via hydrodynamic compression to predict the column performance is well documented (Chang 2011; Davies and Bellhouse 1989; Dorsey *et al.* 1998; Stickel and Fotopoulos 2001; Tran *et al.* 2007).

However, the availability of certain parameters to determine the degree of homogeneity within a column, such as porosity is still limited. Knox stated that a voidage space (ε) less than 0.3 is due to poorly packed columns (Koh, 1998). However,

little has been done to compare the effect of hydrodynamic and mechanical compression on bed porosity for a range of preparative chromatography resins. In preparative columns, voids are known to appear at the top of the column when insufficiently packed (Farkas *et al.* 1994). In addition, the theoretical understanding of the interparticle and intraparticle environment under mechanical compression of beads of differing rigidity are unknown (Dorn *et al.* 2017). It is well known that an evenly packed column is essential for flow velocity distribution and uniform sample concentration (Carta and Jungbauer 2010).

The packing homogeneity and interparticle interactions of preparative columns under different methods of compression need systematic investigation. This chapter examines the porosity of the bed when different methods of compressions are applied and also discusses the effects of particle size, rigidity and resin type on the levels of compression seen.

3.3 Material and Methods

3.3.1 Voidage, ε

The voidage, ε is the interstitial porosity of the packed bed (Hagel *et al.* 2008b; Jungbauer 2005). An excluded tracer (blue dextran) was used to measure the voidage at each level of compression. A loading volume of 2% column volume of 2 mg mL^{-1} Blue Dextran in 1 M NaCl was used.

Dextran is a glucose polymer of molecular weight 2×10^3 kDa with covalently attached reactive blue dye molecules. The volume in which the dextran elutes represents the void space between the resin particles. The voidage space was obtained by subtracting the mean extra column volume from the mean retention volume as determined by blue dextran (Koh and Guiochon 1998); (Hagel *et al.* 2008a).

3.3.2 Intraparticle porosity, ε_p

The intraparticle porosity was determined by injecting a pulse of 2% of the column volume of 2% v/v acetone and 2 mg mL^{-1} Blue Dextran. Intraparticle porosity, ε_p represents the porosity of the chromatography bead or particle and is determined

from the ratio of the pore volume to the total particle volume (Hagel *et al.* 2008c). The intraparticle porosity is defined as:

$$\varepsilon_p = \frac{EV_d - EV_a}{EV_a} \qquad \textbf{Eq. 3-1}$$

where EV_d is the elution volume of dextran and EV_a is the elution volume of acetone (Chiu *et al.* 2018). From these results, the intraparticle porosity was determined for all five resins under hydrodynamic and mechanical compression. Figure 3-1 shows typical dextran and acetone profiles used to determine the intraparticle porosity of resins.

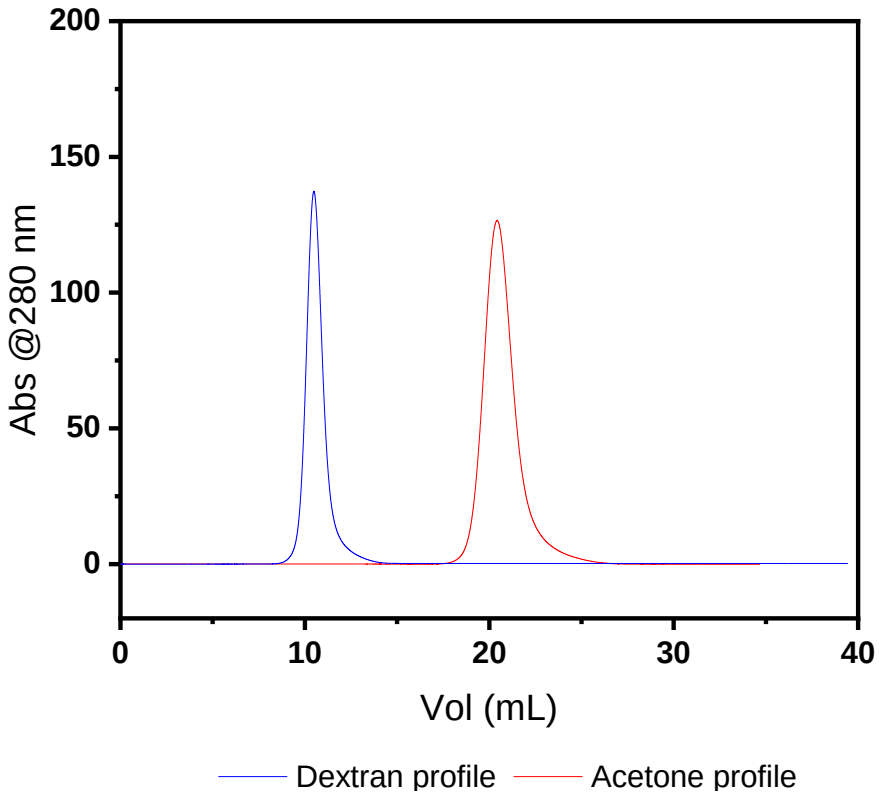

Figure 3-1 Summary of combined voidage and intraparticle porosity profiles of Sepharose CL-6B. Results obtained from the 2 mg mL^{-1} dextran blue and 2% v/v acetone determined by injecting a pulse of 2% of the column volume. Measurements were repeated three times with a relative standard deviation of less than 5% in all measurements. A XK16 column was used at a bed height of 20 ± 0.1 cm. Diagram of dextran and acetone profiles used to determine intraparticle porosity.

3.3.3 Particle Size Distribution (PSD)

The particle size distribution of the anion exchange resins were analysed using a Malvern Mastersizer 3000 laser sizer; (Malvern Instruments, Worcestershire, UK) which is able to detect particle size ranging from 0.01µm – 3500 µm. The particles were all assumed spherical. All solutions used in the analysis were filtered using 0.22 µm Stericup filter units (Merck & Co., Darmstadt, Germany) and the electrolytic buffers used for size-analysis were vacuum-degassed for 1 hr prior to use. Measurements were repeated three times with a relative standard deviation of less than 5% in all measurements.

3.4 Results and Discussion

3.4.1 Effect of compression on voidage

Having established the effects of hydrodynamic and mechanical compression on column efficiency, the next step was to evaluate and understand the effect of compression on bed porosity on five chromatography resins: Sepharose CL-6B, DEAE Sephacel, Q Sepharose FF, Q Sepharose HP, and Capto Q.

Figure 3-2 shows the variation in voidage as a function of both hydrodynamic and mechanical multiple incremental step compression for four anion exchange resins. As the compression factor increased, the voidage decreased. The voidage results are consistent with earlier work by Koh and Guiochon (Koh and Guiochon 1998), however only hydrodynamic compression was examined in that earlier study. Poor packing is defined when the voidage space $\varepsilon < 0.3$. A porosity of 0.5 – 0.6 is expected with randomly packed spheres under gravity settling (De Smet *et al.* 2005). When the bed is compressed to below a voidage space of 0.3, it is described to be less evenly packed and further compression can cause channelling within the column (Koh and Guiochon 1998).

At the highest compression factor under hydrodynamic compression, the voidage space for all four anion exchange resins fell below 0.3. When hydrodynamic compression was applied, stress on the stationary phase accumulates in the direction of flow culminating in greater compaction at the outlet of the column as seen with the anion exchange resins. This phenomenon is probably related to the non-uniform stress distribution as a result of over-compression inside the column, leading to uneven flow and band broadening (Stanley *et al.* 1996). Under hydrodynamic compression, high velocity flow passing through the adapter and frit can cause uneven currents to flow onto the fragile top of the column bed. This causes irregular patches of direct stress onto the column; reducing the homogeneity and permeability of the column (Dorn *et al.* 2017). Whereas, mechanical compression applies even pressure to the whole cross-section directly onto the surface of the bed, where excess liquid can escape from the top of the column, lessening the stress at the bottom of the bed. Distributing the pressure along the axial direction of the column therefore causes a uniform packed bed when compressed mechanically.

Interestingly, the softest resin (DEAE Sephacel) achieved a voidage space above 0.3 under both methods of compression. This is because DEAE Sephacel was flow packed at a lower velocity of 30 cm h^{-1} to avoid reaching maximum pressure of the resin. Whereas, the other resins were flow packed at a higher liquid velocity of 50 cm h^{-1}. This difference in velocity clearly affects the level of voidage space.

The overall change in voidage was highest for softer resins. For instance, DEAE Sephacel showed an overall change of 53% under hydrodynamic compression from 0.0 to 0.15 CF. By comparison to Capto Q showed an overall change of 34%. Capto Q (the harder resin) consistently showed a better voidage range due to it's additional dextran surface extender for additional rigidity. Capto Q maintained a bed voidage above 0.3 for both mechanical and hydrodynamic compression.

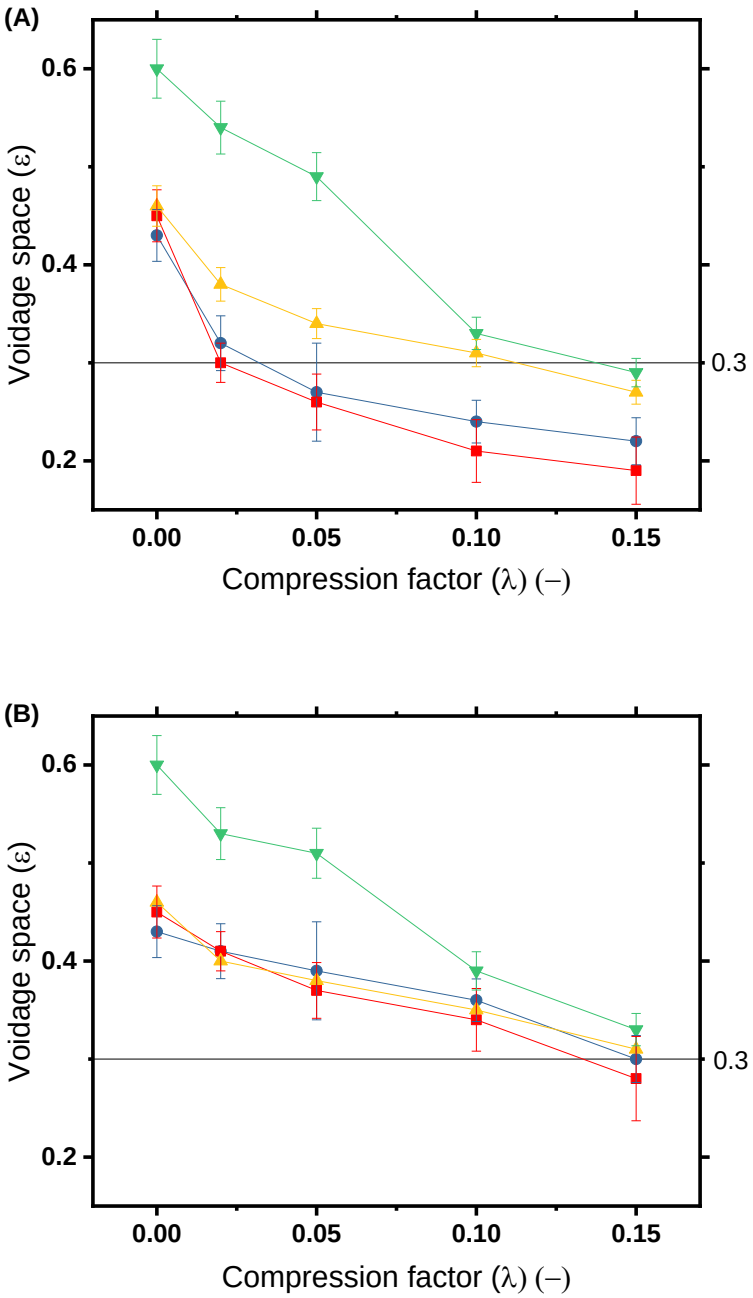

Figure 3-2 Examination of the impact of (A) Hydrodynamic and (B) Mechanical multiple incremental step compression on voidage space. Four anion exchange resins were examined; Q Sepharose Fast Flow (■), Q Sepharose High Performance (●), Capto Q (▲) and DEAE Sephacel (▼). A XK16 column was used at a bed height of 10 ± 0.1 cm. Poor packing is defined when the voidage ε < 0.3. Measurements were repeated three times with a relative standard deviation of less than 5% in all measurements.

Furthermore, the particle size distribution of the resins influenced the overall voidage space. Mechanical compression maintained a voidage space above 0.3 for three resins, expect for Q Sepharose FF. Compared with Q Sepharose HP, with a mean particle size of 34 µm, Q Sepharose FF has a mean particle size of 90 µm and has a broader particle size distribution, as seen in Figure 3-3. Broader particle size distribution behaves in a different way to monodisperse particles. Broader PSD can give smaller bed voidage as tiny particles fit in between gaps; this is one of the reasons why the voidage space decreases more rapidly with increasing compression factor with Q Sepharose FF (Koh and Guiochon 1998).

For Q Sepharose HP, under hydrodynamic and mechanical compression the voidage was higher compared to Q Sepharose FF, in particular above 0.3 under mechanical compression; poor packing is defined when the voidage $\varepsilon < 0.3$. Koh and Guiochon stated that columns packed with a tighter and uniform particle distribution showed a more homogenous packed bed during the compression process (Koh and Guiochon 1998). For Q Sepharose FF, larger particles will create larger gaps of voidage and result in uneven packing of the column (Sarker and Guiochon 1996).

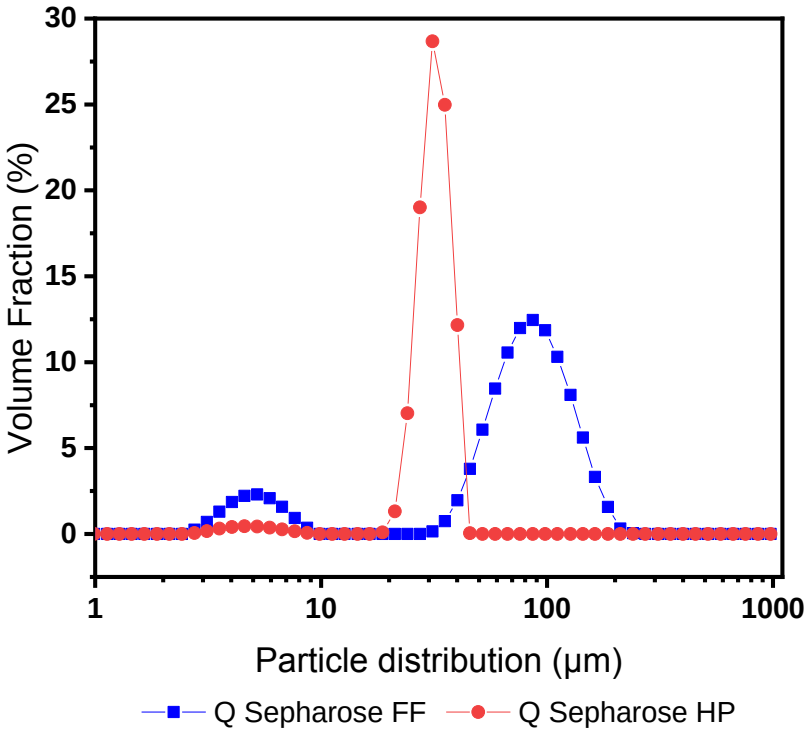

Figure 3-3 Comparison of the particle size distribution of Sepharose Fast Flow (▪) and Q Sepharose High Performance (●). The average bead diameter was determined using a Malvern 3000E Particle Sizer with Mastersizer 2000 control software under the conditions described in Section (3.3.3).

3.4.2 Effect of compression on intraparticle porosity

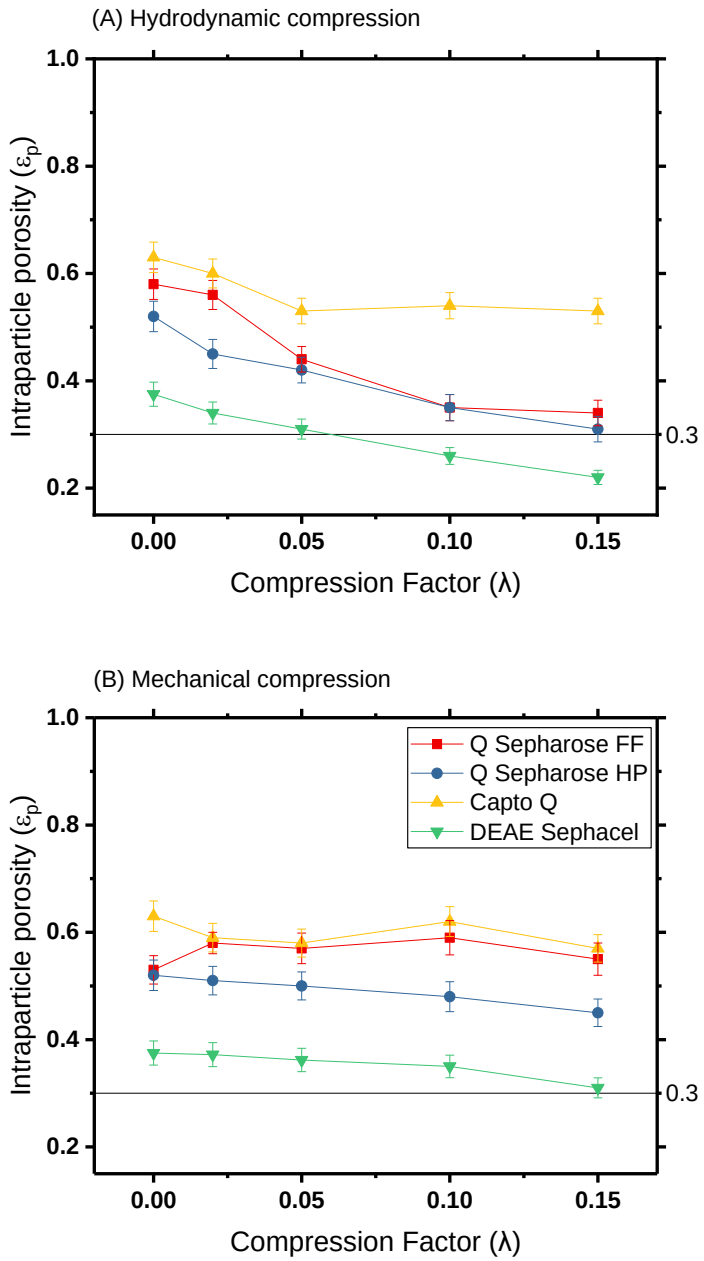

Figure 3-4 Examination of the impact of (A) Hydrodynamic and (B) Mechanical multiple incremental step compression on intraparticle porosity. Four anion exchange resins were examined; Q Sepharose Fast Flow (■), Q Sepharose High Performance (●), Capto Q (▲) and DEAE Sephacel (▼). A XK16 column was used at a bed height of 10 ± 0.1 cm. Measurements were repeated three times with a relative standard deviation of less than 5% in all measurements.

Figure 3-4 shows the intraparticle porosity as a function of compression factor of four anion exchange resins. By measuring the dextran and acetone elution profiles at different compression factors, the intraparticle porosity was calculated according to Eq. 3-1. At a 0.15 CF, hydrodynamic compression on DEAE Sephacel showed an intraparticle porosity below 0.3. When compared to the control, hydrodynamic compression showed a greater degree of change of 45%, compared to 23% under mechanical compression. This indicated the interior volume within the resins is influence more when a high fluid velocity is applied, whereas mechanical compression maintained the intraparticle porosity above 0.3. The main difference between these two types of compression is the application of stress. Fluid flow serves to accumulate stress in the direction of flow suggesting a higher degree of compaction at the outlet of the column. Mechanical compression by contrast allows the excess liquid to escape from the top of the bed easing tension from the already densely packed bottom of the bed.

Mechanical compression showed intraparticle porosities above 0.3 for all resins. In preparative columns, voids are known to appear at the top of the column when insufficiently packed (Farkas *et al.* 1994). The additional downward force on the upper regions of the column caused by the movement of the top adapter resulted in more homogenously packed beds. As previously discussed, this method of compression has shown to improved column efficiency as captured in reduced plate height and asymmetry. By applying pressure mechanically, the morphology of the resins appears to remain intact while only reducing the voidage spaces, resulting in a more evenly compacted bed.

Capto Q showed stable values of intraparticle porosity of above 0.45 at 0.15 compression factor under both hydrodynamic and mechanical compression. This result was as expected, considering the extra dextran support on Capto Q providing a stronger matrix compared to the other strong anion exchange resins (Q Sepharose FF and Q Sepharose HP) which were made with only 6% cross-linked agarose (Pezzini *et al.* 2009). As a result, Capto Q can withstand higher pressures. In the case where compression is applied above the recommended pressure drop, over-compression or mechanical shocks can cause further collapses, especially with columns of longer lengths (Koh and Guiochon 1998) (Nweke *et al.* 2017).

3.4.3 Influence of compression on Sepharose CL-6B

Table 3-1 Summary of voidage space and intraparticle porosity of Sepharose CL-6B under hydrodynamic and mechanical multiple incremental step compression. Results obtained from the dextran blue and acetone elution profile data with Sepharose CL-6B. Measurements were repeated three times with a relative standard deviation of less than 5% in all measurements. A XK16 column was used at a bed height of 20 ± 0.1 cm.

Compression factor (λ)	Voidage space (ε)		Intraparticle Porosity (ε_p)	
	Hydrodynamic	Mechanical	Hydrodynamic	Mechanical
0.00	0.41	0.41	0.63	0.63
0.02	0.37	0.39	0.60	0.60
0.05	0.33	0.36	0.58	0.63
0.10	0.29	0.33	0.57	0.62
0.15	0.26	0.31	0.54	0.60

Mechanical compression led to a decrease in voidage but no discernible effect on intraparticle porosity. The voidage data is consistent with earlier work (Davies and Bellhouse 1989). It is believed that pore diffusion is enhanced as voidage within the column falls (De Smet *et al.* 2005). This allows for greater surface area for diffusion between the resins and analytes to be presented to the molecules (Balke *et al.* 1969; Chang *et al.* 2012). The consistent intraparticle porosity even under significant levels of mechanical compression may be explained by considering the elastic properties of the agarose material. Porosity moved from about 0.4 at no compression to 0.3 at a compression factor of 0.15 with mechanical compression. A porosity of 0.4 – 0.5 is expected with randomly packed spheres under gravity settling (De Smet *et al.* 2005). When hydrodynamic compression is applied, stress on the stationary phase accumulates in the direction of flow indicating greater compaction at the outlet of the column as seen with the anion exchange resins. In addition, different regions of voidage space, particularly at the top of the column, result in uneven flow distribution when hydrodynamic compression is applied. In contrast, under mechanical compression, pressure is applied to the entire cross-section at the top of the bed. This gives an opportunity to compress further the top regions with larger voidage to create a more uniform packed bed along the length of the column. This allows for a more even distribution of pressure along the length of the column when mechanical compression is used compared with hydrodynamic compression.

Insights of the location of voidage spaces have been gained using static magnetic resonance imaging (MRI) (Keener *et al.* 2004; Yuan *et al.* 1999). Others have reported that the void fraction is lower near the column wall than in central and upper regions of the column for gel filtration resins (Yuan *et al.* 1999). In addition, near-wall packing may be a possible source of poor performance under hydrodynamic compression, since uneven pressure across the cross-section may cause an uneven velocity distribution, particularly at higher flow rates.

This study suggests that compression achieved by applying pressure through the movement of the top adapter results in a better quality of packing. The fact that the voidage decreases means that interparticle distances are reduced and hence diffusion is expected to rise.

3.5 Conclusion

The bed porosities of five chromatographic resins under hydrodynamic and mechanical compression at a range of compression factors were investigated. Examining bed porosities gives additional information about the packing structure of the whole column. A detailed investigation of different matrixes were studied on DEAE Sephacel, Q Sepharose FF, Q Sepharose HP, Capto Q and Sepharose CL-6B.

By looking at the voidage and intraparticle porosity of resins under different methods of compression, the data suggests that bed porosity is highly dependent on the choice and composition of the matrix material and to the application of axial pressure force upon the inlet of the bed. This is because the rigidity of a matrix will depend on a number of factors including the material from which the resin is made, the size and microscopic structure of the matrix particles, and hence the porosity of the beads.

As the data suggests, the packing behaviour and the stability of a particle is greatly influenced by the method of compression. Based on the porosity results, the voidage and intraparticle porosity were less impacted when mechanical compression was applied. Hydrodynamic compression produced greatest changes in the intraparticle porosities with larger (Q Sepharose FF) and softer resins (DEAE Sephacel). The results indicate that the shape of the resins deformed when porosities fell below 0.3. Columns packed with Capto Q under both hydrodynamic and mechanical compression

exhibited higher external and internal porosity values when compared with the other resins most likely due to its extra dextran surface giving addition matrix strength and hence bed support.

Bed porosities are strongly influenced by the level of bed compression as well as the method by which compression is applied. Examining bed porosities gives addition information about the packing structure of the whole column. There is a need to understand further the effect of different methods of compression beyond examining bed porosity along the whole bed. The next chapter aims to investigate the phenomenon of band broadening effects along the separate axial sections of a chromatography column to elucidate changes in the internal structure not describable from a gross average determination.

4 Quantifying the dispersive effects of hydrodynamic and mechanical compression along the axial sections of the chromatographic bed using an extended reverse flow technique

4.1 Abstract

This chapter discusses the development of a reverse-flow technique designed to examine band broadening in different axial sections of the chromatography column. The experimental protocols utilising reverse-flow technique have been described in detail in numerous publications (Kamiński 1992; Kamiński *et al.* 1982; Moscariello *et al.* 2001; Siu *et al.* 2014). This chapter describes the development of an experimental methodology that characterises microscopic dispersion and band broadening in order to characterise the homogeneity of the chromatographic column packing. The results show that hydrodynamic packing achieves evenly packed columns more rapidly, though over-compression will occur earlier, particularly at the bottom of the bed. Over-compression will occur in the top section of beds packed via mechanical compression due to the increasing force from the top adapter. This phenomena is seen with softer resins (Q Sepharose FF and DEAE Sephacel), where Q Sepharose HP (2 - 3 times smaller resin) was less effected at a compression factor of 0.15. Capto Q (hardest resin examined) showed consistent equal proportions in microscopic dispersion across the bed, even at high levels of compression. The results illustrates that compression can improve bed uniformity, although the effect of compression is resin dependent and favours stronger more rigid resins.

4.2 Introduction

During the last decades, considerable effort has been devoted to the improvement of chromatographic performance. Effort has been focused to the understanding and prediction of column hydrodynamics; correlation of the pressure drop and the influence of compression on the packing structures were previously studied (Hekmat *et al.* 2013; Müller *et al.* 2005; Sarker and Guiochon 1996; Yew *et al.* 2003).

However, conventional methods used in industry for diagnosing the condition of a packed bed column only provide an indication of the overall condition of the column, as described in Chapters 2 and 3. Column efficiency and porosity tests will not necessarily identify the location where the effects of compression are most severe or

illustrate where the packing differences between mechanical and hydrodynamic compression reside. This missing information can be vital during process development and when designing packing protocols to mitigate excessive compression effects. This chapter sets out to examine a simple, non-destructive technique that can access the structure within a packed column based on band broadening effects due to over-compression which cannot be gained by using traditional techniques.

Poorly packed columns can lead to subsequent loss of product yield, as columns may need to be repacked or even completely replaced. In industry, methods of column packing vary and different packing methods and conditions results in beds with different structural characteristics (Kaminski et al 1982, Klawiter *et al.* 1982, Guiochon et al 1997). Guiochon (1997) pointed out that both axial and radial inhomogeneity depends on the packing method applied. It is well known that packing homogeneity is required for uniform sample concentration and flow velocity distribution. It was shown that HETP (Height Equivalent to Theoretical Plate) values vary along the column when radially compressed (Guiochon and Sarker 1995). Hence, it is established knowledge that the chromatographic packing exhibits intrinsic consolidation dynamics during column operation that is governed by particle rearrangement and migration as described by Guiochon and Kaminski (1995). In recent studies, packing homogeneity along the chromatographic column was analysed using the reverse flow technique when fouled with BSA (Siu *et al.* 2014). The reverse flow technique indicated the amount of fouling material was shown to greatly influence the overall dispersive effects especially at the top section of the column. However, understanding the impact of hydrodynamic and mechanical compression and its influence on packing structures along the column is still limited.

Two separate methodologies have been shown to have the ability to analyse the levels of dispersion along different axial sections within the column. The first being an extended reverse-flow technique using an acetone tracer to quantify the dispersive effect of compression (Kamiński 1992) and the second being the use of computational fluid dynamic (CFD) (Billen *et al.* 2005). In summary, the advantage using reverse-flow technique over CFD is that it allows quick and easy evaluation of column packing without the need to expensive equipment and programming expertise.

In this thesis, the compression factor was the main parameter used to set the desired bed height of the column. It was also imperative that the reverse-flow technique was automated to enable one to study the multiple experimental conditions and reduce manual handling. In addition, automation can reduce error from experiment to experiment, hence results can be compared using the same method with confidence.

The key to the reverse-flow technique is the reversible quality of macroscopic flow maldistribution. Under low Reynolds number (Re), the flow in such chromatography systems are proportional to velocity and by reversing the driving pressure the fluid element would retrace its path in the opposite direction (Bird 2002).

$$\boldsymbol{Re = \frac{d_p v \rho}{\mu} \ll 1} \qquad \textbf{Eq. 4-1}$$

where d_p is the diameter of the chromatographic bead, v is the interstitial fluid velocity, ρ is the density of the fluid and μ is the viscosity of the fluid. When referencing the Blake-Kozeny equation (Eq. 4-7).

Bird et al. (2002) also states,

> "All contributions to the plate height in one-dimensional models are localized to the size scale of the packing particle diameter are irreversible, whereas fluid motion on a size scale of the particle diameter is reversible".

$$\boldsymbol{\frac{dP}{dL} = \frac{150\,\mu}{d_p^2}\,\frac{(1-\varepsilon)^2}{\varepsilon^3}\,.\,v} \qquad \textbf{Eq. 4-2}$$

where dP is the pressure drop, L is the total height of the bed, μ is the viscosity of the fluid, d_p is the diameter of the chromatographic bead, ε is the porosity of the bed, and v is the interstitial fluid velocity. The usefulness of the reverse flow techniques is that macroscopic disturbances are eliminated when the flow is revered and microscopic variances are simply doubled (Moscariello et al. 2001). If a pulse of tracer was introduced into the system in the normal (down-flow) direction until it has reached the desired section of the bed, the flow can be reversed and the distribution of the tracer peak measured. Any effects due to macroscopic flow variations would have been eliminated.

The heterogeneity of a packed bed consisting of particles is quantified by the particle dispersion of the mobile phase flowing through the packed bed. The $\sigma^2_{micro,total}$ describes the heterogeneity of the bed and can be isolated into different sections.

4.3 Materials and Methods

4.3.1 Chromatography system

A bench-scale column with adjustable column length and inner diameter of 1.6 cm (model XK16, GE Healthcare, Uppsala, Sweden) was used. This was operated on an AKTA Pure (GE Healthcare, Uppsala, Sweden) pumping and monitoring apparatus. The control software UNICORN 6.0 (GE Healthcare, Little Chalfont, Buckinghamshire, UK) was used.

4.3.2 Stationary phases

Three strong anion exchangers (quaternary amine) were investigated; Q Sepharose Fast Flow, Q Sepharose High Performance and Capto Q (GE Healthcare Uppsala, Sweden). Both Q Sepharose resins are highly cross-linked agarose beads, whereas Capto Q has an additional dextran surface extender. Both Q Sepharose FF and Capto Q have a particle size, d_p of ~ 90 µm, whilst Q Sepharose HP has a size distribution of average particle size, d_p of 34 µm (quoted by the manufacturer).

Studies were also carried out on a weak anion exchanger; DEAE Sephacel (GE Healthcare Uppsala, Sweden). The resin has a cross-linked cellulose structure with a diethylaminoethyl functional group. The average bead diameter was determined to be, d_p = 96 µm ± 5 µm using a Malvern 3000E Particle Sizer with MastersizerTM 2000 control software (Malvern Mastersizer 3000 laser sizer; Malvern Instruments, Worcestershire, UK). Five different lot batches of DEAE Sephacel were examined to investigate the consistency and reliability of the experiments.

4.3.3 Packing procedure

All resins were made up to 80% (w/v) slurry in a 50 mL measuring cylinder. The total slurry volume was calculated based on achieving a desired gravity settled bed height of 10 cm. The slurry was poured into the column and allowed to gravity settle

overnight. The adapter was lowered into the supernatant to start the flow pack. The column was then compressed as described in Section (2.2.8).

4.3.4 Reverse flow methodologies

For all experiments the column bed height was divided equally into five sections. In this procedure, an XK16 column at 10 cm bed height was used. Pulse experiments were carried out at a linear flow rate of 0.5 cm min^{-1} using a 2% CV injection of 2% v/v acetone tracer. This procedure was applied using a V-7 sample injector with a 100 mL loop. Each column was equilibrated with 3 CV of ultrapure water (typically at 18.2 MΩ cm at 25 ℃) until neutral pH was reached. The UV detector was set to measure absorbance at 280 nm. The general procedure of the reverse-flow technique used is given in Figure 4.1.

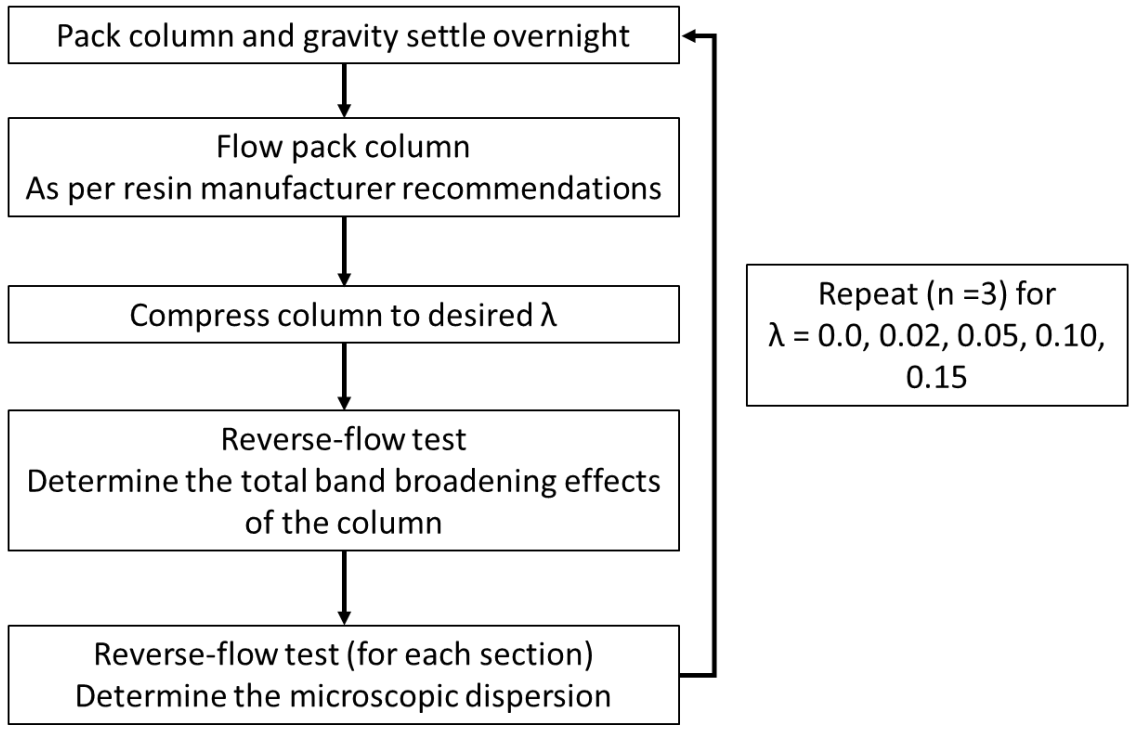

Figure 4-1 Outline procedure for the extended reverse-flow technique.

4.3.5 Determining Extra-column effects

Extra column effects can be subdivided into contributions arising from: dispersion in tubing, dead volumes within the system and finite volumes within the detectors. The total extra-column broadening can be expressed as (Kaltenbrunner *et al.* 1997);

$$\boldsymbol{\sigma_{ex}^2 = \sigma_s^2 + \sigma_t^2 + \sigma_d^2 + \tau_{dead}^2} \qquad \textbf{Eq. 4-3}$$

where σ_{ex}^2 is the cumulative extra-column effect, σ_s^2 is the variance of the initial injection profile, σ_t^2 is the tube broadening effect, σ_d^2 is the finite sensing volume of the detector, and τ_{dead}^2 is the exponential broadening introduced by the dead volumes (Cramers *et al.* 1981).

The extra column dead volume was kept to a minimum by using 0.12 mm I.D. capillary tube to connect the column to the injector. To calculate the dead volume of the system, the tubing leading to the top column was attached directly to the UV detector via a tubing piece of known volume. Subsequently, 20 micro L of 2% v/v acetone tracer was injected to the system at 0.5 mL min-1. By subtracting the known volume of the connecting tube from the retention volume reading of the eluted acetone pulse, the void volume of the system in downward flow mode was determined. The tubing connecting the top and bottom flow adapters in the XK16 columns were also taken into account by disconnecting them from the column and connecting them to the experimental set-up when determining their dead volumes.

4.3.6 Determining the total band broadening effects

For the total chromatographic system, the band broadening was measured at the outlet of the column defined as:

$$\boldsymbol{\sigma_{total}^2 = \sigma_{ex}^2 + \sigma_{macro,total}^2 + \sigma_{micro,total}^2} \qquad \textbf{Eq. 4-4}$$

where σ_{total}^2 relates to the total cumulative variance, σ_{ex}^2 relates to the extra-column effects, σ_{macro}^2 relates to the macroscopic factors, and σ_{micro}^2 relates to the microscopic factors.

A 2% v/v acetone tracer was performed using a 100 mL loop at the sample value of the AKTA system. The acetone pulse was eluted through the column (compressed or uncompressed) in downward flow (refer Section 4.4.3). The mean solute residence time of the acetone peak was determined and the dead volume of the column was calculated. This was necessary in order to calculate the elution volume required to bring the acetone pulse from the injection valve to the specific sections along the column.

4.3.7 Determining the total microscopic dispersion

Since Eq. 4-4 can be experimentally determined, it was possible to calculate $\boldsymbol{\sigma^2_{micro,total}}$. The $\sigma^2_{micro,total}$ describes the heterogeneity of the bed and can be isolated into different sections according to:

$$\boldsymbol{\sigma^2_{micro,total}(t) = \frac{1}{N}\sum_{i=1}^{N}(v_{z,i}(t) - v_z(t))^2} \qquad \textbf{Eq. 4-5}$$

where N is the number of sections, $\boldsymbol{v_{z,i}(t)}$ is the variance attributed to the system in reverse flow at time t averaged over all sections, and $\boldsymbol{v_z(t)}$ is the variance attributed to the section of interest in reverse flow at time ($\boldsymbol{t}$). The direction of flow (downward or upward) was controlled using the in-built function on the UNICORN 6.0 software. The acetone pulse was applied downward flow until the desired section along the axial column was reached at which point is time the direction of flow was reversed (upward flow) causing the acetone pulse to leave the column from the inlet. A peak was then generated within 30 minutes. The resulting acetone peak was analysed in terms of residence time distribution.

A key advantage of the AKTA Avant as a delivery system was that it enabled precise control and automation over the direction of flow along the column. Furthermore, it had the utility of continually generating feedback for all axial sections along the column at each compression factor. With this functionality, the reverse flow technique examines the effect of microscopic dispersion in five equally divided sections of the column under hydrodynamic and mechanical compression. The relationship between dispersion as it varies along the column and the overall level of compression can be

better understood. Figure 4-2 illustrates a diagram representing the five equally divided sections within the column.

A key advantage of the AKTA Avant as a delivery system was that it enabled precise control and automation over the direction of flow along the column. Furthermore, it had the utility of continually generating feedback for all axial sections along the column at each compression factor. With this functionality, the reverse flow technique examines the effect of microscopic dispersion in five equally divided sections of the column under hydrodynamic and mechanical compression. The relationship between dispersion as it varies along the column and the overall level of compression can be better understood. Figure 4-2 illustrates a diagram representing the five equally divided sections within the column.

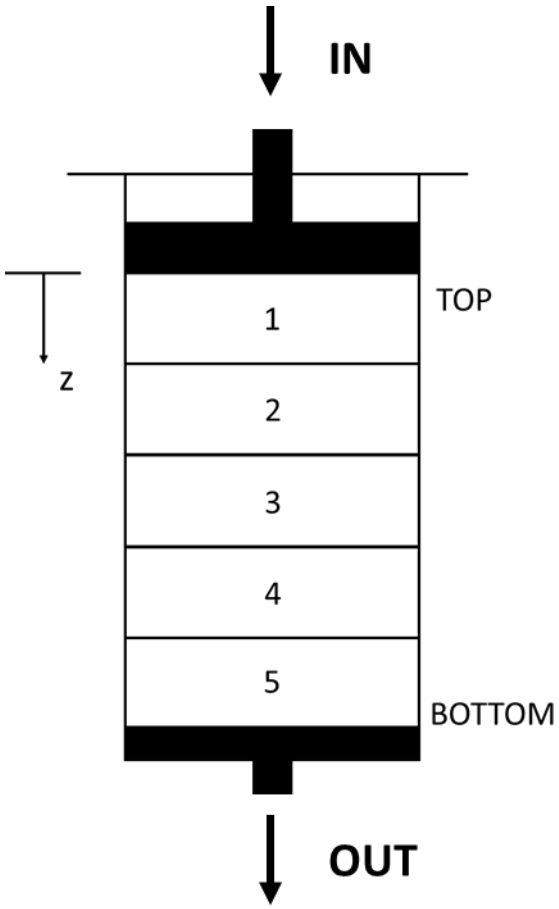

Figure 4-2 Diagram illustrating the five equally divided sections of the column to show the effects of microscopic dispersions.

Prior to compression, large voidage spaces are known to appear in the top section meaning the column is likely to be loosely packed (Yuan *et al.* 1999). With mechanical and hydrodynamic compression, these voidage spaces decrease (as described in Chapter 3) leading towards a column which is more densely and hopefully more uniformly packed. Evidence have shown that well packed columns under compression lead to improved protein separation (Kong *et al.* 2018) and column efficiency (Edwards and Helft 1970) for size exclusion resins, however little is known for AEX resins of different morphologies (particle size and rigidity). Nevertheless, over-compression is undesirable as channelling can occur and unevenly packing can lead to greater band broadening effects. This chapter examines the effects of hydrodynamic and mechanical compression on the microscopic dispersions across the whole column and along different sections within the column, with the aim to understand where band broadening is likely to occur for AEX resins with varying morphologies.

4.4 Results and Discussion

4.4.1 Examining the total band broadening effect

Before analysing the microscopic dispersions of individual sections along the column, the total microscopic dispersion was determined. Reverse-flow experiments were conducted to determine the total microscopic dispersion, σ^2_{total} to measure the total band broadening effects as a function of hydrodynamic and mechanical compression for four anion exchange resins. Figure 4-1 shows that the level of total band broadening decreased for both methods of compression, however band broadening increased when hydrodynamic compression was applied above 0.05 CF for Q Sepharose FF and DEAE Sephacel. Q Sepharose HP showed increasing band broadening at a higher level of 0.10 CF, whereas Capto Q indicated the lowest levels of microscopic dispersion at 0.15 CF. Both Q Sepharose HP and Capto Q displayed greater tendencies to withstand band broadening effects compared with Q Sepharose FF and DEAE Sephacel. Since Q Sepharose HP is smaller in size compared to Q Sepharose FF the results possibly indicate that a smaller particle diameter can resist higher hydrodynamic force while achieving a more densely packed bed. Capto Q is similar in size compared to DEAE Sephacel and Q Sepharose FF, however it has a stronger matrix able to withstand higher pressures from both hydrodynamic and mechanical compression, allowing a well-packed bed to form.

The data from mechanical compression suggests a similar linear decrease for all four resins below a compression factor of 0.15. Mechanical compression gave a higher level of consistency compared to hydrodynamic compression. This gives evidence that mechanical compression produces well-packed columns over a wider range of compression for the four resins tested. Softer and larger particle sized resins, i.e. DEAE Sephacel, Q Sepharose FF still achieved higher microscopic dispersion compared to Capto Q, suggesting that particle size and morphology plays an important factor at high levels of compression, where less consistency is seen under hydrodynamic compression. This feature is most likely due to the inconsistent distribution of flow via the inlet adapter resulting in uneven flow onto the column bed.

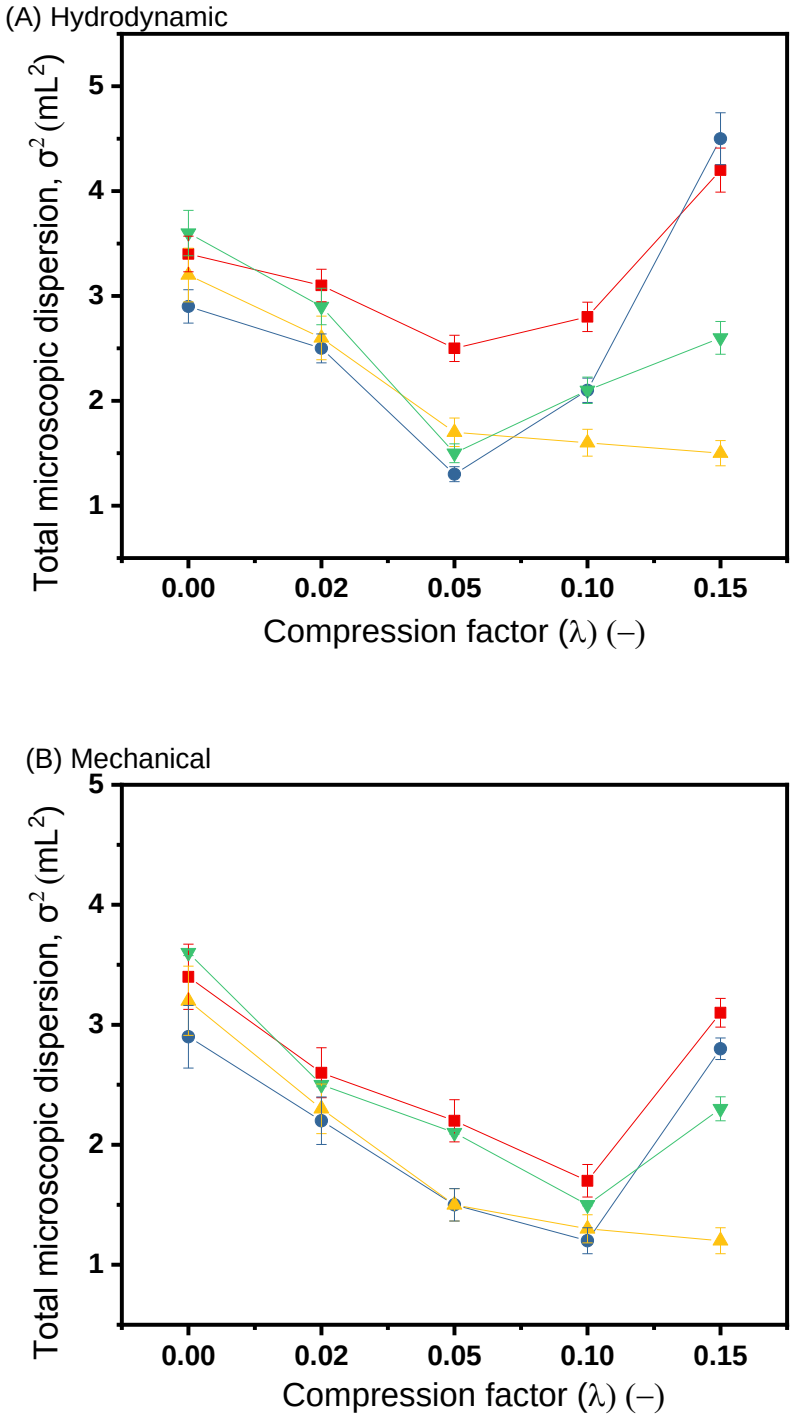

Figure 4-1 (A – B) Examination of total microscopic dispersion as a function of compression factor λ; (A) hydrodynamic compression and (B) mechanical compression. Four anion exchange resins were used; Q Sepharose Fast Flow (■), Q Sepharose High Performance (●), Capto Q (▲) and DEAE Sephacel (▼). A XK column was used at a bed height of 10 ± 0.1 cm at 0.0 CF. Measurements were repeated three times with a relative standard deviation of less than 5% in all measurements.

In general, these results confirm that the total microscopic dispersion was lower under compression. Greater band broadening effects are seen at high levels of compression under both methods of compression, except for resins with a strong matrix base; Capto Q. The next section looks at the evolution of the microscopic dispersion along the axial sections of the column to help understand where the column is likely to be over compressed and to measure band broadening across the bed.

4.4.2 Examining microscopic dispersion along the column

Q Sepharose FF

Running in reverse-flow mode allows isolation of the band broadening effects. This next section shows the measured axial microscopic dispersion profiles for Q Sepharose FF and DEAE Sephacel (two of the softer resins examined) under (A) hydrodynamic and (B) mechanical compression. By using the reverse flow technique at set sections along the axial length of the column, the microscopic factors within a column were calculated according to Eq. 4-8.

Figure 4-3 shows the microscopic dispersions within the column for Q Sepharose FF, it can be seen that both packing methods exhibited different band broadening behaviour. Compressing the slurry material resulted in a homogeneous packing in the axial direction between 0.5 – 0.10 CF, where the microscopic dispersion percentages ranged from 18 – 22%, practically uniform throughout the packed bed. Notably the lowest overall total band broadening effects were also in the range between 0.5 – 0.10 CF for both hydrodynamic and mechanical compression (refer to Figure 4-1).

Talking just the data at 0.15 CF, greater differences between the top and bottom sections are seen when comparing the two methods of compression. For hydrodynamic compression, the microscopic dispersion showed the highest contribution at the bottom section (30%) than in the top section (13%). This disparity in microscopic dispersion suggests over-compression occurred towards the bottom of the column as the tracer took longer to diffuse through the bottom section. At high levels of compression, greater differences in microscopic dispersion along the column were detected. This suggests uneven band broadening effects along the column, resulting in poorer intraparticle diffusion and interparticle dispersion throughout the column as discussed in Chapter 3. These later experiments shed useful mechanistic insights on the earlier phenomenological results.

By contrast, mechanical compression resulted in higher levels of microscopic dispersion in the top of the column (27%) at 0.15 CF. This difference in mechanical compression indicates that over-compression occurs at the top of the column.

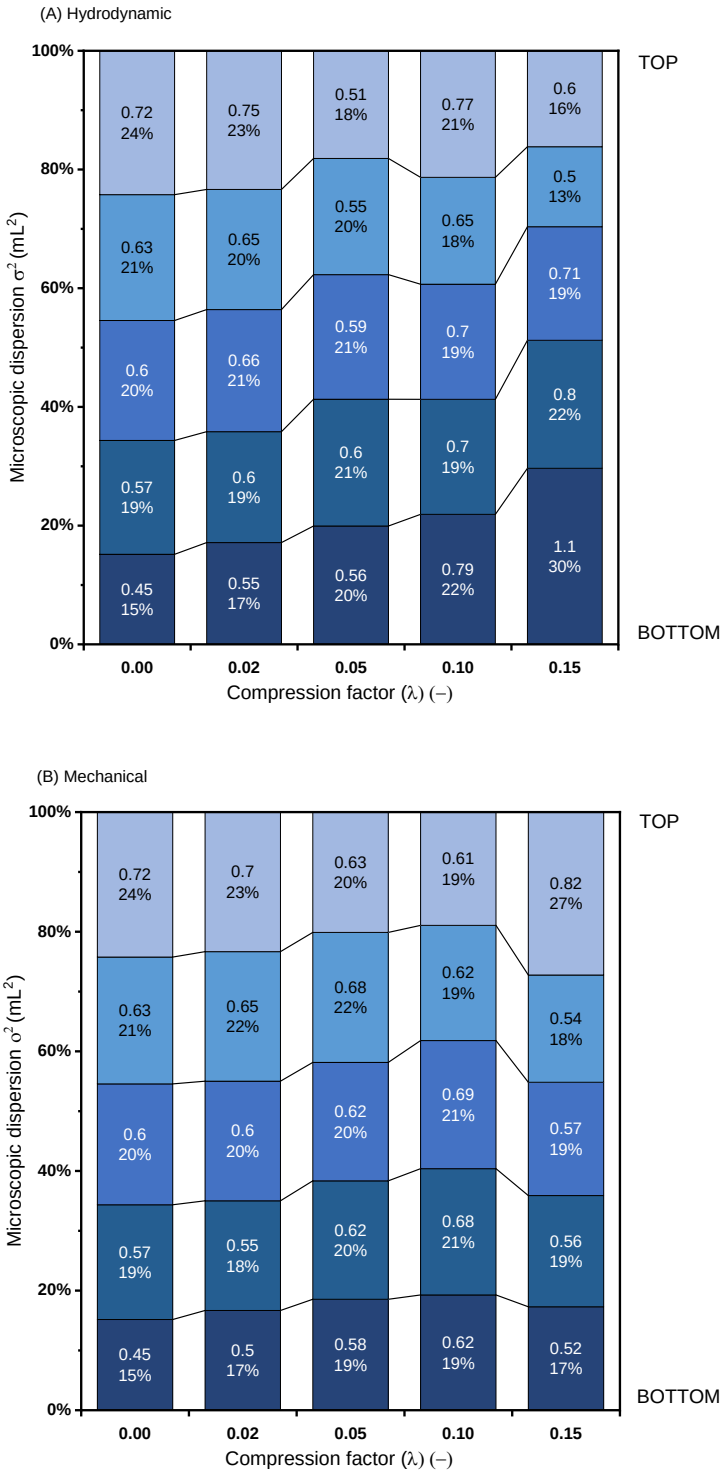

Figure 4-3 Examining the effect of (A) hydrodynamic compression and (B) mechanical compression on the contribution of microscopic dispersion by reverse flow technique on Q Sepharose FF. A range of five equally divided sections along the column was analysed. A XK16 column was used at a bed height of 10 ± 0.1 cm at 0.0 CF. Measurements were repeated three times with a relative standard deviation of less than 5% in all measurements.

A reverse trend in packing phenomenon was observed when mechanical compression was applied. A greater degree of band broadening occurred in the top section of the column, where the microscopic dispersion is highest. This can be attributed directly to the differences in packing methods. Under hydrodynamic compression, a high liquid force is applied throughout the column where fluid escapes through in the outlet valve. However, at the highest compression factor, further compression is expected at the already densely packed bottom section of the bed due to the previous application of compression, adding cumulative pressure towards the end of the column. Mechanical compression uses physical force applied directly to top section where larger voidage space are known to appear (Yuan *et al.* 1999), also where excess liquid can escape through the inlet valve lessening the pressure in the bottom of the column.

For mechanical compression, the highest microscopic dispersion data recorded was 0.82 mL^2 when compared with hydrodynamic compression at 1.1 mL^2, suggesting hydrodynamic compression enforces greater microscopic dispersion for Q Sepharose FF at high levels of compression. In the next part of the study, we will examine the effects of compression on microscopic dispersion in beds of softer AEX resin, DEAE Sephacel were studied.

DEAE Sephacel

Figure 4-2 shows the isolation of microscopic dispersion within a column packed with DEAE Sephacel under (A) hydrodynamic and (B) mechanical compression. Prior to compression, the top section of the column had slightly higher levels of microscopic dispersion compared to the bottom section of the column. After compressing the column, the microscopic dispersion showed approximately equal dispersion under hydrodynamic compression at 0.05 CF, ranging from 0.52 – 0.58 mL^2 (19 – 21 %). In contrast, mechanical compression indicated larger disparities of microscopic dispersions at 0.05 CF, ranging from 0.30 – 0.47 mL^2 (17 – 26 %). Though when mechanically compressed to 0.10 CF, the microscopic dispersion achieved approximately equal microscopic dispersions ranging from 0.31 – 0.34 mL^2 (19 – 21 %). Possibly the reason why the total microscopic dispersion under mechanical compression was lower across a wider range of compression, refer to Figure 4-1.

Uniform dispersion across the bed was achieved at a higher compression factor with mechanical compression compared to hydrodynamic compression. This suggest for softer resins, hydrodynamic compression can achieve a better-packed bed with less compression than when compared to mechanical compression. Although, DEAE Sephacel withstood higher levels of compression under mechanical compression; by achieving an optimum level of compression at 0.10 CF, possibly due to the gradual application of pressure where the top adapter was evenly applied across the whole cross section at the top surface of the bed.

Talking just the data at 0.15 CF, both methods of compression showed vast differences in microscopic dispersions ranging from 14 – 35% under hydrodynamic compression and 12 – 36 % under mechanical compression. Where a greater degree of microscopic dispersion is seen in the bottom section of the column under hydrodynamic compression and vice versa for mechanical compression. These trends are similar to those seen for Q Sepharose FF when compressed at high levels. Q Sepharose FF achieved a wide range of uniform dispersion between 0.05 – 0.10 CF for both methods of compression. Unsurprisingly, this suggests softer resins (DEAE Sephacel and Q Sepharose FF) are more sensitive to compression and less able to withstand high levels of compression. The next target was to examine the effects of compression on microscopic dispersion on beds packed with smaller resin and to see how band broadening is impacted.

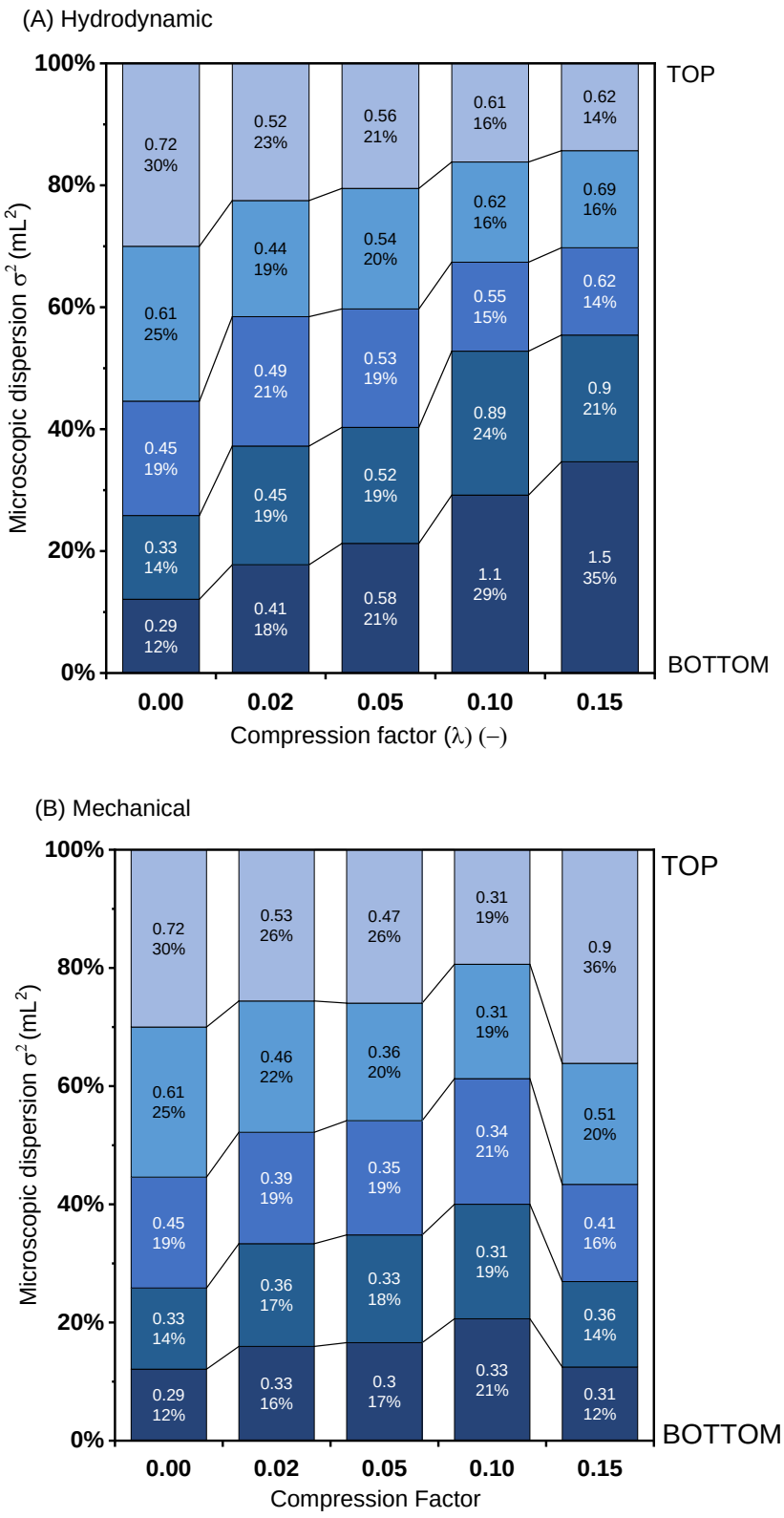

Figure 4-2 Examining the effect of (A) hydrodynamic compression and (B) mechanical compression on the contribution of microscopic dispersion by reverse flow technique on DEAE Sephacel. A range of five equally divided sections along the column was analysed. A XK16 column was used at a bed height of 10 ± 0.1 cm at 0.0 CF. Measurements were repeated three times with a relative standard deviation of less than 5% in all measurements.

Q Sepharose HP

Figure 4-3 illustrates the effect of compression on microscopic dispersion across the chromatographic bed packed with Q Sepharose HP. The average particle size of Q Sepharose HP is 2 – 3 times smaller than Q Sepharose FF and DEAE Sephacel. After compressing the column, the microscopic dispersion showed gradual improvement between 0.02 – 0.05 CF under hydrodynamic compression, with approximately equal sections throughout the bed at 0.10 CF, ranging from 19 – 22 %. This trend is similar to that obtained with the softer resins. Likewise, mechanical compression also showed improvements in microscopic dispersions across the bed with approximately equal microscopic dispersion at 0.10 CF, ranging from 19 – 21 %.

Taking just data at 0.15 CF, the highest level of microscopic dispersion under hydrodynamic and mechanical compression was 0.84 mL^2 (28 %) and 0.82 mL^2 (27 %), respectively. As expected, hydrodynamic compression showed highest band broadening effects in the bottom section of the bed, whereas mechanical compression indicated the opposite effect achieving the highest microscopic dispersion in the top section of the bed. Although, this trend was similar with the previous larger resins, the microscopic dispersions observed with Q Sepharose FF and DEAE Sepharose when compressed at 0.15 CF were more than 35 % higher compared to Q Sepharose HP. Under both methods of compression, Q Sepharose HP produced lower disparities of band broadening effects across the bed even at high levels of compression. This suggests smaller particles are more resistant to changes to structural re-arrangement and hence results in more consistent levels of microscopic dispersions at higher levels of compression.

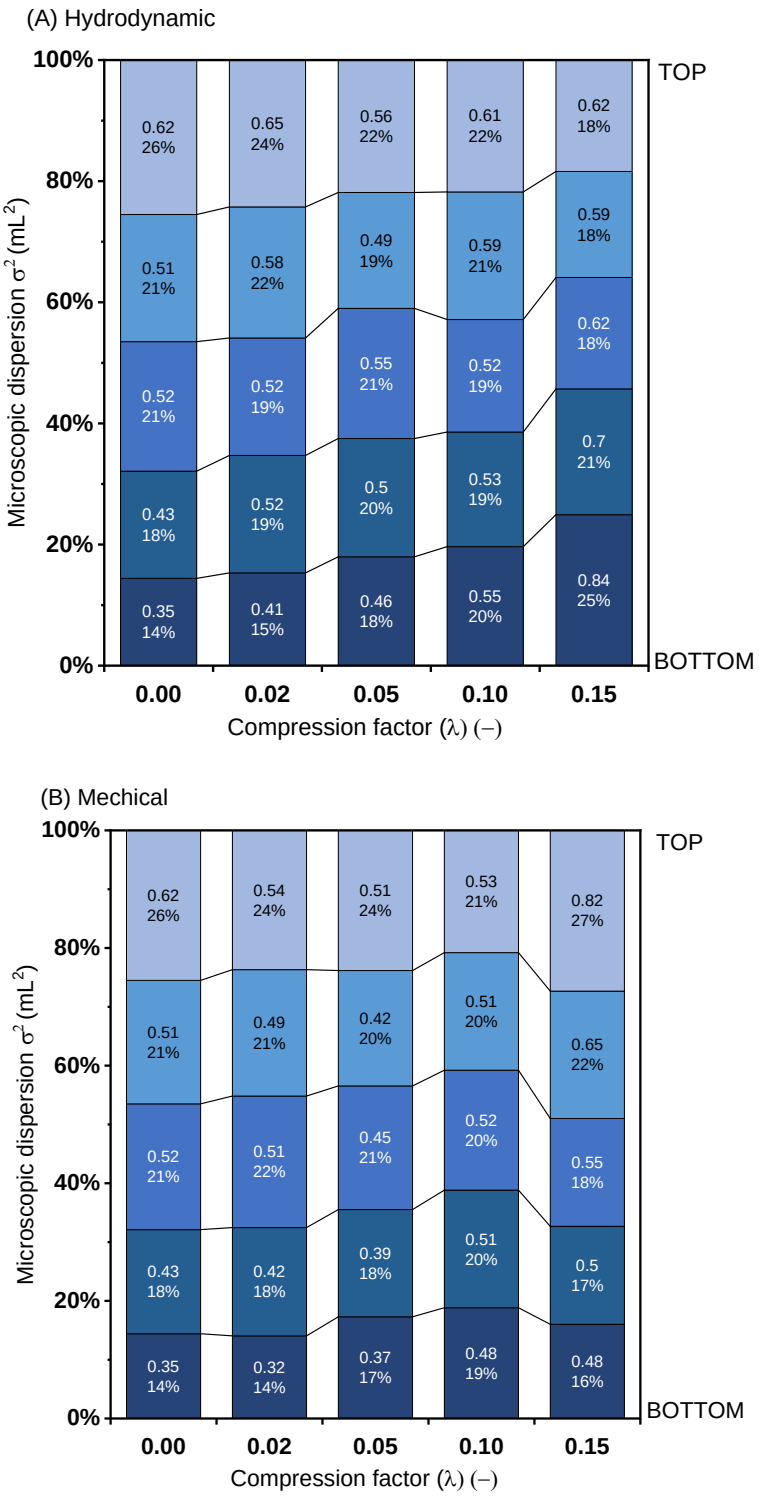

Figure 4-3 Examining the effect of (A) hydrodynamic compression and (B) mechanical compression on the contribution of microscopic dispersion by reverse flow technique on Q Sepharose HP. A range of five equally divided sections along the column was analysed. A XK16 column was used at a bed height of 10 ± 0.1 cm at 0.0 CF. Measurements were repeated three times with a relative standard deviation of less than 5% in all measurements.

As the compression factor increased, the smaller resin particles appear to pack more closely together forming a more stable bed structure and is more susceptible to higher pressures. This can be described by the number transfer unit equation, where band broadening (or column efficiency) is inversely dependent on particle size:

$$N = 60\,(1-\varepsilon)\frac{D_e}{{d_p}^2}\frac{L}{u} \qquad \textbf{Eq. 4-6}$$

This equation shows that smaller resins result in higher column efficiency. This may indicate why smaller resins are able to withstand high levels of compression while forming homogenously packed bed; shown by lower variability of microscopic dispersion. However, there is a limitation to how small the particle size can be, due to column pressures given by the limitation of the resin as described in the Kozeny equation (refer to Eq. 4-2).

This next study was to examine the effects of compression with resins with stronger structures (Capto Q) and also to characterise the effects of microscopic dispersions across the bed.

Capto Q

Figure 4-4 illustrates the effect of compression on microscopic dispersion across the chromatographic bed packed with Capto Q; the hardest resin examined. Capto Q demonstrated approximately equal distribution of microscopic dispersions from 0.05 – 0.15 CF ranging from 18 – 21 %, under hydrodynamic compression. Even at the extreme levels of compression, Capto Q showed evenly distributed microscopic dispersions throughout the whole bed. As expected, stronger resins are able to withstand higher levels of compression, indicating the effects of compression on microscopic dispersion is resin dependent and favours resins that are more rigid.

Even though both methods showed stable levels of band broadening more at 0.15 CF, hydrodynamic compression achieved an evenly compressed column at a lower compression factor than when compared to mechanical compression at 0.05 CF (dispersion ranging from 20 – 21 %). Mechanical compression showed higher

disparities of microscopic dispersion at 0.05 CF, ranging from 17 – 26 %. Mechanical compression achieved the best levels of microscopic dispersion at 0.10 CF, ranging from 19 – 20 %. Since homogenous packing was achieved with lower compression factor with hydrodynamic compression, flow packing is believed to apply pressure more uniformly throughout the whole column with harder resins. Thus achieving evenly packed sections sooner than in the case of mechanical compression.

Via hydrodynamic compression, fluid was flowed throughout the column at a higher velocity, compressing the column at a faster rate compared with mechanical compression. Even though mechanical compression achieved the same compression factor, the rate at which compression was applied was manually applied and more gradual. Perhaps mechanical compression is preferable with softer resins, which are more sensitive to pressure changes, while still achieving an evenly packed bed.

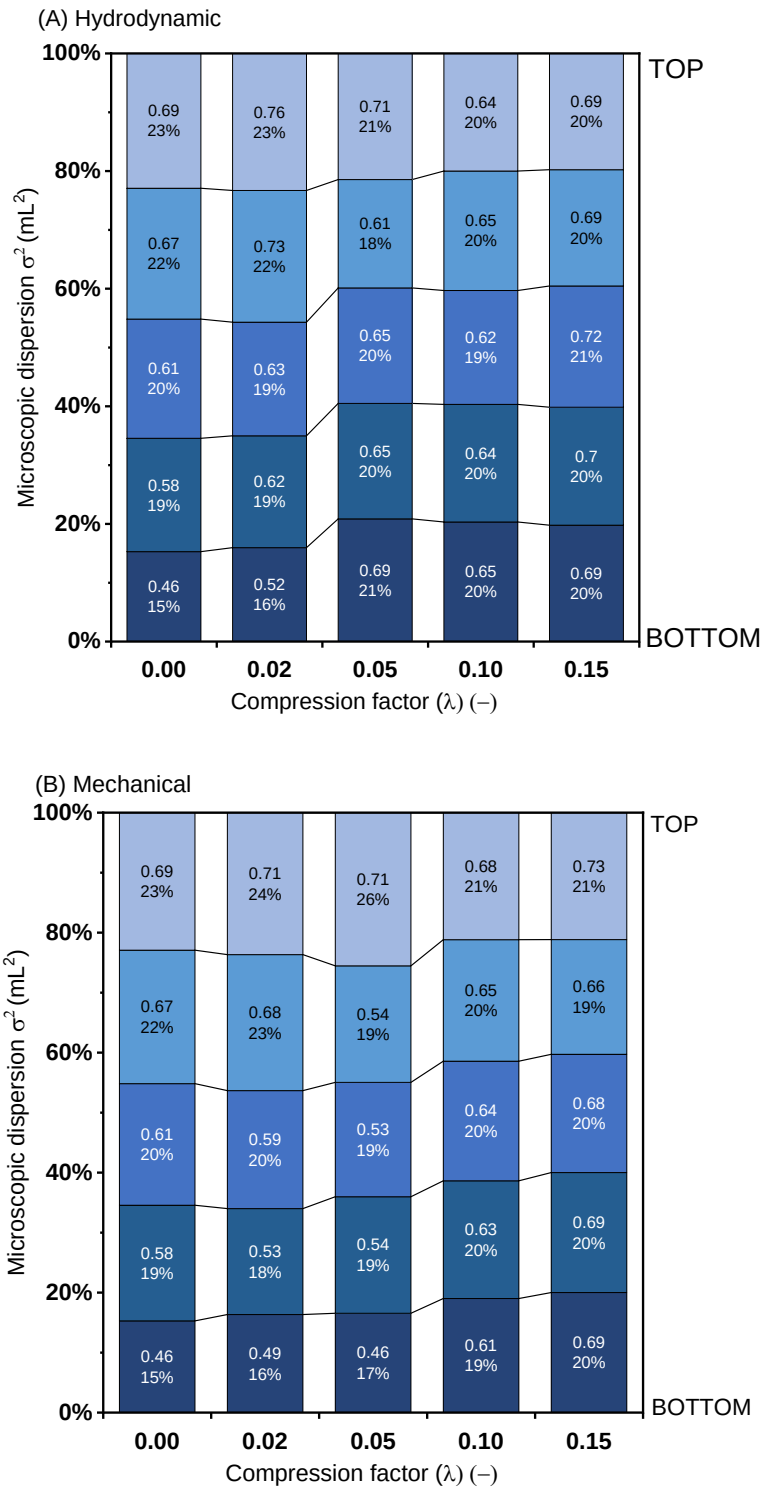

Figure 4-4 Examining the effect of (A) hydrodynamic compression and (B) mechanical compression on the contribution of microscopic dispersion by reverse flow technique on Capto Q. A range of five equally divided sections along the column was analysed. A XK16 column was used at a bed height of 10 ± 0.1 cm at 0.0 CF. Measurements were repeated three times with a relative standard deviation of less than 5% in all measurements.

4.5 Conclusion

The studies described so far have demonstrated the ability of the reverse-flow technique to examine axial packing heterogeneity of four ion exchange resins under different methods of compression for slurry packed chromatography beds. This technique has been shown to be simple, non-destructive, and able to reveal the total microscopic dispersion across the whole bed. In addition, uncovering the microscopic dispersion at different sections of the column, illustrate the effects of over-compression associated at high levels of compression.

Clearly, there are trade-offs between the two different methods of compression; hydrodynamic achieves faster levels of evenly packed columns, though over-compression will occur at lower compression factor, particularly at the bottom of the bed. Over-compression will occur in the top section of the bed via mechanical compression due to the increasing force from the top adapter. This phenomena is more readily seen with softer resins (Q Sepharose FF and DEAE Sephacel), where Q Sepharose HP (2 -3 times smaller resin) was less effected at a compression factor of 0.15. Only Capto Q (hardest resin examined) showed consistent equal distribution in microscopic dispersion across the bed, even at high levels of compression. The results illustrate that compression can improve bed uniformity, although the negative effects of compression is resin dependent and favours stronger resins.

5 Examining the impact of different methods of compression on the binding capacities on AEX resins

5.1 Abstract

In this chapter, the impact of hydrodynamic or physical compression on the binding capacity and breakthrough performance of three anion exchange resins was studied. Hydrodynamic and mechanical compression were applied to three different AEX resins: Q Sepharose Fast Flow, Q Sepharose High Performance and Capto Q selected to cover a range of bead rigidity and particles sizes. Column performance was assessed by analysing the breakthrough curves obtained using BSA as a model protein. Change in column performance was evaluated by comparing breakthrough curves upon two different methods of compressed columns.

The overall impact of compression on breakthrough performance depends heavily on the method of compression applied to the bed. For both hydrodynamic and mechanical compression, the dynamic binding capacity (DBC) increased by 60% for Capto Q. However, when Q Sepharose FF, a softer resin was hydrodynamically compressed the DBC decreased by 10% at 0.15 CF. By contrast, when Q Sepharose HP (2 – 3 times smaller than Q Sepharose FF) was hydrodynamically compressed to the equivalent compression factor, the DBC increased by 20%. This suggests that the particle size also influenced changes in breakthrough behaviour when compressed. For all three resins tested, mechanical compression produced the largest increases in DBC. It is hypothesized that this is a result of homogenously packed beds allowing a greater degree of mass transfer between proteins and resins.

5.2 Introduction

Downstream processing, which is not limited to just chromatography processes, has become an important manufacturing technique used in the biopharmaceutical sector (Carta and Jungbauer 2010; Jungbauer 2005). Chromatography is an adaptable and scalable unit operation used for the purifying of proteins and other biomolecules in typical capture and polishing steps. Manufacturers are able to produce large quantities of matrices at an industrial scale. However, chromatography performances is

influenced by structural differences of the stationary phases (surface modifications, resin morphologies) so there is a need to evaluate the performance of specific resins.

Resins properties can be informative in determine the impact of compression on the performance of the chromatography column. The shape and position of the breakthrough curve with respect to the volume of material processed depends on the capacity of the adsorbent, the binding kinetics and mass transfer characteristics of the solute in the system (Chase 1984; Cooney 1990, 1993). Over estimating the binding capacity can result in process related issues such as a decrease in the purity of the product, or underestimating binding capacity may result in uneconomical operation (Jagschies *et al.* 2007). Therefore, estimating the binding capacity under compression is of importance.

Only a few investigations on the effects of compression on column packed chromatography columns have been reported in the literature (Colby *et al.* 1996b; Edwards and Helft 1970; Freitag *et al.* 1994). A fundamental analysis of the way binding capacity is affected by the various methods of compression or the level of compression is still limited. Guiochon stated that axial and radial inhomogeneity depends on the packing method applied (Guiochon and Sarker 1995). Therefore, it follows that different methods of compression might cause changes in column capacity and column resolution, all of which are critical process parameters that determine product consistency between batches (Knox and Pyper 1986). A quantitative analysis of the factors affecting the dynamic binding capacity and hence the behaviour of breakthrough curves has been presented by Carta (G. Carta 2005). The ability to characterise the specific interactions that occur between proteins during adsorption and the matrix chemistry to which they bind under different methods of compression is key to achieving efficient bioprocess performance. Comparison of the breakthrough curves for columns packed using both hydrodynamic and mechanical compression can be informative in determining the effect of compression on the performance of chromatographic separations.

In this chapter, experimental studies were conducted to examine the changes in breakthrough curves upon applying two different methods of compression on chromatographic columns packed with AEX resins. Change in column performance

was evaluated by comparing dynamic binding capacities, obtained using BSA as a test protein, loaded onto a range of ion exchange resins of varying rigidity. The maximum binding capacity is determined by the adsorption isotherms (Cooney 1990). Changes in performance was assessed as a function of hydrodynamic and mechanical compression applied to the column at 4 levels of compression factor (0.02, 0.05, 0.10, 0.15).

5.3 Materials and methods

5.3.1 Chemicals

All reagents were from a single supplier (Sigma–Aldrich, Poole, Dorset, UK) unless stated otherwise. The loading material for this study was analytical grade Bovine Serum Albumin (BSA).

5.3.2 Description of equipment

Chromatographic procedures were performed using an ÄKTA Avant 25 (GE Healthcare, Little Chalfont, Buckinghamshire, UK) fast protein liquid chromatography system supplying an XK16 column, manually packed with four anion exchange resins: Q Sepharose FF, Q Sepharose HP, Capto Q and DEAE Sephacel (GE Healthcare, Uppsala, Sweden) to a bed height of 10.0 ± 0.1 cm. The ÄKTA Avant 25 built-in UV monitoring and conductivity measuring functions sent data to a control software UNICORN 6.0 (GE Healthcare, Little Chalfont, Buckinghamshire, UK). Spectrophotometric assays were performed off-line using a Beckman DU 650 spectrophotometer (Beckman Instruments Ltd, High Wycombe, Buckinghamshire, UK). All chromatography experiments were performed in triplicate and at room temperature 20 ± 5 ℃.

5.3.3 Process description

All solutions were filtered using 0.22 µm Stericup filter units (Merck & Co., Darmstadt, Germany) and were vacuum-degassed for 1 hr prior to use before loading onto the column. All resins were made up to 80% (w/v) slurry in a 50 mL measuring cylinder. The total slurry volume was calculated based on achieving a desired bed height of 10 cm. Each bed was initially gravity settled overnight before flow packing

at a velocity of 30 cm h^{-1} for 5 column volumes (CV). Once flow packed at this flow rate, a constant initial bed height of 10 cm ± 0.1 cm was achieved. Each column was operated at 30 cm h^{-1} and equilibrated with 3 CV of 50 mM Tris-HCL at pH 8.5 before loading the sample directly onto the column. The protein concentration of BSA was 5 mg mL^{-1} and the loading challenge was 180 mg mL^{-1}. Bound BSA was eluted using a step change of 1 CV of 50 mM Tris-HCL 1 M NaCl pH 8.5. Eluate fractions were collected until the UV trace (280 nm) returned to the baseline. Following elution, the column was cleaned with 3 CV of 0.5 mol L^{-1} NaCl and 0.1 mol L^{-1} NaOH solution and then washed with ultrapure water (typically at 18.2 MΩ cm at 25 °C) until neutral pH was reached. Columns were stored in 20% v/v ethanol solution, as per the manufacturer's recommendations. Columns stored in 20% v/v ethanol were washed with 5 CV of packing buffer prior the equilibration step.

5.3.4 BSA breakthrough curve determination

The following method was used to determine the breakthrough curves in all the frontal analysis tests. BSA at 5 mg ml^{-1} in 50 mM Tris-HCL at a pH 8.5 was fed to the column until the BSA effluent concentration, as measured by UV absorption at 280 nm (A280) equalled the feed concentration. Results for the breakthrough curves are presented graphically as the ratio of output concentration of BSA to input concentration of BSA; (C/C_0) versus column volume. The dynamic capacity at the 5% breakthrough level was calculated by taking the amount of BSA which had flowed through the column, determined as the area below the breakthrough curve at $C/C_0 = 0.05$.

Assay techniques

Protein concentration determination

Protein concentration was determined using a commercially available protein assay kit from Bio-Rad (Hertfordshire, UK). Reproducibility of the assay was typically ± 5% for triplicate samples.

Equilibrium binding capacity

The maximum equilibrium binding capacity (EBC) in batch mode was determined experimentally as the maximum amount of protein bound to the chromatographic media at given solvent and protein concentration conditions (Ghose *et al.* 2014). For each resin a 5 mL aliquot and 200 mL of 25 mg mL^{-1} of BSA was left overnight in a tumbler to promote mixing. Since the stationary phase was kept in high BSA concentration overnight to promote best levels of binding, the resins were allowed to reach maximum binding capacity. The supernatant was analysed and a mass balance was performed to obtain the EBC.

Particle Size Distribution (PSD)

The particle size distribution of the anion exchange resins were analysed using a Malvern Mastersizer 3000 laser sizer; (Malvern Instruments, Worcestershire, UK) which is able to detect particle size ranging from 0.01µm – 3500 µm. The particles were all assumed spherical. All solutions used in the analysis were filtered using 0.22 µm Stericup filter units (Merck & Co., Darmstadt, Germany) and the electrolytic buffers used for size-analysis were vacuum-degassed for 1 hr prior to use. Measurements were repeated three times with a relative standard deviation of less than 5% in all measurements.

5.4 Results

5.4.1 Equilibrium binding capacity

The equilibrium binding capacity (EBC) of the three anion exchange resins studied in this thesis Q Sepharose FF, Q Sepharose HP and Capto Q, are shown in Figure 5-1. To facilitate a comparison under identical experimental conditions, mass balances were performed to obtain the EBC. The maximum binding capacity of BSA for Q Sepharose FF, Q Sepharose HP and Capto Q were determined to be 110 ± 2, 114 ± 3 and 180 ± 3 mg mL^{-1}, respectively. The capacities of Q Sepharose FF and Q Sepharose HP were about 30% lower compared to Capto Q. Values found in these studies matched closely with earlier published data from (Zagorodni 2006) where EBC analysis of BSA were examined to determine the levels of capacity of binding for a range of ion exchange resins. When comparing EBC to particle sizes (Q Sepharose FF and Q Sepharose HP) little difference was seen.

Capto Q showed the highest EBC compared to the other resins. The binding capacity of proteins onto the resin and inside the pores are highly dependent on the structural characteristics of the beads (Martin *et al.* 2005). Capto Q has a rigid structure with additional dextran surface extenders. Resins with surface extenders, much like tentacle, servers to minimise mass transfer resistances; so-called enhanced ligands. Thus, the multi-site binding availability offered by these extensive structures enhances their binding capacity.

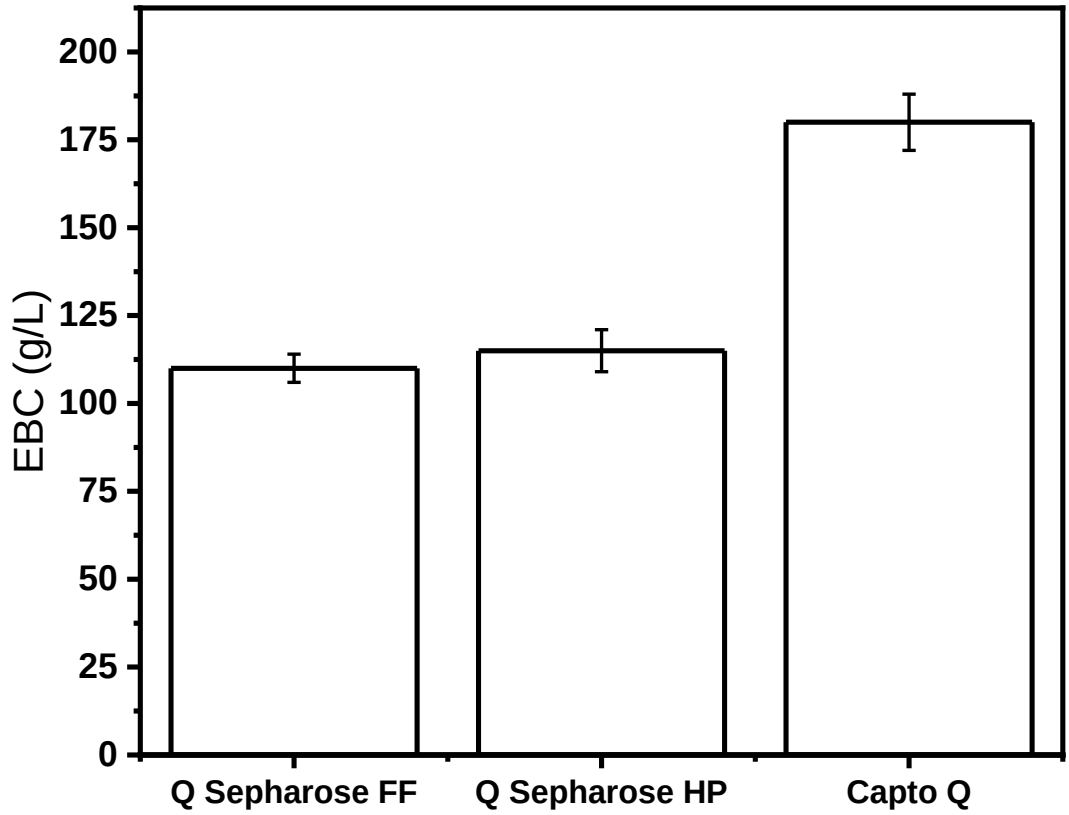

Figure 5-1 Equilibrium binding capacity (EBC) data of BSA adsorbed per mL of anion exchange medium. Data was derived from batch uptake experiments. The loading challenge for each resin was 200 mg mL^{-1} of BSA. Measurements were repeated three times with a relative standard deviation of less than 5% in all measurements.

5.4.2 Influence of bed compression on dynamic binding capacity

The next step was to determine the dynamic binding capacity as a function of the mode of compression: hydrodynamic or mechanical. Results are summarised in Figure 5-2. The effect of hydrodynamic and mechanical compression on dynamic binding capacity was determined by analysing the breakthrough curves at 5% obtained at four different compression factors. At 0.0 CF, the DBC of BSA for Q Sepharose FF, Q Sepharose HP and Capto Q were determined to be 45 ± 2, 58 ± 2 and 91 ± 3 mg mL^{-1} at 5% breakthrough, respectively. In general, trends showed gradual improvements in the DBC across all resins under mechanical compression, with a decrease in DBC above 0.10 CF. An earlier decrease in DBC under hydrodynamic compression was shown above 0.05 CF for softer resins (Q Sepharose FF and Q Sepharose HP), but remained unaffected for Capto Q.

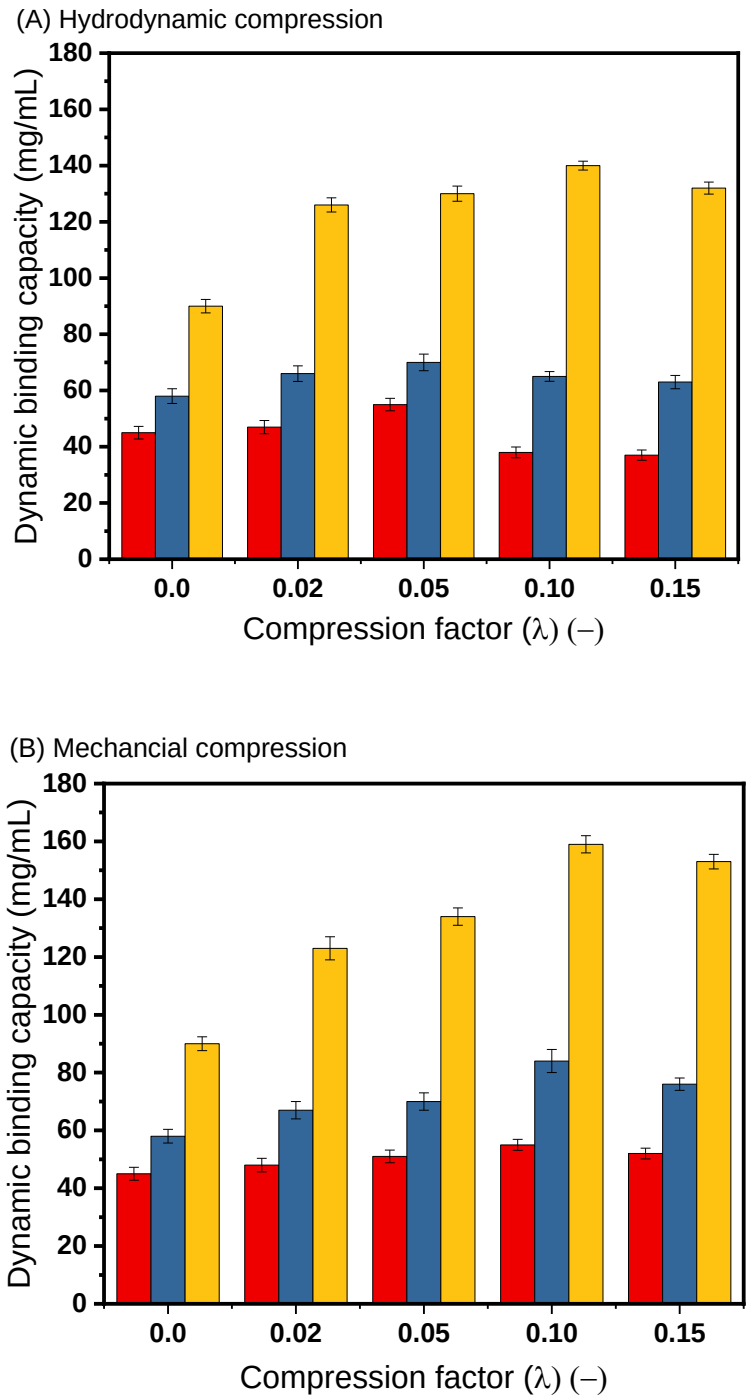

Figure 5-2 Examining the impact of (A) Hydrodynamic and (B) Mechanical compression on dynamic binding capacity (DBC). Three anion exchange resins were tested; Q Sepharose Fast Flow (red), Q Sepharose High Performance (blue) and Capto Q (yellow). The loading concentration for this study was 5 mg mL^{-1} of BSA. Studies were based on an XK16 column to a bed height of 10 ± 0.1 cm at CF = 0.0.

Q Sepharose FF

Figure 5-3 illustrates the breakthrough curves for Q Sepharose FF under both methods of compression. As the hydrodynamic compression increased, the breakthrough curves eluted later, indicated by a higher DBC with compression. However, at high levels of hydrodynamic compression, only Q Sepharose FF showed a decrease in binding capacity of - 5 % at 0.10 CF and - 8 % at 0.15 CF. Q Sepharose FF has been shown previously (refer to Chapter 2 & Chapter 3) to yield poor column efficiencies and variations in porosity at high levels of compression. These are linked to a decrease in DBC. When hydrodynamic compression was applied, the DBC for Q Sepharose FF ranged from 38 - 50 mg mL^{-1} compared to 45 – 53 mg mL^{-1} when under mechanical compression.

For easy DBC comparison, Figure 5-4 illustrates the relative changes determined at each compression factor in DBC with respect to the binding capacity compared at 0.0 CF. The determination of dynamic binding capacities were found to be reproducible to within 5% (95% CI) of the mean based on three repeated determinations. Changes in binding capacities greater than 5% were judged as significant.

The optimal level of dynamic binding capacity for Q Sepharose FF was achieved at a compression factor of 0.05 for hydrodynamic and 0.10 CF for mechanical compression. Mechanical compression provided higher DBC values across a wider acceptable range of compressible conditions (0.02 – 0.10 CF) compared to hydrodynamic compression where compression factors ranged from (0.02 – 0.05 CF).

At 0.15 CF, the dynamic binding capacity had decreased by approximately 5 - 15 % when compared to the optimal DBC for both methods of compression. The sharpest decrease was seen with Q Sepharose FF (softest resin) with a decrease of 15 % under hydrodynamic compression. At 0.15 CF under mechanical compression, the DBC showed a decrease of 5 % when compared to the optimal DBC; far lower than 15 % under hydrodynamic compression.

Based on these findings, the difference in compression factor of hydrodynamic and mechanical compression can be explained. During hydrodynamic compression, high liquid forces can result to over-compression, which contributes to uneven flow within the column. This leads to an early breakthrough suggesting proteins and ligand interaction will have less time to interact with each other promoting a lower DBC. In contrast to this, the axial compression force in mechanical compression is distributed more evenly in the radial direction by the top adapter that promotes even dispersion of force in the top surface of the bed. The packing compression behaviour of mechanical compression is governed by allowing excess liquid to escape through the top outlet allowing the excess voidage near the top to leave promoting a more homogenously packed column. This resulted in mechanical compression achieving an overall increase in DBC of BSA for all resins.

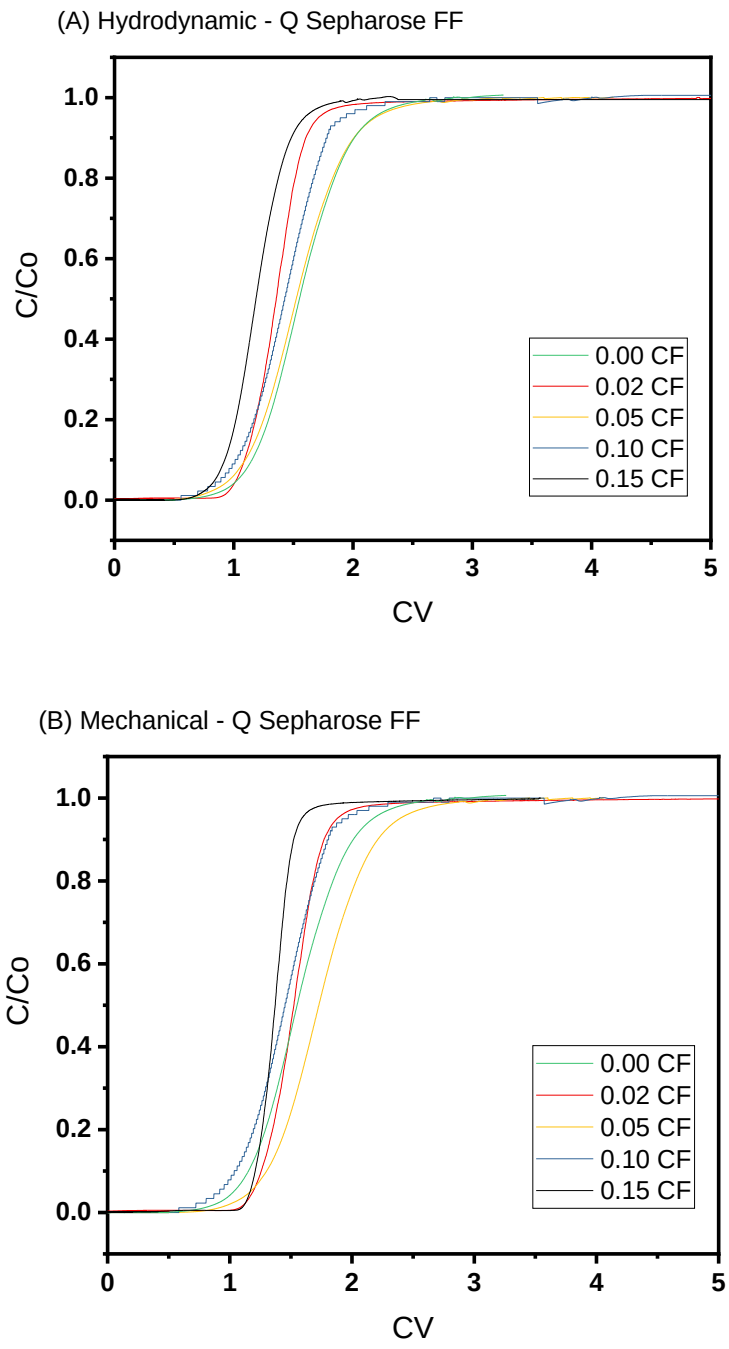

Figure 5-3 The effect of (A) Hydrodynamic and (B) Mechanical compression on the breakthrough curves for Q Sepharose FF. The loading challenge for this study was 180 mg mL^{-1} of BSA. Studies based on an XK16 column to a bed height of 10 ± 0.1 cm at CF = 0.0.

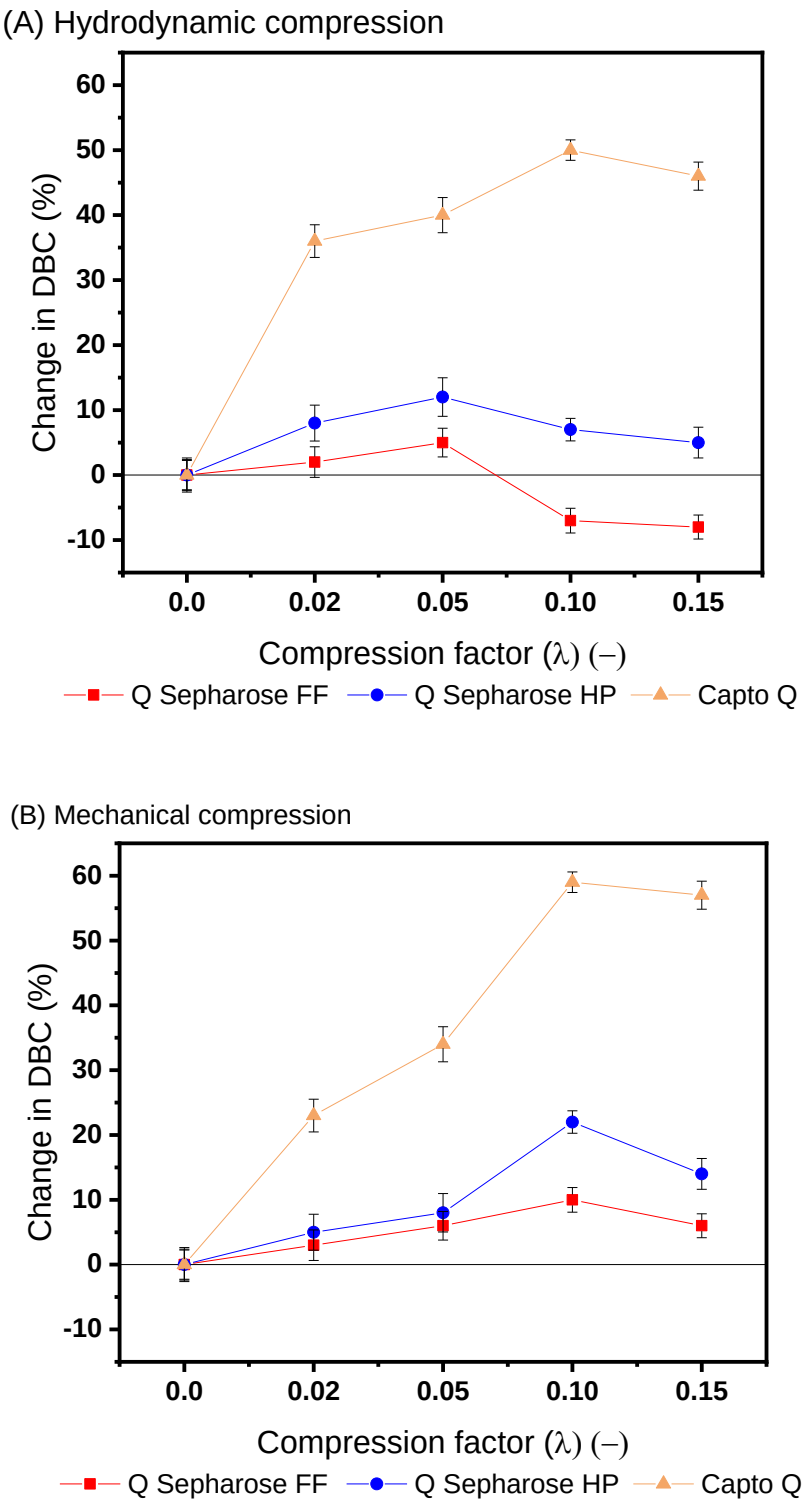

Figure 5-4 A study comparing the change of dynamic binding capacity of three anion exchange resins at (A) Hydrodynamic and (B) Mechanical compression. Change of capacity was measured with respect to the average capacity determined at CF = 0.0 quoted at: 45 ± 2.1 mg mL^{-1} (95% CI), 58 ± 2.5 mg mL^{-1} (95% CI), 90 ± 2.1 mg mL^{-1} (95% CI) for Q Sepharose Fast Flow (■), Q Sepharose High Performance (●) and Capto Q (▲), respectively. Studies based on an XK16 column packed to a bed height of 10 ± 0.1 cm at CF = 0.0.

Q Sepharose HP

In recent studies, Kaczmarski showed DBC is inversely depended on particle size, however no literature was found in regards to the changing levels of compression (Kaczmarski 2011). In this thesis, both resins are made of crossed-linked 6% agarose with quaternary ammonium strong anion exchange group with an experimentally acquired particle size of 90 µm and 34 µm for Q Sepharose FF and Q Sepharose HP, respectively.

Figure 5-4 illustrates the breakthrough curves for Q Sepharose HP under both methods of compression. Just taking data at 0.0 CF, Q Sepharose HP showed approximately 22 % higher DBC compared to Q Sepharose FF. This indicates columns packed with smaller resins show higher adsorption rates. As described by Martin and co-authors, the DBC is influenced by adsorption rates determined by mass transfer resistance, which are dependent on resin size and morphology (Martin *et al.* 2005). Since the morphological properties of Q Sepharose FF and Q Sepharose HP are the same except for their mean particle sizes, it can be concluded that changes in size morphology plays a role in DBC.

At 0.0 CF, columns were initially packed to the same bed height by gravity settling and flow packed at 30 cm h^{-1} for 5 CV. This allowed smaller resins to pack more closely together, evident by the lower voidage space for Q Sepharose HP (as described in 3). As the voidage space reduces, the occupied volume goes down, facilitating a higher surface area to volume ratio, as a result higher rates of BSA adsorption onto the beads were seen. Figure 5-5 illustrates the breakthrough curves for Q Sepharose HP under both methods of compression.

Larger resins allow larger voidage spaces to form around matrix particles, leading to a less compact bed (Chiu *et al.* 2018). After the bed is gravity settled, high levels of voidage space are located in the upper region close to the adapter as shown in MRI analysis (Yuan *et al.* 1999). During both methods of compression, the high axial force reduces voidage and increases the surface area to volume ration between the protein and resin. It can be noticed that the column efficiency is improved when the voidage decreases as long as the morphology of the resin remains constant.

At 0.15 CF, both methods of compression showed a decrease in DBC for Q Sepharose HP. This was expected since over-compression is likely to happen under high levels of fluid force throughout the column, adding further pressure at the bottom section of the column (as previously discussed in 4). Over-compression leads to uneven packing resulting in uneven flow and therefore contributes to early breakthrough of BSA. This trend is similarly seen with Q Sepharose FF; a softer larger resin.

Packing with hydrodynamic compression forces higher levels of compression towards the bottom compared to mechanical compression, which showed higher compression at the top. This had subsequent consequences on the DBC profiles for both methods of achieving compressed columns shown in (Figure 5-4). Over-compression at the bottom of the bed seems to give worse performance in DBC compared to over-compression at the top of the column.

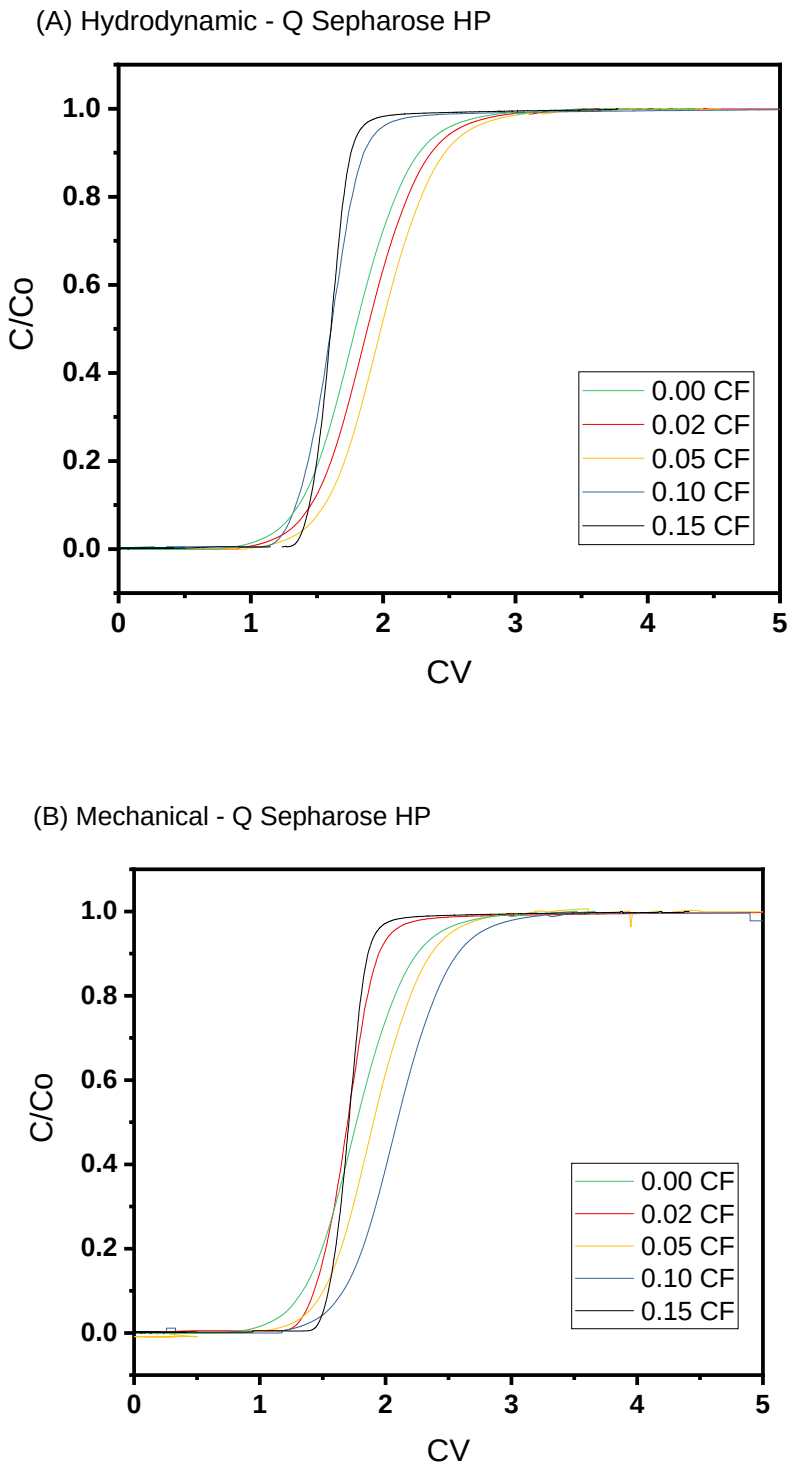

Figure 5-5 The effect of (A) Hydrodynamic and (B) Mechanical compression on the breakthrough curves for Q Sepharose HP. The loading challenge for this study was 180 mg mL^{-1} of BSA. Studies based on an XK16 column to a bed height of 10 ± 0.1 cm at CF = 0.0.

Capto Q

Capto Q is made more rigid by the introduction of an extra dextran linker, showed the sharpest increase in DBC for both hydrodynamic and mechanical compression. Figure 5-6 illustrates the breakthrough curves for Capto Q under both methods of compression. Both methods of compression showed optimal DBC at 0.10 CF, with mechanical compression achieving the highest DBC of 159 mg mL^{-1} compared to hydrodynamic compression achieving DBC of 143 mg mL^{-1}. From 0.10 – 0.15 CF, mechanical compression demonstrated higher improvements in DBC ranging from 53 – 59% compared to hydrodynamic compression with improvements in DBC ranging from 42 -48 %. Similar trends showed Capto Q to yield better column efficiencies and variations in porosity at high levels of compression (as shown previously in Chapter 2 & Chapter 3). These are linked to an increase in DBC.

Comparison of the breakthrough curves for non-compressed and compressed columns can be informative in determining the effect of packing methods on the performance of chromatography columns. For both methods of compression between 0.02 – 0.05 CF, the breakthrough curves were characterised by later breakthrough peaks but also showed severe tailing. Under higher levels of mechanical compression, the breakthrough curves showed steeper slopes in the initial phase ($C/C_0 < 0.2$). The leading edge of the breakthrough curve, $C/C_0 < 0.5$, is dominated by the mass transfer of solute in the fluid film, whereas the tailing edge, $C/C_0 > 0.5$, is dominated by diffusion of the solute in the matrix pores (Helfferich and Carr 1993). From 0.10 – 0.15 CF under mechanical compression, the breakthrough curve occurred considerably later and the shape of the breakthrough curve was significantly sharper compared to the same column before it was compressed. This suggests under high mechanical compression, the column is packed in such a way that promotes lower mass transfer resistances. Since, the breakthrough curve also showed a small occurrence of tailing, this could imply diffusion within the matrix pores is significantly improved with mechanical compression.

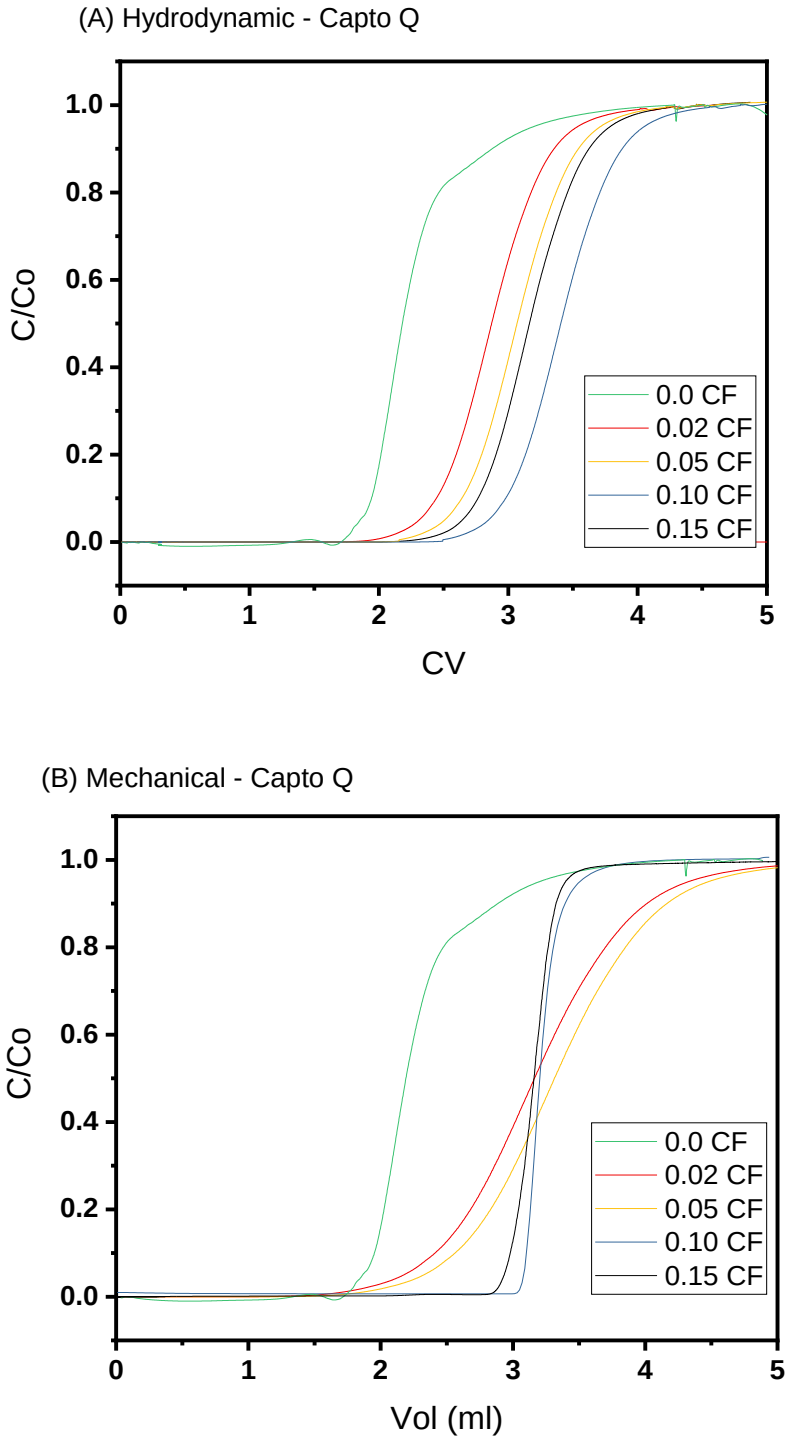

Figure 5-6 The effect of (A) Hydrodynamic and (B) Mechanical compression on the breakthrough curves for Capto Q. The loading challenge for this study was 180 mg mL^{-1} of BSA. Studies based on an XK16 column to a bed height of 10 ± 0.1 cm at CF = 0.0.

5.5 Conclusion

In this work, the variations in dynamic binding capacities were monitored as a function of two different methods of packing; hydrodynamic and mechanical. Performance was assessed in terms of the breakthrough characteristics obtained for binding of a test protein, BSA. The effect of bed compression by hydrodynamic and mechanical compression was studied for Q Sepharose FF, Q Sepharose HP and Capto Q. Performance was assessed in terms of the dynamic binding capacity (DBC) analysis at 5% breakthrough obtained for binding of BSA.

Only Q Sepharose FF showed a decrease in DBC when hydrodynamic compression was applied, indicating that changes in DBC are resin dependent when different methods of compression are applied. Q Sepharose HP showed a higher DBC compared to Q Sepharose FF under hydrodynamic and mechanical compression, this indicates smaller particle sizes (34 µm) can achieve higher DBC performance. Capto Q showed the greatest change in dynamic binding capacity as evidenced by a sharper breakthrough at increasing values of the compression factor. For all resins, the DBCs were expressly higher under mechanical compression.

The effect of mechanical compression on column breakthrough characteristics was more significant than those observed with hydrodynamic compression. For mechanical methods, following compression, breakthrough was delayed and the shape of the breakthrough curve was altered compared to the non-compressed states. These behaviours are most likely due a reduction in voidage space allowing a greater degree of mass transfer between proteins and resins. The DBC breakthrough behaviour is very dependent on the resin base matrix and is effected by the mode of compression.

6 Effect of bed compression on protein separation on gel filtration and anion exchange chromatography

6.1 Abstract

This chapter sets out to examine the effects of hydrodynamic and mechanical compression on the level of anion exchange achieved resins on protein separation. The influence of the mode of compression via one-step or multiple incremental step compression was also studied. Data presented in previous chapters show a strong correlation between column efficiency and interstitial porosity on protein adsorption. Results showed higher purification factor was achieved under multiple incremental step compression compared to one-step compression. Mechanical compression resulted in higher levels of purity and resolution compared to hydrodynamic compression. Q Sepharose HP showed higher levels of separation compared to Q Sepharose FF, which is 2 -3 times larger in size. Beyond 0.10 CF, Q Sepharose FF showed worse bed performance compared to an non-compressed bed, indicating protein separation is resin dependent and varies across the level of compression, with softer resin achieving optimal bed performance earlier. Whereas Capto Q has an additional dextran surface extender, which yields a stronger matrix structure compared to the two softer resins and this showed the greatest level of product purity and yield of the AEX matrices studied.

6.2 Introduction

Previous chapters explored the column efficiency (see Chapter 2) and bed porosity (see Chapter 3) of five chromatography resins - Sepharose CL-6B, DEAE Sephacel, Q Sepharose FF, Q Sepharose HP and Capto Q - using acetone and dextran to access the reduced plate height and intraparticle porosity. The resins were structurally characterised based on particle size and bead rigidity. Each resin exhibited different packing behaviours under hydrodynamic and mechanical compression. Capto Q showed significant improvements in reduced plate height and asymmetry under both hydrodynamic and mechanical compression, whereas Q Sepharose FF and HP (softer resins) showed poor packing quality above 0.05 CF. This indicates that the addition of the dextran surface extender on Capto Q makes this resin more resistant to the highest levels of compression compared to all other resins.

The reverse-flow technique was then used to determine the extent of microscopic dispersion along the axial sections of the column and was used to characterise the homogeneity along the chromatographic bed (see Chapter 4). The results show that hydrodynamic packing achieves evenly packed columns more rapidly, though over-compression will occur earlier, particularly at the bottom of the bed. This flow technique has been shown to be simple, non-destructive, and able to reveal the microscopic dispersion at different sections of the column, and hence to illustrate the effects of over-compression associated at high levels of compression. Capto Q (hardest resin examined) showed a consistently even distribution in microscopic dispersion across the bed, even at high levels of compression. The results illustrate that compression can improve bed uniformity, although the negative effects of compression are resin dependent and less in more rigid resins.

DBC analysis was then used to determine whether different methods of compression were linked to breakthrough performance for three anion exchange resins - Q Sepharose FF, Q Sepharose HP, and Capto Q. DBC increased by 60% for Capto Q under both hydrodynamic and mechanical compression. However, when Q Sepharose FF, a softer resin was hydrodynamically compressed the DBC decreased by 10% at 0.15 CF.

For all three resins tested, mechanical compression produced the largest increases in DBC. Capto Q showed the highest DBC, followed by Q Sepharose HP whilst Q Sepharose FF had the lowest DBC (see Chapter 5).

Only a few investigations on the effects of compression on packed bed chromatography columns have been reported in the literature. These show how packing quality can be can be improved with hydrodynamic compression (Colby *et al.* 1996a; Freitag *et al.* 1994; Guiochon and Sarker 1995). Several articles on the different methods of compression on column packing and efficiency have been studied (Luo *et al.* 2013; Mohammad *et al.* 1992b). Whilst, no literature describing the effects of hydrodynamic and mechanical compression on protein separation is seen in the literature for preparative chromatography systems.

For preparative chromatography, a qualitative analysis of a protein mixture based on the chromatogram can give rise to complex overlapping of peaks from which it is difficult to identify the purity of the proteins directly. In preparative chromatography, multiple components are unlikely to resolve fully from one another compared to analytical chromatography where baseline separation can be revealed. This is because analytical chromatography uses lower amounts of protein relative to the number of binding sites on the column. Whereas, in preparative chromatography it is necessary to maximize the loading of the column to reduce the cost of goods for the process. This means the eluate will need to be processed further in order to identify the individual components from the overlapping peaks. This process includes the separation of the eluate into fractions and subsequent analysis to determine the product from impurities.

An alternative method to calculate product purity, is modelling protein absorbance directly from the chromatogram to predict individual protein purity (Gerontas *et al.* 2010). The use of UV absorbance at 280 nm where proteins typically absorb UV light can determine the concentration of proteins (Aitken and Learmonth 1996). The concentration profiles for each component has been used as the basis for modelling chromatographic processes. Edwards-Parton *et al.* (2008) used such an approach to fit peak parameters for predicting large-scale elution profiles. Programmed scripts based on theoretical equations have also been used to resolve peaks into single components from small scale by applying correction factors that correct for the dispersion and retention effects. Modelling of small-scale process to predict large-scale performance can give an immediate quantitative indication of the process performance. Nevertheless, this procedure requires several pre-processing steps and makes assumptions that the peak takes the form of an ideal Gaussian distribution. Both of which are potential sources of error (Hutchinson and Edwards-Parton 2009).

An approach for reducing the complexity of concentration profiles and producing quantitative data from which to quantify the performance of the process is to calculate the maximum purification factor vs. yield (PFY) diagrams. PFY diagrams were originally used to compare precipitation processes, until Ngiam *et al.* (2001) adapted these diagrams for analysing the trade-offs between the purity and yield for chromatography separation. In preparative chromatography, the product and impurities are rarely well resolved; therefore, it is vital to know when to start collecting

from the eluate to maximize product yield and purity. However, changing peak cuts to maximize the yield will result in more impurities being collected resulting in a lower purity and vice versa. The PFY diagram illustrates the trade-offs between the purity and yield by plotting the purification factor at all possible yields that can be achieved.

In this chapter, the effects of hydrodynamic and mechanical compression on protein separation on anion exchange chromatography using purification factor vs. yield (PFY) diagrams is studied. In addition, the effects of one-step and multiple incremental step compression on protein separation on gel filtration chromatography are considered. The use of resolution and purification factor is made to compare the effects of two different methods of compression on the overall column performance and productivity.

6.3 Material and methods

Detailed description of one-step and multiple incremental step compression is located in Section 2.3.8, Modes of Compression.

Bench-scale setup

Bench-scale experiments were carried out using the ÄKTA Avant 25 (GE Healthcare, Little Chalfont, Buckinghamshire, UK) fast protein liquid chromatography system equipped with pump unit P-903, cell (280 nm, 2 mm path length), conductivity cell, and auto sampler A-900. The control software UNICORN 6.0 (GE Healthcare, Little Chalfont, Buckinghamshire, UK) was used. The extra column dead volume was kept to a minimum by using 0.12 mm I.D. capillary tube to connect the column to the injector. An XK16 column (GE Healthcare, Uppsala, Sweden) was used with an inner diameter (I.D.) of 0.016 m (XK16, with adjustable column lengths). All chromatography experiments were performed in triplicate and at room temperature 20 $\pm$ 5 ℃.

Stationary phases and loading samples

All reagents were from a single supplier (Sigma–Aldrich, Poole, Dorset, UK) unless stated otherwise. Studies were carried out using a gel filtration resin; Sepharose CL-

6B (GE Healthcare Uppsala, Sweden). It is a 6% cross-linked agarose gel filtration based matrix which may be used to separate samples of diverse molecular weight; 1 x 10^4 – 1 x 10^6 Da. The resin is available in both Sepharose and Sepharose CL forms where the cross-linked form is chemically and physically more resistant, allowing identical selectivity but at increased flow conditions. The spherical resins had a size distribution of 45 – 165 µm (quoted by the manufacturer). The average bead diameter was determined to be, dp = 98 µm ± 5 µm (Malvern Mastersizer 3000 laser sizer; Malvern Instruments, Worcestershire, UK). For gel filtration studies, the loading materials were ovalbumin from chicken, Bovine Serum Albumin (BSA) and ɣ-globulin (bovine) with molecular weights of 44, 67 and 18 kDa.

In addition to studying gel filtration resins, three strong anion exchangers (quaternary amine) were investigated; Q Sepharose Fast Flow, Q Sepharose High Performance and Capto Q (GE Healthcare Uppsala, Sweden). Both Q Sepharose resins are highly cross-linked agarose beads, whereas Capto Q has an additional dextran surface extender. Both Q Sepharose FF and Capto Q have a particle size, d_p of ~ 90 µm, whilst Q Sepharose HP has a size distribution of average particle size, d_p of 34 µm (quoted by the manufacturer). For anion exchange studies, the loading materials were ovalbumin (chicken), BSA and β-Lactoglobulin (bovine) with isoelectric points of 4.5, 4.7 and 5.1, respectively.

A total protein concentration of 5 mgmL^{-1} was used. The concentration of the protein mixture was equally divided in thirds. Therefore, the initial purity of the sample with respect to ovalbumin was 33%. All samples were filtered using 0.22 µm Stericup filter units (Merck & Co., Darmstadt, Germany).

Process description

Gel filtration

An equilibration step of 3 CV of PBS at pH 7.2 was used before loading the sample directly onto the column. A loading volume of 0.5 CV of 5 mg mL^{-1} of total protein was used. Eluate fractions were collected until the UV trace returned to the baseline. A wash step of 2 CV was used to remove any remaining traces of sample. Following elution, the column was cleaned with 2 CV of 0.5 M NaCl and 0.1 M NaOH solution and then washed with ultrapure water (typically at 18.2 MΩ cm at 25 ℃) until neutral pH was reached. Columns were stored in 20% v/v ethanol solution, as per the manufacturer's recommendations. Columns stored in 20% v/v ethanol were washed with 5 CV of packing buffer prior to commencing the equilibration step.

Anion exchange

An equilibration step of 5 CV of 50 mM Tris-HCL at pH 8.5 was used before loading the sample directly onto the column. A loading volume of 0.5 CV of 5 mg mL^{-1} of total protein was used. A wash step of 2 CV was used to remove any remaining traces of sample. Separation was achieved using a linear gradient of 5 CV 50 mM Tris-HCL 1 M NaCl pH 8.5. Eluate fractions were collected until the UV trace returned to the baseline. Following elution, the column was cleaned with 6 CV of 1 M NaCl and 0.1 mM NaOH solution and then washed with ultrapure water (typically at 18.2 MΩ cm at 25 ℃) until neutral pH was reached. Columns were stored in 20% v/v ethanol solution, as per the manufacturer's recommendations. Columns stored in 20% v/v ethanol were washed with 5 CV of packing buffer prior to initialising the equilibration step.

6.3.1 Assay techniques

HPLC-SEC protein mixture

SEC-HPLC was used to determine the purity of the eluting protein mixture. This was performed using an Agilent 1100 HPLC system with ChemStation software and an Agilent ZORBAX GF T-250 column (Agilent Technologies UK Ltd, Berkshire, UK).

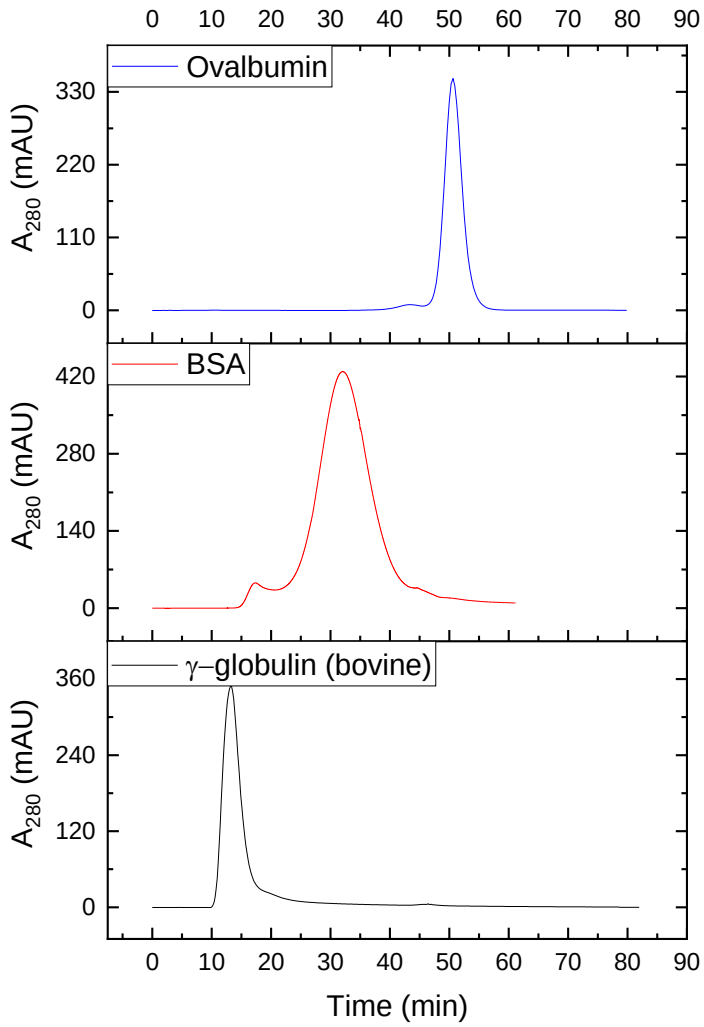

Figure 6-1 Screening of individual protein peaks on SEC-HPLC column using HPLC-SEC column. Protein sample: 2 mg mL^{-1} of ovalbumin, BSA, and γ-globulin measured at A_{280} nm (mAU). Equilibration buffer: PBS at pH 7.2 at 0.5 mL min $^{-1}$. All samples were filtered through 0.45 µm Stericup filter units.

The total protein concentration was determined using the Bradford method with Brilliant Blue G Protein Assay reagent (Sigma–Aldrich, St. Louis, MO, USA). Gel filtration standards (Bio-Rad Laboratories Ltd, Hertfordshire, UK) were used to calibrate the accuracy of the SEC-HPLC column (data not shown).

Fractionation diagram

Based on the SEC-HPLC data collected from the eluate fractions, the fractionation diagram was plotted. The fractionation diagram is a plot of *y vs. x* where x represents the fractional mass of the total protein and y represents the fractional mass of the product (BSA) as defined in Eq. 6-1 and Eq. 6-2.

$$\boldsymbol{x} = \frac{\sum_{i=0}^{i} \boldsymbol{M_{t,i}}}{\sum_{i=o}^{N} \boldsymbol{M_{t,i}}} \qquad \textbf{Eq. 6-1}$$

where the eluate is divided into i = 1, 2, 3 … N fractions and $M_{t,i}$ is the mass of the total protein in fraction i.

$$\boldsymbol{y} = \frac{\sum_{i=0}^{i} \boldsymbol{M_{P,i}}}{\sum_{i=o}^{N} \boldsymbol{M_{P,i}}} \qquad \textbf{Eq. 6-2}$$

where $M_{P,i}$ is the mass of product in fraction i.

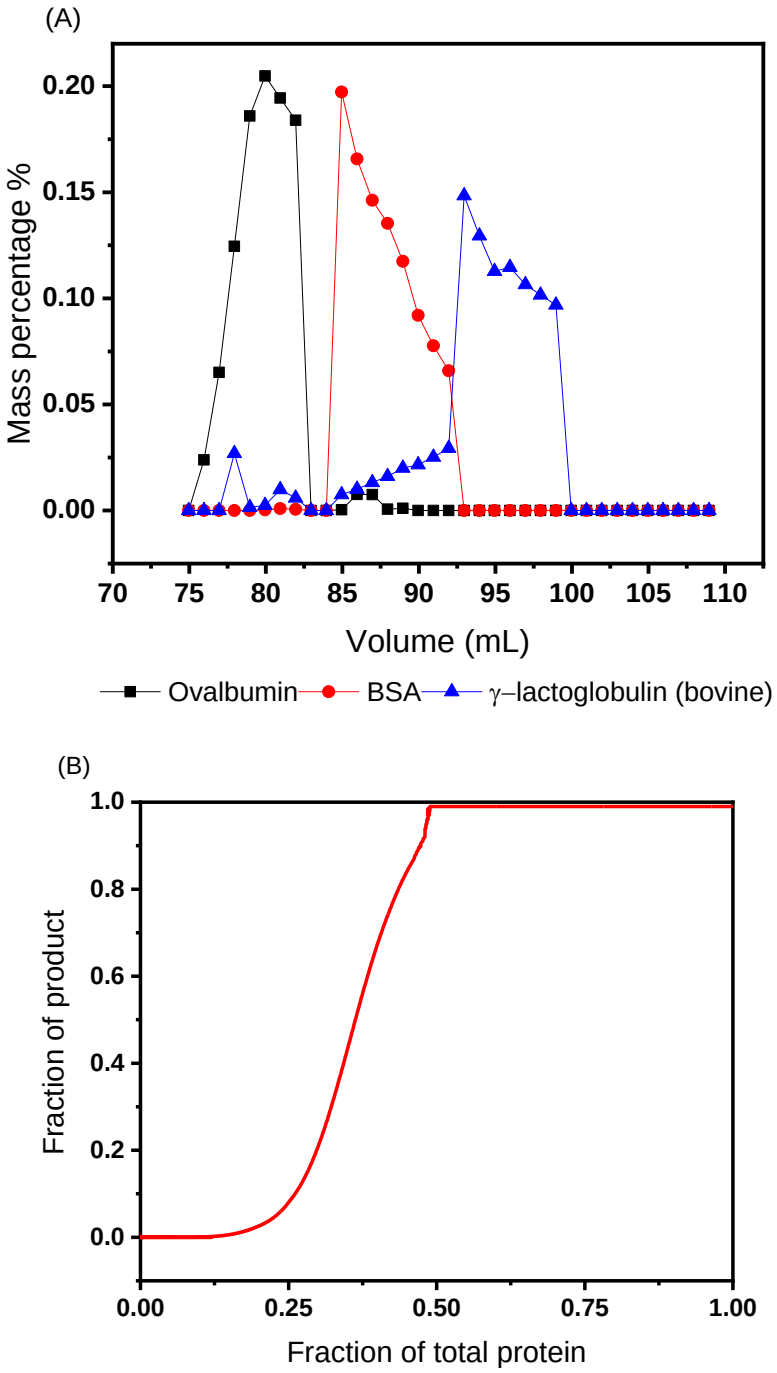

Figure 6-2 The fractionation diagram (6-2B) is calculated from the given mass percentage chromatograms (6-2A) for the separation of ovalbumin, BSA, and ɣ- globulin (bovine) using SEC-HPLC.

Once the fractionation diagrams had been plotted, the separation performance was evaluated based on the purification factor (PF). The impurities in the sample load chosen to be; ovalbumin (44 kDa) and γ-globulin (158 kDa) for SEC studies, and; ovalbumin (44 kDa) and β-Lactoglobulin (18.4 kDa) for AEX studies, BSA (67 kDa) was selected as the product in all cases. The separation of smaller and larger impurities was therefore simulated.

The PF is described as the ratio between the final purity of BSA after purification to the initial purity of the sample load. For a pair of collection cuts the fractionation diagram can be used to calculate the purification factor and yield using Eq. 6-3 and Eq. 6-4. On the fractionation diagram, these correspond to the gradient between the two points and the difference in *y* coordinates respectively.

$$\boldsymbol{PF = \frac{y_2 - y_1}{x_2 - x_1}} \qquad \textbf{Eq. 6-3}$$

$$\boldsymbol{Y = y_2 - y_1} \qquad \textbf{Eq. 6-4}$$

where PF is the purification factor and Y is the yield and y_1, y_2, x_1 and x_2 are the coordinates of the two cuts on the fractionation diagram. MATLAB scripts were written to obtain the maximum purification factor at each yield and produce the PF vs. yield diagram (see Appendices).

Resolution determination

Resolution was calculated as follows;

$$\boldsymbol{R_s = \frac{(V_{R2} - V_{R1})}{(W_{h2} + W_{h1})}\, x\, 1.177} \qquad \textbf{Eq. 6-5}$$

where R_s is the resolution, V_{R1} and W_{h1} are the retention and the width at half height of the early peak and V_{R2} and W_{h2} are the retention and width at half height of the late peak.

6.4 Results and Discussion

In Chapter 2, we examined the effect of one-step and multiple incremental step compression on column efficiency on gel filtration chromatography. In this section, the impact of one-step vs. multiple incremental step compression under hydrodynamic and mechanical compression on protein separation are examined.

6.4.1 Effect of one-step vs. multiple incremental step compression on protein separation on gel filtration chromatography

Figure 6-3 displays the purification factor as a function of yield for separating a fixed protein mixture obtained with columns that had undergone; (A) one-step (B) multiple incremental step via hydrodynamic compression on Sepharose CL-6B. Both modes of compression showed improvements of the purification factor across all yields. Nevertheless, results show that hydrodynamic multiple incremental step compression lead to greater levels of product purity and yields than hydrodynamic one-step compression. This suggests packing quality and protein separation is influenced by the packing history of the bed. Multiple incremental steps changes the chromatography bed by undergoing several steps to achieve the desired level of compression. Whereas under hydrodynamic one-step compression, the desired compression factor is achieved by applying high levels of fluid flow directly once onto the bed.

The maximum PF achieved for one-step compression was seen at 0.05 CF, whereas, multiple step compression was seen at 0.10 CF. Above 0.05 CF under one-step compression, the column separation performance deteriorated indicating a poorly packed column. This was evident when compared with column efficiency data where the asymmetry and reduced plate height were outside the acceptable range (see Section 2.4). Above 0.05 CF, the one-step method suggests signs of over-compression likely caused by high levels of hydrodynamic force on to the top of the bed for a longer length of time. By contrast, at high levels of compression under multiple incremental steps, the bed underwent a gradual increase in compression that allowed the bed to stabilise at each level of compression. This method of compression may cause less physical deformation of the beads by allowing time for the bed to acclimatise and form

more stable particle arrangements. Multiple incremental step compression yielded highest purification factors at 0.10 – 0.15 CF, indicating better quality of packed beds in terms of column efficiency, as evidenced by lower reduced plate heights and asymmetry values closer to 1.0 (see Section 2.4).

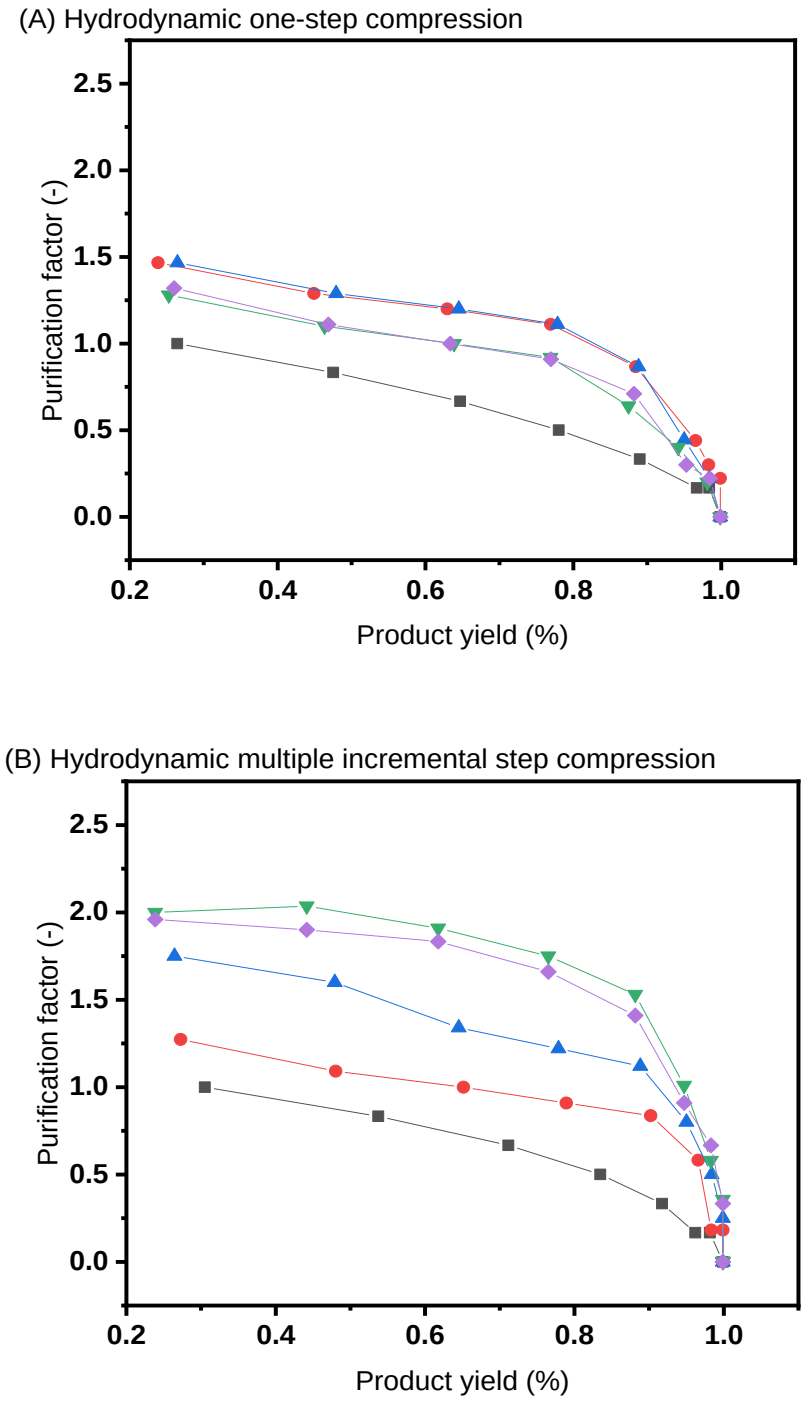

Figure 6-3 Influence of hydrodynamic compression on separation performance of a fixed protein mixture. Purification factor vs product yield of a protein mixture of 5 mg mL^{-1} with hydrodynamic compression on Sepharose CL-6B. (A) Hydrodynamic one-step compression; (B) Hydrodynamic multiple incremental step compression (▪) 0.0; (●) 0.02; (▲) 0.05; (▼) 0.10; (♦) 0.15. Measurements were repeated three times with a relative standard deviation of less than 5% in all measurements.

Figure 6-4 displays the purification factor as a function of yield for columns that had undergone mechanical compression; (A) one-step (B) multiple incremental step. As expected, results show that mechanical compression via multiple incremental steps leads to greater levels of product purity and yields than does mechanical compression in one-step. In both hydrodynamic and mechanical compression, the purification factor achieved was higher at all levels of compression compared to a non-compressed bed. As expected, results showed that mechanical compression via multiple incremental steps lead to greater levels of product purity and yields than mechanical compression in one-step.

The results indicate that performance of protein separation is better the higher the level of mechanical compression achieved, but that compression by multiple incremental step protocols created separation with significantly higher purification factor (PF) values for all yields. This was especially pronounced for compression levels CF > 0.05. For example, at a typical specification of product yield of 0.9 the PF at 0.15 CF was 1.25 for mechanical compression achieved in one-step and 1.80 for mechanical compression in multiple incremental steps. Such increases in PF offers the ability to increase purity at a set yield target or to increase yield with no detrimental impact on purity. Similarly, the PF at 0.15 CF at a product yield of 0.9 was 0.85 for hydrodynamic compression achieved in one-step compression and 1.55 for hydrodynamic compression in multiple incremental steps. Hydrodynamic one-step compression applied at higher levels of compression showed significantly lower PF values compared to multiple incremental step compression. High levels of fluid flow for a longer duration seems to increase the chance of instability and heterogeneity within the column, resulting in lower performance in terms of protein separation.

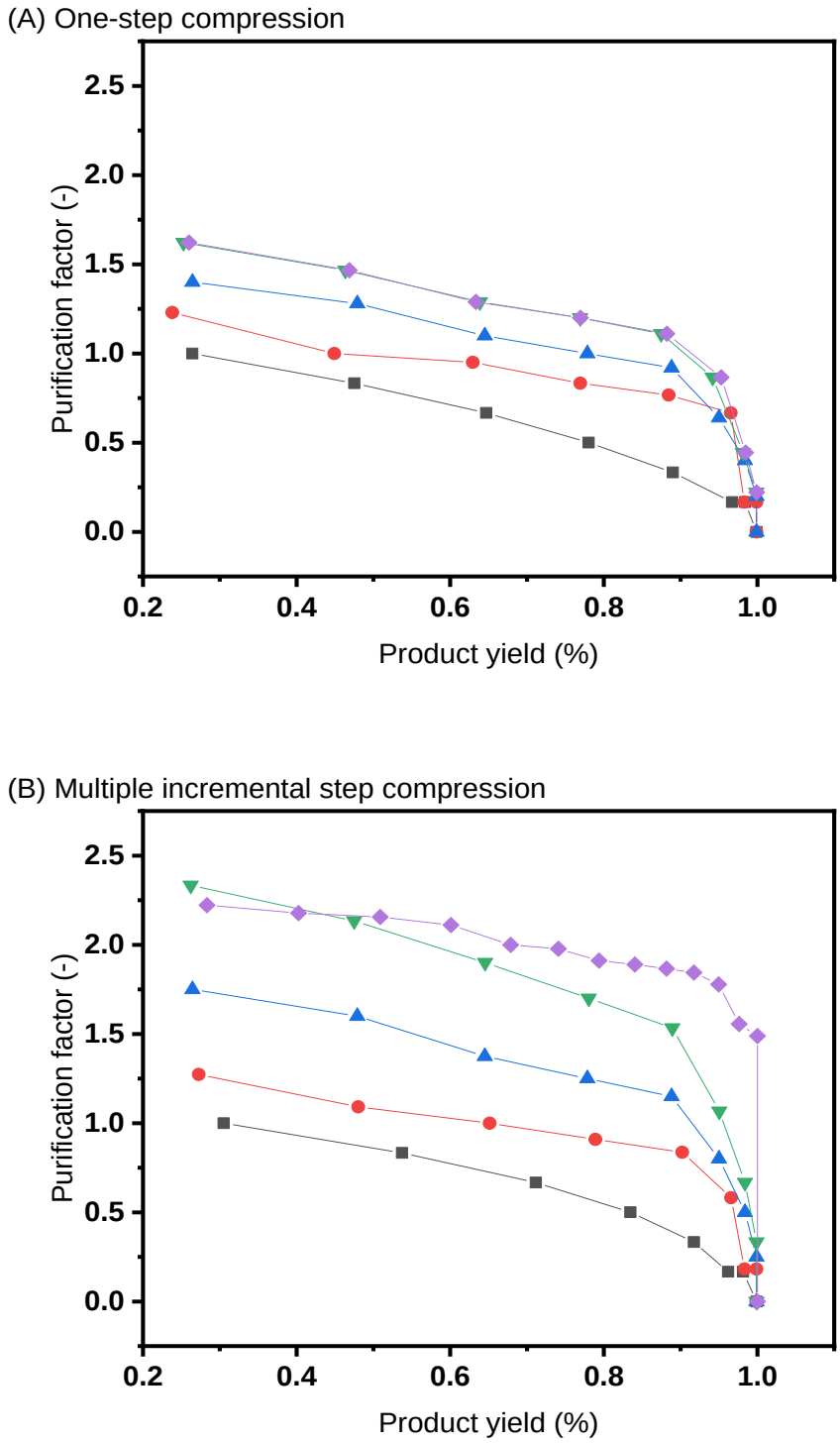

Figure 6-4 Impact of mechanical compression on separation performance of a fixed protein mixture. Purification factor vs product yield of a protein mixture of 5 mg mL^{-1} with mechanical compression on Sepharose CL-6B. (A) Mechanical one-step compression; (B) Mechanical multiple incremental step compression (▪) 0.0; (●) 0.02; (▲) 0.05; (▼) 0.10; (♦) 0.15.

Since compression via multiple incremental steps created separation with significantly higher PF values compared with one-step compression, the next set of studies was to examine the impact of multiple incremental steps on protein separation for anion exchange resins.

6.4.2 Effect of compression on protein separation on anion exchange chromatography

This study investigated the impact of hydrodynamic and mechanical compression via multiple incremental steps on three anion exchangers (quaternary amine); Q Sepharose FF, Q Sepharose HP, and Capto Q. The effect of compression on protein resolution was determined by analysing the chromatograms at each compression factor studied, as shown in Figure 6-5. The determination of peak resolution were found to be reproducible to within 5% (95% CI) of the mean based on three repeated determinations.

At 0.0 CF, the resolution between the first and second peak (β-Lactoglobulin and BSA) for Q Sepharose FF, Q Sepharose HP, and Capto Q were determined to be 0.6 ± 0.03, 0.72 ± 0.05, and 0.92 ± 0.04, respectively. In general, trends showed gradual improvements in protein resolution across all resins under both methods of compression, with a decrease in resolution above 0.10 CF for softer resins (Q Sepharose FF and Q Sepharose HP), but remained unaffected for Capto Q. This suggests the relationship between the quality of packing via compression and protein separation of proteins are highly dependent on the structural characteristics of the beads.

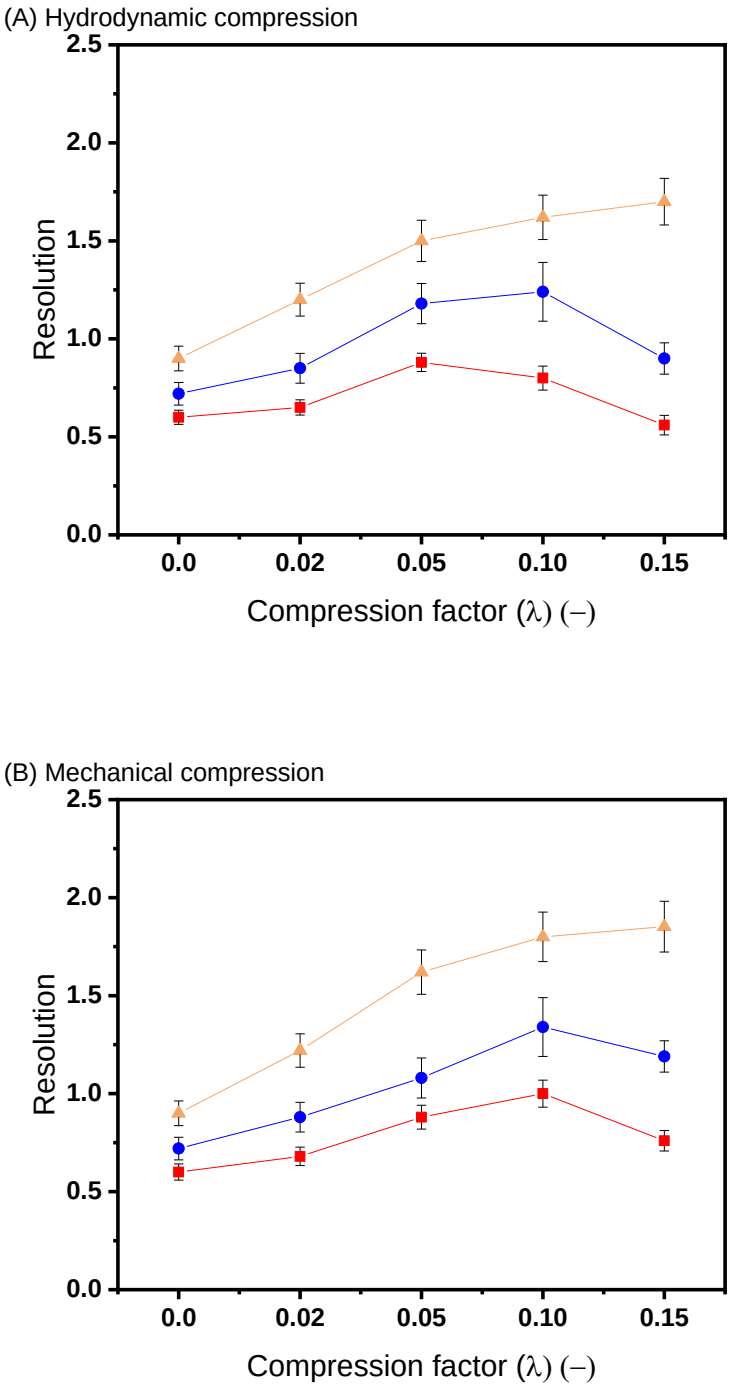

Figure 6-5 A study comparing the resolution of three anion exchange resins under (A) Hydrodynamic and (B) Mechanical compression. Resolution was obtained from the chromatogram of the early peak (β-Lactoglobulin) and the late peak (BSA). Three anion exchange resins were tested; Q Sepharose Fast Flow (■), Q Sepharose High Performance (●) and Capto Q (▲). The loading concentration for this study was 5 mg mL^{-1} of total protein. Studies were based on an XK16 column to a bed height of 10 ± 0.1 cm at CF = 0.0. Measurements were repeated three times with a relative standard deviation of less than 5% in all measurements.

Q Sepharose FF

Figure 6-6 illustrates the PFY diagram for Q Sepharose FF under both methods of compression. In general, as the level of hydrodynamic compression increased, the purification factor showed small improvements in purity. Although, at the high levels of hydrodynamic compression (0.15 CF), only Q Sepharose FF showed a decrease in PF. At 0.15 CF under hydrodynamic compression, the resolution showed a decreased of approximately 5% when compared to the non-compressed column. Above 0.05 CF, Q Sepharose FF has been shown previously to yield lower plate numbers and poorer asymmetry (refer to Chapter 2). Poor quality of packing has been linked to a decrease in protein separation (Kong *et al.* 2018; Luo *et al.* 2013).

When hydrodynamic compression was applied, the resolution for Q Sepharose FF ranged from 0.56 – 0.89 compared to 0.60 – 1.1 under mechanical compression. The highest resolution achieved was achieved at 0.05 CF for hydrodynamic and 0.10 CF for mechanical compression.

Based on these findings, the difference in compression via hydrodynamic and mechanical compression can be explained. At high levels of hydrodynamic compression, over-compression is likely to occur particularly for softer resins. Under high liquid force, microscopic dispersion has been reported to increase towards the bottom of the column (as described in Chapter 4). This disparity in microscopic dispersion along the bed length promotes greater heterogeneity within the column resulting in poorer column efficiencies. Mechanical compression uses evenly distributed force applied directly to the column top section where larger voidage space are known to appear (Yuan *et al.* 1999), also where excess liquid can escape through the inlet valve lessening the pressure at the bottom of the column. The packing compression behaviour of mechanical compression is governed by allowing excess liquid to escape through the top outlet allowing the excess voidage near the top to leave promoting a more homogenously packed column. This resulted in mechanical compression achieving an overall increase in purification factor.

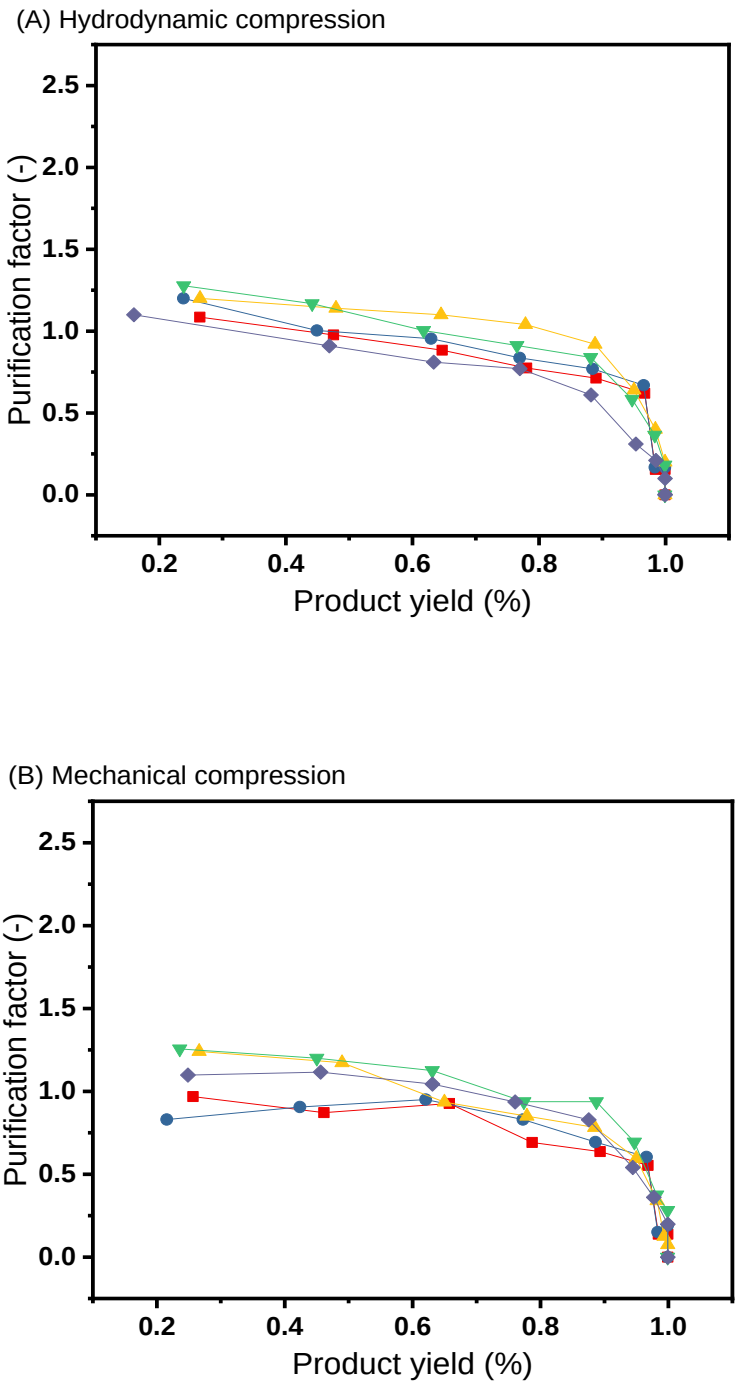

Figure 6-6 Impact of (A) Hydrodynamic (B) Mechanical multiple incremental step compression on separation performance of a fixed protein mixture. Purification factor vs product yield of a protein mixture of 5 mg mL^{-1} on Q Sepharose FF at CF = (▪) 0.0; (●) 0.02; (▲) 0.05; (▼) 0.10; (♦) 0.15. Studies based on an XK16 column to a bed height of 10 ± 0.1 cm at CF = 0.0.

Q Sepharose HP

Figure 6-7 illustrates the PFY diagram for Q Sepharose FF under hydrodynamic and mechanical compression. Both methods of compression showed optimal purification factor at 0.10 CF. Q Sepharose HP showed approximately 22 % higher DBC compared to Q Sepharose FF under zero compression conditions, CF = 0.0 (refer to Figure 6-5).

Under both methods of compression, Q Sepharose HP showed improvements in resolution at all levels of compression compared to the control. Both resins are made of crossed-linked 6% agarose with quaternary ammonium strong anion exchange group with an acquired average particle size of 34 µm and 90 µm for Q Sepharose HP and Q Sepharose FF, respectively. Since the morphological properties of Q Sepharose FF and Q Sepharose HP are the same except for their mean particle sizes, it can be concluded that changes in size plays a key role in determining protein resolution and that columns packed with smaller resins result in improved levels of protein separation.

Based on these findings, the difference in resolution between Q Sepharose FF and Q Sepharose HP can be explained. Larger resins (Q Sepharose FF) allow larger voidage spaces to form around the matrix particles, leading to a less compacted bed (Chiu *et al.* 2018). As compression increased, the voidage space reduced as the occupied volume goes down, facilitating a higher surface area to volume ratio. As a result, smaller resins (Q Sepharose HP) form a closely packed bed creating a more homogenously packed column (as discussed in Chapter 2 & Chpater 3); smaller plate heights and asymmetry values closer to 1.0. It can be noticed that the column efficiency is improved when the voidage space decreases as long as the morphology of the resin remains intact.

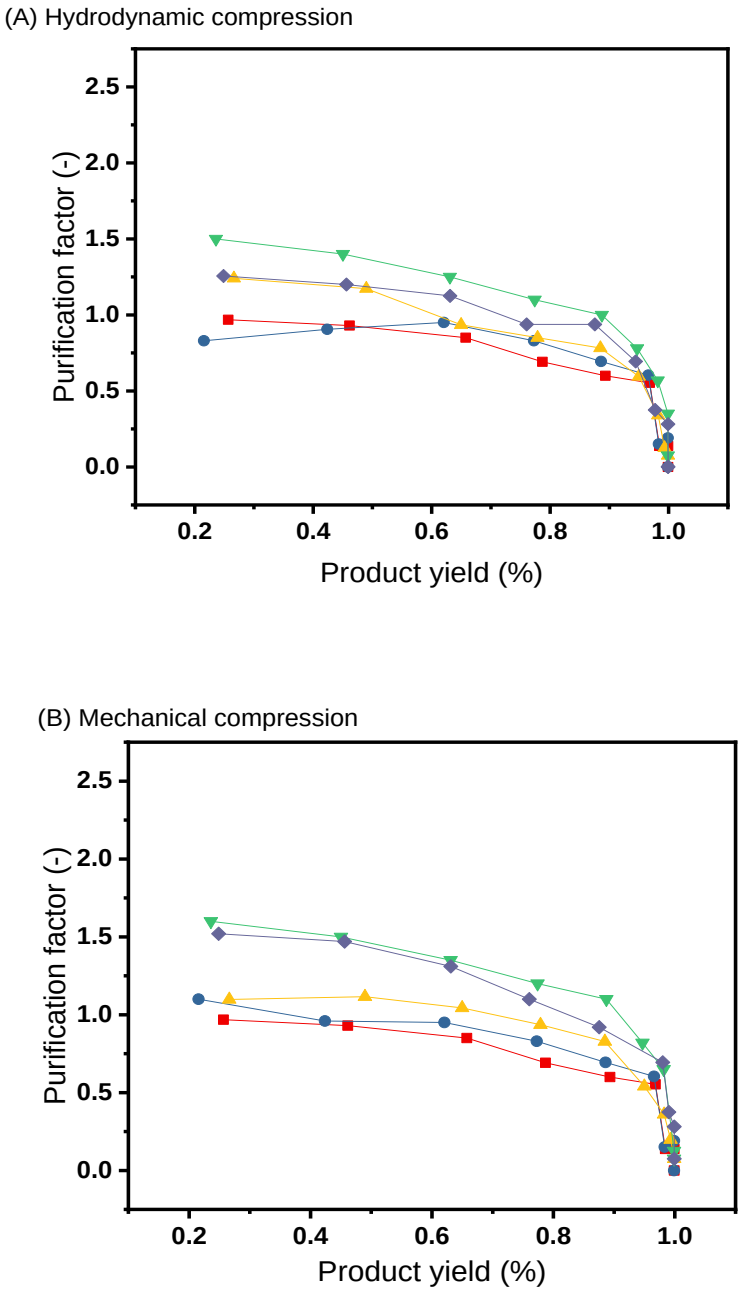

Figure 6-7 Impact of (A) Hydrodynamic (B) Mechanical multiple incremental step compression on separation performance of a fixed protein mixture. Purification factor vs product yield of a protein mixture of 5 mg mL^{-1} on Q Sepharose HP at CF = (▪) 0.0; (●) 0.02; (▲) 0.05; (▼) 0.10; (♦) 0.15. Studies based on an XK16 column to a bed height of 10 ± 0.1 cm at CF = 0.0.

Capto Q

At 0.0 CF, Capto Q showed the highest resolution (1.74). Capto Q is made more rigid than the softer resins by the introduction of an extra dextran linker. This showed the sharpest increase in protein resolution for both hydrodynamic and mechanical compression, as seen in Figure 6-5. Similar trends demonstrate Capto Q yielded better column efficiencies and variations in porosity at high levels of compression (as shown previously in Chapter 2 & Chapter 3). These factors are expected to be linked to an increase in protein separation. Both methods of compression showed optimal DBC at 0.15 CF. The results indicate that performance of protein separation is better the higher the level of hydrodynamic and mechanical compression achieved. Hydrodynamic compression showed slightly lower resolutions compared to mechanical compression, however greater differences were seen the two softer resins were examined. From 0.10 – 0.15 CF, mechanical compression demonstrated higher improvements in resolution ranging from 80 – 85% compared to hydrodynamic compression with improvements in resolution ranging from 70 - 76%.

Figure 6-8 illustrates the PFY diagrams for Capto Q under both methods of compression. At a typical specification of product yield at 0.9 at 0.15 CF, mechanical compression achieved the highest purification factor of 1.70 and hydrodynamic compression achieved a purification factor of 1.55. Hydrodynamic compression showed lower purification factor compared to mechanical compression, especially for the two softer resins examined. The results indicate protein separation is resin dependent and the optimum level of compression varies across resin structures, with mechanical compression achieving superior separation compared to hydrodynamic compression.

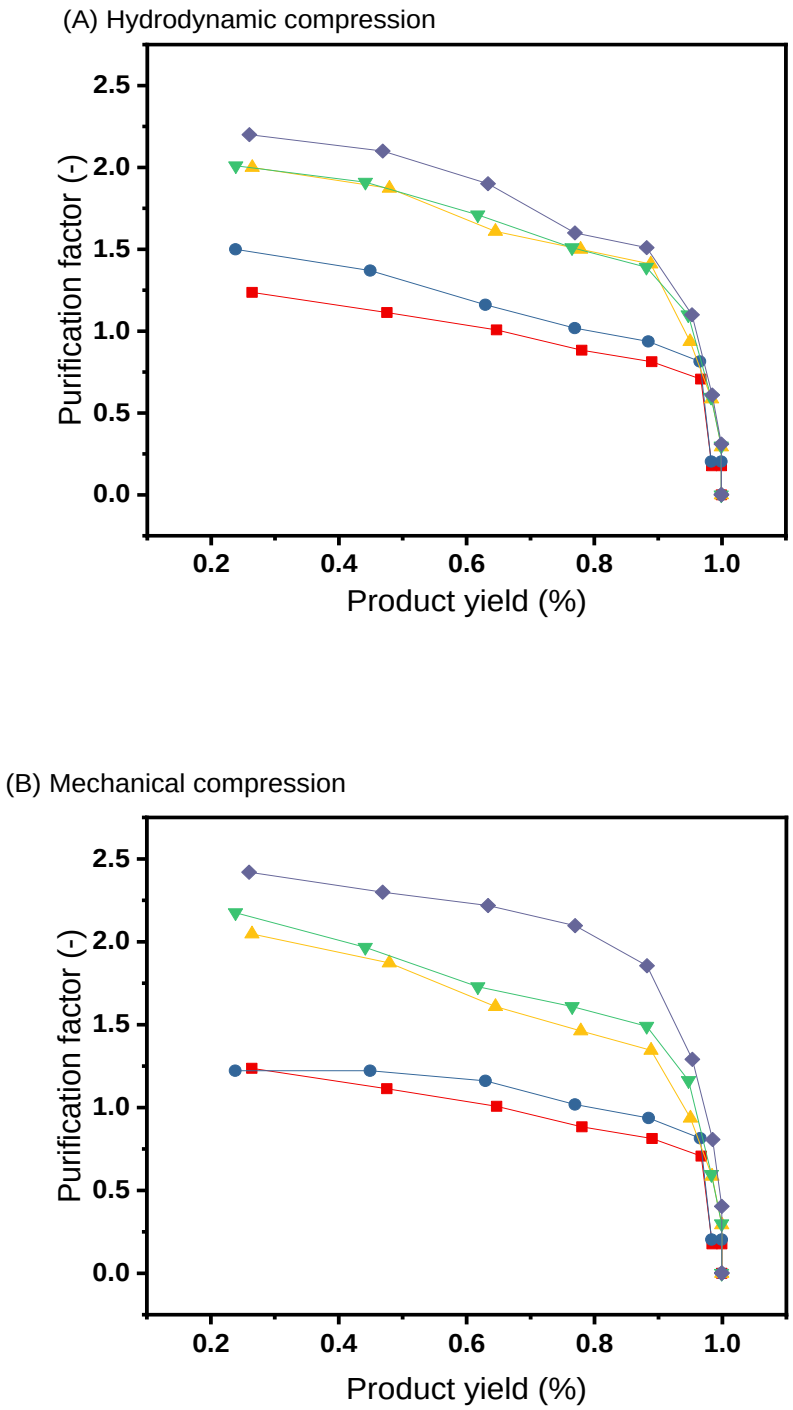

Figure 6-8 Impact of (A) Hydrodynamic (B) Mechanical multiple incremental step compression on separation performance of a fixed protein mixture. Purification factor vs product yield of a protein mixture of 5 mg mL^{-1} on Capto Q at CF = (▪) 0.0; (●) 0.02; (▲) 0.05; (▼) 0.10; (♦) 0.15. Studies based on an XK16 column to a bed height of 10 ± 0.1 cm at CF = 0.0.

6.5 Conclusion

Results showed higher purification factor was achieved under multiple incremental step compression compared to one-step compression. Hydrodynamic compression caused flow instability towards to bottom section of the column that resulted in poorer protein separation. With mechanical compression, an even distribution of pressure was applied from the top column diameter that is known to have larger voidage space. This resulted in higher levels of purity and resolution compared to hydrodynamic compression. Q Sepharose HP showed higher levels of separation compared to Q Sepharose FF, which is 2 - 3 times larger in size. As voidage decreased with compression, this translated to a more tightly packed bed for Q Sepharose HP and consequently in better column efficiency thus separation. Beyond 0.10 CF, Q Sepharose FF showed worse bed performance compared to a non-compressed bed, indicating protein separation resin depended and varies across the level of compression, with softer resin achieving optimal bed performance earlier. Whereas Capto Q has an additional dextran surface extender, which has a stronger matrix structure compared to the two softer resins showed the greatest level of product purity and yield.

Column performance has been shown to be strongly influenced by the level of bed compression as well as the method by which compression is applied. These behaviours are most likely due a reduction in voidage space allowing a greater degree of mass transfer between proteins and resins. Protein separation behaviour is very dependent on the resin base matrix and is effected by the mode of compression.

7 Overall Conclusions

The work presented in this thesis examined new approaches to evaluate the effects of hydrodynamic and mechanical compression on process chromatography to further enhance the understanding of the quality of packing when the bed is exposed to different levels of compression.

Column efficiency test (Chapter 2)

The first results chapter (Chapter 2) measured the column efficiency to observe the impact of hydrodynamic and mechanical compression on five chromatography resins – Q Sepharose FF, Q Sepharose HP, DEAE Sephacel, Capto Q, and Sepharose CL-6B. The impact of bed compression was found to be dependent on the method of bed compression used. In general, bed compression lead to improved reduced plate height and asymmetry across all resins. When challenged with one-step and multiple incremental step compression, mechanical compression led to a significant improvement in column efficiency for both modes of compression for Sepharose CL-6B. Whereas when hydrodynamic compression one-step compression was applied above 0.5 CF, the results showed worsening reduced plate height and asymmetry compared to non-compressed columns.

Four anion exchange resins were studied with different matrix strengths. Capto Q showed significant improvement under hydrodynamic and mechanical compression, whereas Q Sepharose FF and HP showed poor packing quality above 0.05 CF. The addition of dextran surface extender on Capto Q showed greatest benefit compared to all other resins.

Interestingly, mechanical compression provided a greater level of uniformity and column efficiency at both scales bench and pilot scale for DEAE Sephacel. Signs of over-compression via hydrodynamic compression was shown earlier at pilot scale. This was attributed to poorer packing quality indicated by broader peaks resulting in larger peak heights and asymmetry factors below 0.8.

Bed porosity tests (Chapter 3)

The dextran and acetone peaks were analysed to assess the voidage space and intraparticle porosities across the five chromatography resins. The data suggest the packing behaviour and the rigidity of a particle is greatly influenced by the method of compression. Hydrodynamic compression showed significant problems at higher compression factors, showing greatest changes to intraparticle porosities. Mechanical compression showed less change in external and internal porosity across a greater range of resins. Columns packed with Capto Q under both hydrodynamic and mechanical compression had higher external and internal porosity comparable with the other resins due to its extra dextran surface giving addition matrix support. Hydrodynamic compression gave significant problems at higher compression factors, greatest changes to intraparticle porosities appeared with larger (Q Sepharose FF) and softer resins (DEAE Sephacel) indicating the shape of the resins had deformed when porosities fell below 0.3.

The main challenge faced when using conventional methods to investigate column efficiency and bed porosity is that the data only gives a reading of the whole column. This proved difficult to investigate areas of poor packing across the axial section of the column. Therefore, the reverse-flow technique using an acetone tracer was developed as a novel technique in this field to quantify the microscopic dispersion effects due to bed compression on defined axial sections within a packed bed.

Reverse-flow technique (Chapter 4)

This chapter discussed the development of a reverse-flow technique designed to examine the microscopic dispersion and band broadening in different axial sections of the chromatography column in order to characterise the homogeneity of the packed bed. The experimental protocols utilising reverse-flow technique have been described in detail in numerus publications (Kamiński 1992; Kamiński *et al.* 1982; Moscariello *et al.* 2001; Siu *et al.* 2014). The results showed hydrodynamic achieved levels of evenly packed columns at a lower compression factor, though over-compression will occur earlier, particularly at the bottom of the bed. Over-compression will occur in the top section of the bed via mechanical compression due to the increasing force from the

top adapter. This phenomena is seen with softer resins (Q Sepharose FF and DEAE Sephacel), where Q Sepharose HP (2 -3 times smaller resin) was less effected at a compression factor of 0.15. Only Capto Q (hardest resin examined) showed consistent equal distributions and decrease in microscopic dispersion across the bed, even at high levels of compression. These results illustrate that compression can improve bed uniformity, although the effect of compression is resin dependent and favours stronger resins.

The main challenge faced when using this technique is that it only allows examination of microscopic dispersion in the axial direction but not the radial direction across the bed diameter. Quantification of radial dispersion within a bed might warrant further research especially for larger diameter systems.

Dynamic binding capacity (Chapter 5)

In this chapter, the impact of hydrodynamic or physical compression on binding capacity and breakthrough performance of three anion exchange resins were examined; Q Sepharose Fast Flow, Q Sepharose High Performance and Capto Q. The resins were selected to cover a range of bead rigidity and particles sizes. Column performance was assessed by analysing the breakthrough curves obtained using BSA as a model protein. Changes in column performance were evaluated by comparing breakthrough curves upon two different methods of column compression.

The results indicated that the overall impact of compression on breakthrough performance depended heavily on the method of compression applied to the bed. For both hydrodynamic and mechanical compression, the dynamic binding capacity (DBC) increased by 60% for Capto Q. However, when Q Sepharose FF, a softer resin was hydrodynamically compressed the DBC decreased by 10% at 0.15 CF. By contrast, when Q Sepharose HP was hydrodynamically compressed to the equivalent compression factor, the DBC increased by 20%. This suggests that the particle size distribution also influenced changes in breakthrough behaviour when compressed. For all three resins tested, mechanical compression produced the largest increases in DBC. It is hypothesized that this is a result of decreasing voidage space allowing a greater degree of mass transfer between proteins and resins.

Purification factor vs. yield diagram (Chapter 6)

Finally, this last chapter examined the effects of hydrodynamic and mechanical compression on protein separation. Due to the quantity of data generated, the chromatograms can become complex and often do not directly indicate the performance of the process. To reduce the complexity of concentration profiles and producing quantitative data to quantify the performance of the process the purification factor vs. yield (PFY) diagrams were derived.

Results showed higher purification factor was achieved under multiple incremental step compression compared to one-step compression. As expected, mechanical compression resulted in higher levels of purity and resolution compared to hydrodynamic compression. Beyond 0.10 CF, Q Sepharose FF showed worse bed performance compared to a non-compressed bed. Whereas Capto Q showed the greatest level of product purity and yield.

The results indicate that different methods of compression can affect the packing quality of the beds and therefore an impact on the protein separation. The packing behaviour of chromatographic columns is largely dependent on the type of resin; where smaller and harder resins tend to be less impacted by high levels of compression. In order to maintain a well-packed column, these results would indicate the need for two things. Firstly, a review of the column packing protocol used. Secondly, to conduct studies to quantify the quality of packing to determine the ideal level of compression needed to alleviate poorly packed chromatographic columns.

The relationship between process chromatography and the resolution of protein separation is highly influenced by the quality of resins and proteins used. The use of different proteins (products) will therefore behave differently in influencing the chromatographic results achieved. Several techniques and pore models have been conducted in order to determine the quality of packing for a range of commercially available media. However, with the provision of information concerning to certain aspects of this thesis, a range of secondary objectives could have been explore, further outlined in Chapter 8.

8 Future work

Process chromatography continues to be the dominant purification technique in the biopharmaceutical industry for the purification and recovery of therapeutics. For affinity chromatography, ti is accepted to be the most expensive part of downstream processing. Poorly packed columns can lead to detrimental effects on the separation performance and result in failed manufacturing batches. Therefore, there is a need to understand the effects of bed compression prior to protein separation and this thesis aims to prove advancements in this area. The techniques examined in this thesis can be used to investigate the effects of bed compression on process chromatography. Suggestions of possible future work seek to further develop the techniques and to enhance the knowledge of bed compression are given below.

To meet stringent and exact purification specifications required by the regulation authorities, it is a requirement to demonstrate process and product understanding to ensure each process consistently meets defined quality attributes. Hence, there is a need to further understand what critical process parameters (CPPs) which influences quality of packing and its linking them to critical quality attributes (CQAs).

Due to these pressures, there is a requirement to identify better techniques to assess quantitatively the column efficiency to predict when packing failure will occur. Understanding the alterations in process conditions, such as method of bed compression can act as troubleshooting practices for the extension of well-packed columns. In 2017, Dorn *et al.* reported that by combining both flow packing and axial compression resulted in the most homogeneous packing resulting in improved column efficiency (Dorn *et al.* 2017). This so-called hybrid method showed highest packing stability during long-term operation. The following section briefly describes a series of secondary experiments that can be applied to enhance the results of this study and to promote greater understanding of bed compression on process chromatography.

Large-scale studies

Throughout the work of this thesis, the chromatography columns were packed at laboratory-scale, as large-scale operations would require vast amounts of expensive

resins and impractical within the EngD budget. Consequently, the effect of bed compression was studied for only bench-scale operations and may reveal different consequences using industrial scale columns. Nevertheless, an evaluation on the impact of bed compression was studied on Sepharose CL-6B at pilot-scale that showed results of similar trends of column efficiency (cf. Chapter 2) with signs of "wall-effects" occurring at high levels of compression. The techniques developed in this thesis could be easily applied to large-scale chromatographic processes, and would be interesting to compared the obtain results with those in this thesis.

In addition, the reverse flow technique was demonstrated at laboratory-scale. Even at large-scale this technique is a simple non-invasive technique. With this understanding, the effects of bed compression at large-scale could be correlated with heterogeneity across the different sections of the column. More recently, Pathak *et al.* 2017 studied different sections of the column combing transmission electron microscopy (TEM) to analyse the structural stability during and post-column operation. This combination of studies could potentially increase our understanding of bed compression and column efficiency. However, limitations include uncontrolled temperatures in the microtoming chamber an extensive labour required for sample preparation.

Explore new resins

Choosing suitable resins for specific protein separation is critical. The degree of resins reported in this thesis covered agarose-based and cellulose-based resins of various sizes that only cover a small range of the commercially available matrixes available. However, it may also be interesting to investigate the effects of bed compression of different base materials, particularly hard bead support matrices, such as ceramic-based, resin whereas agarose-based resins exhibit limitations in back pressures. Alternatively, resins that can prove benefits that are more economical. For instance, Protein A is one of the most expensive resin due to its high selectivity; estimated to cost up to 60% of downstream cost from chromatography alone and is 50% more expensive than other types of chromatography media (Rathore *et al.* 2018). Further studies on how different methods of compression to optimise packing to produce even higher efficiency efficiencies that could lead to more economically optimised

processes. The information collected could then be correlated to other chromatography performance characteristics such as purity etc. (cf. Chapter 6).

Mathematical modelling

The future of bioprocessing will involve greater automation and modelling to help predict packing stability of the chromatography step. Keener *et al.* 2004 reported a framework to model flow packing and mechanical compression to predict theoretical relationships of column geometry upon compression, however, only a one-dimensional model of column packing was evaluated. They also reported the model is able to describe mechanical compression of any chromatographic resin for any column diameter. Similarly, McCue at al. 2009 established chromatography models to determine the effect of column packing quality on separation of monomer and aggregate species. However, the simulation showed poor predictions when the theoretical plates was above 150 and only hydrodynamic packing was evaluated on Phenyl Sepharose Fast Flow. More recently, Dorn. et. al 2017 used Euler-Lagrange modelling by coupling Computational Fluid Dynamics (CFD) and the Discrete Element Method (DEM) to measure packing behaviour for both hydrodynamic and mechanical compression pack with a diameter of 9.6 mm and bed height of 30 mm. The benefit of CFD-DEM modelling provides valuable information regarding intrinsic packing properties that up to now have been inaccessible. The employment of more successful models, as well as large-scale studies allows for better process understanding of column packing in the not-too-distant future. Understanding the impact of bed compression can potentially improve packing quality without repacking the column or unnecessary disposal. This could lead to significant cost saving and the potential to achieve higher chromatographic performance.

References

Albanese J, Blehaut J, Chochois H, Colin H, Guillerm J (2011) Industrial-scale biochromatography columns address challenging purification needs. BioProcess International 9 (2):60-63

Amsterdam A, Er-El Z, Shaltiel S (1975) Ultrastructure of beaded agarose. Archives of biochemistry and biophysics 171 (2):673-677

Balke ST, Hamielec AE, LeClair BP, Pearce SL (1969) Gel Permeation Chromatography. Product R&D 8 (1):54-57. doi:10.1021/i360029a008

Billen J, Gzil P, Vervoort N, Baron G, Desmet G (2005) Influence of the packing heterogeneity on the performance of liquid chromatography supports. Journal of Chromatography A 1073 (1-2):53-61

Carta G, Jungbauer A (2010) Protein Chromatography. Process development and scale-up. Wiley-VCH Verlag GmbH, Weinheim

Chang Y-C (2011) Practical investigation on the hydrodynamic behaviour of chromatographic columns packed with compressible media. Univeristy College London,

Chang Y-C, Gerontas S, Titchener-Hooker NJ (2012) Automated methods for accurate determination of the critical velocity of packed bed chromatography. Biotechnology Progress 28 (3):740-745. doi:10.1002/btpr.1544

Chase HA (1984) Prediction of the performance of preparative affinity chromatography. Journal of Chromatography A 297:179-202

Cherrak DE, Al-Bokari M, Drumm EC, Guiochon G (2002) Behavior of packing materials in axially compressed chromatographic columns. Journal of Chromatography A 943 (1):15-31. doi: 10.1016/S0021-9673(01)01432-7

Colby CB, O'Neill BK, Vaughan F, Middelberg AP (1996a) Simulation of Compression Effects during Scaleup of a Commercial Ion-Exchange Process. Biotechnology progress 12 (5):662-681

Colby CB, O'Neill BK, Vaughan F, Middelberg APJ (1996b) Simulation of Compression Effects during Scaleup of a Commercial Ion-Exchange Process. Biotechnology Progress 12 (5):662-681. doi:10.1021/bp960051t

Cooney DO (1990) Rapid approximate solutions for adsorption bed concentration profile and breakthrough curve behavior: favorable isotherms and both phase resistances important. Chemical Engineering Communications 91 (1):1-9

Cooney DO (1993) Comparison of simple adsorber breakthrough curve method with exact solution. AIChE journal 39 (2):355-358

Cramers C, Rijks J, Schutjes C (1981) Factors determining flow rate in chromatographic columns. Chromatographia 14 (7):439-444

Davies PA, Bellhouse BJ (1989) Permeability of beds of agarose-based particles. Chemical Engineering Science 44 (2):452-455. doi:10.1016/0009-2509(89)85085-7

De Smet J, Gzil P, Vervoort N, Verelst H, Baron GV, Desmet G (2005) On the optimisation of the bed porosity and the particle shape of ordered chromatographic separation media. Journal of Chromatography A 1073 (1):43-51. doi: 10.1016/j.chroma.2004.10.008

Dileo AJ, McCue J, Moya W, Quinones-Garcia I, Soice NP, Thom V, Yuan S (2010) Porous adsorptive or chromatographic media. Google Patents,

Dorn M, Eschbach F, Hekmat D, Weuster-Botz D (2017) Influence of different packing methods on the hydrodynamic stability of chromatography columns.

Journal of Chromatography A 1516:89-101. doi: 10.1016/j.chroma.2017.08.019
Dorn M, Hekmat D (2016) Simulation of the dynamic packing behavior of preparative chromatography columns via discrete particle modeling. Biotechnology Progress 32 (2):363-371. doi:10.1002/btpr.2210
Dorsey JG, Cooper WT, Siles BA, Foley JP, Barth HG (1998) Liquid chromatography: theory and methodology. Analytical Chemistry 70 (12):591-644
Edwards VH, Helft JM (1970) Gel chromatography: Improved resolution through compressed beds. Journal of Chromatography A 47:490-493. doi: 10.1016/0021-9673(70)80074-7
Eghbali H, De Malsche W, De Smet J, Billen J, De Pra M, Kok WT, Schoenmakers PJ, Gardeniers H, Desmet G (2007) Experimental investigation of the band broadening originating from the top and bottom walls in micromachined nonporous pillar array columns. Journal of separation science 30 (16):2605-2613
Eghbali H, Verdoold V, Vankeerberghen L, Gardeniers H, Desmet G (2008) Experimental investigation of the band broadening arising from short-range interchannel heterogeneities in chromatographic beds under the condition of identical external porosity. Analytical chemistry 81 (2):705-715
Eon CH (1978) Comparison of broadening patterns in regular and radially compressed large-diameter columns. Journal of Chromatography A 149:29-42. doi: 10.1016/S0021-9673(00)80977-2
Fang Z (2010) Large-Scale Chromatography Columns, Modeling Flow Distribution. Encyclopedia of Industrial Biotechnology
Farkas T, Chambers JQ, Guiochon G (1994) Column efficiency and radial homogeneity in liquid chromatography. Journal of Chromatography A 679 (2):231-245. doi: 10.1016/0021-9673(94)80565-2
Fishman ML, Barford RA (1970) Increased resolution of polymers through longitudinal compression of agarose gel columns. Journal of Chromatography A 52:494-496. doi: 10.1016/S0021-9673(01)96603-8
Freitag R, Frey D, Horváth C (1994) Effect of bed compression on high-performance liquid chromatography columns with gigaporous polymeric packings. Journal of Chromatography A 686 (2):165-177. doi: 10.1016/0021-9673(94)00697-0
G. Carta ARU, T.M. Pabst (2005) Protein Mass Transfer in Ion Exchange Media: Measurements and interpretations. Chemical Engineering Technology 28 (11):1252-1264
Gassmann O, Schuhmacher A, von Zedtwitz M, Reepmeyer G (2018) The Industry Challenge: Who Would Want to Be in This Business? In: Leading Pharmaceutical Innovation. Springer, pp 17-39
Gerontas S, Asplund M, Hjorth R, Bracewell DG (2010) Integration of scale-down experimentation and general rate modelling to predict manufacturing scale chromatographic separations. Journal of chromatography A 1217 (44):6917-6926. doi:10.1016/j.chroma.2010.08.063
Ghose S, Zhang J, Conley L, Caple R, Williams KP, Cecchini D (2014) Maximizing binding capacity for protein A chromatography. Biotechnology Progress 30 (6):1335-1340. doi:10.1002/btpr.1980
Gibson M (2018) Manufacturing and Process Controls. Pharmaceutical Quality by Design: A Practical Approach:281
Golshan-Shirazi S, Guiochon G (1989) Theory of optimization of the experimental conditions of preparative elution chromatography: optimization of the column

efficiency. Analytical Chemistry 61 (13):1368-1382. doi:10.1021/ac00188a014
Grier S, Yakabu S (2016) Prepacked chromatography columns: evaluation for use in pilot and large-scale bioprocessing. BioProcess International 14 (4)
Grushka E (1972) Characterization of exponentially modified Gaussian peaks in chromatography. Analytical Chemistry 44 (11):1733-1738. doi:10.1021/ac60319a011
Guan H, Guiochon G (1996) Study of physico-chemical properties of some packing materials: I. Measurements of the external porosity of packed columns by inverse size-exclusion chromatography. Journal of Chromatography A 731 (1):27-40. doi: 10.1016/0021-9673(95)01197-8
Guiochon G, Sarker M (1995) Consolidation of the packing material in chromatographic columns under dynamic axial compression. I. Fundamental study. Journal of Chromatography A 704 (2):247-268. doi: 10.1016/0021-9673(95)00242-F
Hagel L, Jagschies G, Sofer G (2008a) 7 - Validation. In: Hagel L, Jagschies G, Sofer G (eds) Handbook of Process Chromatography (Second Edition). Academic Press, Amsterdam, pp 161-188. doi: 10.1016/B978-012374023-6.50009-9
Hagel L, Jagschies G, Sofer G (2008b) 12 - Column Packing. In: Hagel L, Jagschies G, Sofer G (eds) Handbook of Process Chromatography (Second Edition). Academic Press, Amsterdam, pp 321-330. doi: 10.1016/B978-012374023-6.50014-2
Hagel L, Jagschies G, Sofer G (2008c) Appendix A - Symbols and Definitions in Liquid Chromatography. In: Hagel L, Jagschies G, Sofer G (eds) Handbook of Process Chromatography (Second Edition). Academic Press, Amsterdam, pp 331-336. doi: 10.1016/B978-012374023-6.50015-4
Healthcare G (2000) Gel Filtration Principles and Methods. Amersham Biosciences, Uppsala Sweden
Hekmat D, Kuhn M, Meinhardt V, Weuster-Botz D (2013) Modeling of transient flow through a viscoelastic preparative chromatography packing. Biotechnology Progress 29 (4):958-967. doi:10.1002/btpr.1768
Helfferich FG, Carr PW (1993) Non-linear waves in chromatography: I. Waves, shocks, and shapes. Journal of Chromatography A 629 (2):97-122. doi: 10.1016/0021-9673(93)87026-I
Hentschel N (2013) EMA Expert Workshop on Validation of Manufacturing for Biological Medicinal Products.222
Hernandez R (2015) Continuous manufacturing: a changing processing paradigm.
Ioannidis N, Bowen J, Pacek A, Zhang Z (2012) Manufacturing of agarose-based chromatographic adsorbents–Effect of ionic strength and cooling conditions on particle structure and mechanical strength. Journal of colloid and interface science 367 (1):153-160
Jagschies G, Sofer GK, Hagel L (2007) Handbook of process chromatography: development, manufacturing, validation and economics. Elsevier,
Janson J-C, Hedman P (1982) Large-scale chromatography of proteins. Advances in Biochemical Engineering 25:43-99
Johnson SA, Walsh A, Brown MR, Lute SC, Roush DJ, Burnham MS, Brorson KA (2017) The step-wise framework to design a chromatography-based hydrophobicity assay for viral particles. Journal of Chromatography B 1061:430-437

Jungbauer A (2005) Chromatographic media for bioseparation. Journal of Chromatography A 1065 (1):3-12. doi: 10.1016/j.chroma.2004.08.162

Kaczmarski K (2011) On the optimization of the solid core radius of superficially porous particles for finite adsorption rate. Journal of Chromatography A 1218 (7):951-958. doi: 10.1016/j.chroma.2010.12.093

Kaltenbrunner O, Jungbauer A, Yamamoto S (1997) Prediction of the preparative chromatography performance with a very small column. Journal of Chromatography A 760 (1):41-53

Kamiński M (1992) Simple test for determination of the degree of distortion of the liquid-phase flow profile in columns for preparative liquid chromatography. Journal of Chromatography A 589 (1-2):61-70

Kamiński M, Klawiter J, Kowalsczyk J (1982) Investigation of the relationship between packing methods and efficiency of preparative columns: II. Characteristics of the slurry method of packing chromatographic columns. Journal of Chromatography A 243 (2):225-244

Keener RN, Maneval JE, Fernandez EJ (2004) Toward a Robust Model of Packing and Scale-Up for Chromatographic Beds. 1. Mechanical Compression. Biotechnology progress 20 (4):1146-1158

Keener RN, Maneval JE, Östergren KCE, Fernandez EJ (2002) Mechanical Deformation of Compressible Chromatographic Columns. Biotechnology Progress 18 (3). doi:10.1021/bp020051v

Kennedy RM (2003) Qualification of a Chromatographic Column. BioPharm International:31

Khirevich S (2010) High-performance computing of flow, diffusion, and hydrodynamic dispersion in random sphere packings. Philipps-Universitat, Marburg

Kiss I, Bacskay I, Kilár F, Felinger A (2010) Comparison of the mass transfer in totally porous and superficially porous stationary phases in liquid chromatography. Analytical and bioanalytical chemistry 397 (3):1307-1314

Knox JH, Pyper HM (1986) Framework for maximizing throughput in preparative liquid chromatography. Journal of Chromatography A 363 (1):1. doi:10.1016/S0021-9673(00)88988-8

Koh J-H, Guiochon G (1998) Effect of the column length on the characteristics of the packed bed and the column efficiency in a dynamic axial compression column. Journal of Chromatography A 796 (1):41-57. doi: 10.1016/S0021-9673(97)00977-1

Kong DYC, Gerontas S, McCluckie RA, Mewies M, Gruber D, Titchener-Hooker NJ (2018) Effects of Bed Compression on Protein Separation on Gel Filtration Chromatography at Bench and Pilot Scale. Journal of Chemical Technology & Biotechnology:n/a-n/a. doi:10.1002/jctb.5411

Luo J, Zhou W, Su Z, Ma G, Gu T (2013) Comparison of fully-porous beads and cored beads in size exclusion chromatography for protein purification. Chemical engineering science 102:99-105

MacDonald MJ, Chu C-F, Guilloit PP, Ng KM (1991) A generalized Blake-Kozeny equation for multisized spherical particles. AIChE Journal 37 (10):1583-1588. doi:10.1002/aic.690371016

Martin C, Coyne J, Carta G (2005) Properties and performance of novel high-resolution/high-permeability ion-exchange media for protein chromatography. Journal of Chromatography A 1069 (1):43-52. doi: 10.1016/j.chroma.2004.08.114

MHRA (2011) Medicine and Healthcare Regulatory Agency for IPSEN Dyport.
Mohammad AW, Stevenson DG, Wankat PC (1992a) Pressure drop correlations and scale-up of size exclusion chromatography with compressible packings. Industrial and Engineering Chemistry Research 31 (2):549-561
Mohammad AW, Stevenson DG, Wankat PC (1992b) Pressure drop correlations and scale-up of size exclusion chromatography with compressible packings. Industrial & Engineering Chemistry Research 31 (2):549-561. doi:10.1021/ie00002a016
Moscariello J, Purdom G, Coffman J, Root TW, Lightfoot EN (2001) Characterizing the performance of industrial-scale columns. Journal of Chromatography A 908 (1):131-141. doi: 10.1016/S0021-9673(00)01062-1
Müller E, Chung JT, Zhang Z, Sprauer A (2005) Characterization of the mechanical properties of polymeric chromatographic particles by micromanipulation. Journal of Chromatography A 1097 (1):116-123. doi: 10.1016/j.chroma.2005.08.014
Ngiam SH, Bracewell DG, Zhou Y, Titchener-Hooker NJ (2003) Quantifying Process Tradeoffs in the Operation of Chromatographic Sequences. Biotechnology Progress 19 (4):1315-1322. doi:10.1021/bp034039u
Nweke MC, McCartney RG, Bracewell DG (2017) Mechanical characterisation of agarose-based chromatography resins for biopharmaceutical manufacture. Journal of Chromatography A 1530:129-137. doi: 10.1016/j.chroma.2017.11.038
Nweke MC, Rathore AS, Bracewell DG (2018) Lifetime and Aging of Chromatography Resins during Biopharmaceutical Manufacture. Trends in biotechnology
Pezzini J, Cabanne C, Santarelli X (2009) Comparative study of strong anion exchangers: Structure-related chromatographic performances. Journal of Chromatography B 877 (24):2443-2450. doi: 10.1016/j.jchromb.2009.06.044
Rao G, Goyal A (2016) An Overview on Analytical Method Development and Validation by Using HPLC. The Pharmaceutical and Chemical Journal 3 (2):280-289
Rathore AS (2009) Roadmap for implementation of quality by design (QbD) for biotechnology products. Trends in biotechnology 27 (9):546-553
Rathore AS, Kapoor G (2017) Implementation of quality by design toward processing of food products. Preparative Biochemistry and Biotechnology 47 (5):435-440
Rathore AS, Kumar D, Kateja N (2018) Recent developments in chromatographic purification of biopharmaceuticals. Biotechnology Letters:1-11
Rathore AS, Velayudhan A (2002) An overview of scale-up in preparative chromatography. Scale-Up and Optimization in Preparative Chromatography: Principles and Biopharmaceutical Applications 88:1
Read E, Shah R, Riley B, Park J, Brorson K, Rathore A (2010) Process analytical technology (PAT) for biopharmaceutical products: Part II. Concepts and applications. Biotechnology and bioengineering 105 (2):285-295
Sarker M, Guiochon G (1996) Consolidation of the packing material in chromatographic columns under dynamic axial compression III. Effect of the nature of the packing solvent on the consolidation and performance of axial compression columns. Journal of Chromatography A 741 (2):165-173. doi: 10.1016/0021-9673(96)00158-6
Sarker M, Katti AM, Guiochon G (1996) Consolidation of the packing material in Chromatographic columns under dynamic axial compression II. Consolidation

and breakage of several packing materials. Journal of Chromatography A 719 (2):275-289. doi: 10.1016/0021-9673(95)00750-4

Siu SC, Chia C, Mok Y, Pattnaik P (2014) Packing of large-scale chromatography columns with irregularly shaped glass based resins using a stop-flow method. Biotechnology progress 30 (6):1319-1325

Soriano GA, Titchener-Hooker NJ, Shamlou PA (1997) The effects of processing scale on the pressure drop of compressible gel supports in liquid chromatographic columns. Bioprocess Engineering 17:115-119

Stanley BJ, Sarker M, Guiochon G (1996) Consolidation of the packing material in chromatographic columns under dynamic axial compression IV. Mechanical properties of some packing materials. Journal of Chromatography A 741 (2):175-184. doi: 10.1016/0021-9673(96)00163-X

Steinebach F, Müller-Späth T, Morbidelli M (2016) Continuous counter-current chromatography for capture and polishing steps in biopharmaceutical production. Biotechnology journal 11 (9):1126-1141

Stickel JJ, Fotopoulos A (2001) Pressure-Flow Relationships for Packed Beds of Compressible. American Institute of Chemical Engineers 17:744-751

Teepakorn C, Grenier D, Fiaty K, Charcosset C (2016) Characterization of hydrodynamics in membrane chromatography devices using magnetic resonance imaging and computational fluid dynamics. Chemical Engineering Research and Design 113:61-73

Tengliden H (2008) Development of Cleaning-in-Place Procedures for Protein A Chromatography Resins using Design of Experiments and High Throughput Screening Technologies. Institutionen för fysik, kemi och biologi,

Titchener-Hooker NJ, Dunnill P, Hoare M (2007) Micro Biochemical Engineering to Accelerate the Design of Industrial-scale downstream processes for biopharmaceutical proteins. Biotechnology & Bioengineering 100: 473–487

Tran R (2011) Evaluation of challenges to the ubiquitous nature of chromatography. UCL (University College London),

Tran R, Joseph JR, Sinclair A, BracewellY D, Zhou Y, Titchener-Hooker NJ (2007) A Framework for the Prediction of Scale-Up When Using Compressible Chromatographic Packings . Biotechnology & Bioengineering 23:413−422

Turner R, Joseph A, Titchener-Hooker N, Bender J (2017) Manufacturing of Proteins and Antibodies: Chapter Downstream Processing Technologies.

Yew BG, Drumm EC, Guiochon G (2003) Mechanics of column beds: I. Acquisition of the relevant parameters. AIChE Journal 49 (3):626-641. doi:10.1002/aic.690490309

Yuan QS, Rosenfeld A, Root TW, Klingenberg DJ, Lightfoot EN (1999) Flow distribution in chromatographic columns. Journal of Chromatography A 831 (2):149-165. doi: 10.1016/S0021-9673(98)00924-8

Appendix A

MATLAB function for calculating the fractionation diagrams

```
function
[fracProduct,fracTotal]=fractionationDiagram(concProduct,...concImpu
rities)
% Function to calculate the fractionation diagram from a chromatogram
% The inputs 'concProduct' and 'concImpurities' are respectively the
% concentration profiles of the product and the impurities. The
outputs
% 'fracProduct' and 'fracTotal' are the fraction of the product and
the
% fraction of total protein in the calculated fractionation diagram.
%Set all negative values to zero
concImpurities(concImpurities<=0)=0;
concProduct(concProduct<=0)=0;
%Calculate vector for the concentration profile of the total proteins
concTotalProtein=concProduct+concImpurities;
%Cumulative of target protein
sumConcProduct=cumsum(concProduct);

end
```

MATLAB function for calculating maximum purity vs. yield diagram

```
function [yield,purity,cuts]=clearanceCalc(product,impurities)

% Total amount of protein in fractions
totalProtein=impurities+product;

% Fractional cumulative elution profiles
fracProduct=cumsum(product)/sum(product);
%%
fracTotal=cumsum(totalProtein)/sum(totalProtein);

% Calculate purity of monomer in pool of bound proteins
boundPurity=sum(product)/sum(totalProtein);

% Calculate envelope for product
[yield,maxPF,cuts]=maxPFCalc(fracProduct,fracTotal);

% Convert PF to purity
purity=maxPF*boundPurity;

end
```

```
function [yieldEnv,PFEnv,cutsEnv]=maxPFCalc(fracProduct,fracTotal)

% Define size of loop for calculating purification factors
n=size(fracProduct,1)-1;

%Create vector for the PF
purifFact=zeros(sum(1:n),1);

%Create vector for the yield
yield=zeros(sum(1:n),1);

%Create vector for the first cut
PFcut1=zeros(sum(1:n),1);

%Create vector for the second cut
PFcut2=zeros(sum(1:n),1);

%Create count for the number of calculated purification factors
count1=0;

%Loop to calculate the gradient between two points on the
fractionation
%diagram, i.e. the purification factor --> (y2-y1)/(x2-x1)
%First loop through point 1 or the first cut
for iv=1:n-1

    %Second loop through point 2 or the second cut
    for v=iv+1:n

        %Check that x2>x1
        if fracTotal(v)>fracTotal(iv)

            %Check that y2>y1
            if fracProduct(v)>fracProduct(iv)

                %Calculate the purification factor
                gradient=(fracProduct(v)-
fracProduct(iv))/(fracTotal(v)-fracTotal(iv));

                %Update the count of PFs calculated
                count1=count1+1;

                %Add the PF to the vector
                purifFact(count1)=gradient;

                %Add the yield to the vector
                yield(count1)=fracProduct(v)-fracProduct(iv);

                %Add the first cut to the vector
                PFcut1(count1)=iv;

                %Add the second cut to the vector;
                PFcut2(count1)=v;

            end
        end
    end
end
```

```
%Set initial value of 'n' or yield
n=0.001;

% Number of purification factor points
nPF=size(purifFact,1);

%Create 'q' which will take value of the yield at the maxima
q=[];

%Create 'r' which will take the valued of the cuts at the maxima
r=[];

%Create vector for the values of the max PF
maxPF=zeros(1,nPF);

%Create vector for the values of the yield at the max PFs
maxPFYields=zeros(1,nPF);

%Create matrix for the values of the cuts at the max PFs
maxPFCuts=zeros(2,nPF);

%Create count for the number of max PFs found
count2=1;

%Search is carried out starting at the initial value of 'n' until 'n'
%reaches 1.001
while n<=1.001

    %Resetting the value of 'p' after a maximum is found
    p=1;

    %Loop through the calculated values of PF
    for vi=1:nPF

        %Check if this value of yield is greater than value of 'n'
        if yield(vi)>n;

            %and value of PF is greater than the value of 'p'
            if purifFact(vi)>p;

                %Then set value of 'q' to this value of yield
                q=yield(vi);

                %and set value of 'p' to this value of PF
                p=purifFact(vi);

                %'r' takes the values of the cuts
                r=[PFcut1(vi),PFcut2(vi)];

            end
        end
    end

    %If the value of PF for this max. is not equal to the previous
max.
    if maxPF(count2)~=p;
```

```
        %and the value of yield for this max. is not equal to the
previous
        if maxPFYields(count2)~=q;

            %then update the count of the maxPFs
            count2=count2+1;

            %and save the PF of this new maximum
            maxPF(count2)=p;

            %and the yield of this maximum
            maxPFYields(count2)=q;

            %and the cuts at this maximum
            maxPFCuts(:,count2)=r;

        end
    end

    %Increase value of 'n' to restart search
    n=n+0.001;

end

%Remove excess from vectors
PFEnv=maxPF(2:count2-1);
yieldEnv=maxPFYields(2:count2-1);
cutsEnv=maxPFCuts(:,2:count2-1);

PFEnv=PFEnv';
yieldEnv=yieldEnv';
cutsEnv=cutsEnv';


end

    %Loop through the calculated values of PF
    for vi=1:nPF
        %Check if this value of yield is greater than value of 'n'
        if yield(vi)>n;
            %and value of PF is greater than the value of 'p'
            if purifFact(vi)>p;
                %Then set value of 'q' to this value of yield
                q=yield(vi);
                %and set value of 'p' to this value of PF
                p=purifFact(vi);
                %'r' takes the values of the cuts
                r=[PFcut1(vi),PFcut2(vi)];
            end
        end
    end

    %If the value of PF for this max. is not equal to the previous
max.
    if maxPF(count2)~=p;
        %and the value of yield for this max. is not equal to the
previous
        if maxPFYields(count2)~=q;
```

```
            %then update the count of the maxPFs
            count2=count2+1;
            %and save the PF of this new maximum
            maxPF(count2)=p;

            %and the yield of this maximum
            maxPFYields(count2)=q;
            %and the cuts at this maximum
            maxPFCuts(:,count2)=r;
        end
    end
    %Increase value of 'n' to restart search
    n=n+0.001;
end
%Remove excess from vectors
PFEnv=maxPF(2:count2-1);
yieldEnv=maxPFYields(2:count2-1);
cutsEnv=maxPFCuts(:,2:count2-1);
PFEnv=PFEnv';
yieldEnv=yieldEnv';
cutsEnv=cutsEnv';
end
```

Appendix B

Publication

Research Article

Received: 30 June 2017 Revised: 2 August 2017 Accepted article published: 11 August 2017 Published online in Wiley Online Library:

(wileyonlinelibrary.com) DOI 10.1002/jctb.5411

Effects of bed compression on protein separation on gel filtration chromatography at bench and pilot scale

Darryl YC Kong,[a] Spyridon Gerontas,[a] Ross A McCluckie,[b] Martin Mewies,[b] David Gruber[b] and Nigel J Titchener-Hooker[b]*

Abstract

BACKGROUND: Poorly packed chromatography columns are known to reduce drastically the column efficiency and produce broader peaks. Controlled bed compression has been suggested to be a useful approach for solving this problem. Here the relationship between column efficiency and resolution of protein separation are examined when preparative chromatography media were compressed using mechanical and hydrodynamic methods. Sepharose CL-6B, an agarose based size exclusion media was examined at bench and pilot scale. The asymmetry and height equivalent of a theoretical plate (HETP) was determined by using 2% v/v acetone, whereas the void volume and intraparticle porosity ($_p$) were estimated by using blue dextran. A protein mixture of ovalbumin (chicken), bovine serum albumin (BSA) and '- globulin (bovine) with molecular weights of 44, 67 and 158 kDa, respectively, were used as a 'model' separation challenge.

RESULTS: Mechanical compression achieved a reduction in plate height for the column with a concomitant improvement in asymmetry. Furthermore, the theoretical plate height decreased significantly with mechanical compression resulting in a 40% improvement in purity compared with uncompressed columns at the most extreme conditions of compression used.

CONCLUSION: The results suggest that the mechanical bed compression of Sepharose CL-6B can be used to improve the resolution of protein separation.

Keywords: bed compression; size exclusion chromatography; Sepharose CL-6B; HETP; preparative chromatography; protein separation

INTRODUCTION

Chromatography is the workhorse of the bioprocessing industry where it is utilised primarily for the separation of target molecules from impurities. This is achieved by passing a mobile phase, which contains both product and impurities, over a stationary phase; the properties of the stationary phase impart selectivity that results in separation of the target molecule from its impurities. Modifications to the stationary phase can result in selectivity based on size (size exclusion), charge (ion exchange) and hydrophobicity (hydrophobic interaction). The stationary phase can be packed into a variety of formats, the most common of these being cylindrical columns. Size exclusion chromatography (SEC) separates a mixture of molecules according to their size. Smaller molecules diffuse into the stationary phase and hence are retarded through the column compared with molecules of intermediate size, which flow through the void volume in the column. Poorly packed chromatography columns cause uneven flow within the packed bed, this leads to zone mixing, band broadening and ultimately loss of resolving power which can impact the purity and yield of product.

Currently, the use of hydrodynamic flow is often the method of choice for packing size exclusion.[1] However, there are few reports detailing the effect of different procedures of bed compression, i.e. mechanical compression, on packed polymeric particles.[2,3] At high flow rates bed compression occurs with a concomitant decrease in column permeability.[4] Particles follow the direction of flow during column packing and become compressed at the column outlet. The voidage between resin particles is reduced with increasing flow rate, which can deform the particles.[3] Furthermore, it has also been found that the voidage differs between the top and bottom regions of the column, suggesting that the column is not optimally packed.[5] This highlights an opportunity to further compress these regions with large voidage towards the top of the column to create a more uniform packed column. As a result, channelling is reduced and this increases the accessible surface area for mass transfer within the column.[4,6]

Highly cross-linked, polymeric stationary phases with wide protein separation ranges are available for protein separation by SEC.

* *Correspondence to: NJ Titchener-Hooker, University College London, WC1H 0AH, London, UK. E-mail: nigelth@ucl.ac.uk*

a *Department of Biochemical Engineering, University College London, UK*

b *Ipsen Bioinnovation Ltd., Wrexham, UK*

Effective bed compression has been shown to reduce both the time and column size required to achieve optimum separation.[7,8] The particles of Sepharose CL-6B are made of agarose, thus they are porous and mechanically soft. Agarose-based beads are less stable than silica beads due to solvation of the polymer which leads to swelling and thus softening of the support and an inability to withstand high pressures.[4,9,10]

At moderate packing pressures, several investigators have observed that bed compression reduces interstitial porosity, which increases resolution and therefore favours column efficiency.[4,11] Stickel and Fotopoulos investigated the impact of a reduction in void volume, created during hydrodynamic compression, on column efficiency.[12] Their results were interpreted using the Blake-Kozeny equation, which correlates bed porosity as a function of linear velocity.[12] By predicting the impact of operating parameters at industrial scale they were able to identify the most favourable conditions for column efficiency.

Meyer and Hartwick investigated the relationship between column efficiency and packing pressure for narrow-bore columns with siliceous stationary phases and identified the existence of an optimum column packing pressure.[13] However, no evidence based explanations were reported on intraparticle porosity. Though much is known about the hydrodynamic effects of compression on gel filtration beads; no theory is available to account for effects created by mechanical compression during scale up. The aim of this study was to characterize the relationship between the methods of column packing and column efficiency by applying hydrodynamic and mechanical methods of compression. This was achieved by using a commercially available gel filtration media, Sepharose CL-6B (GE Healthcare, Uppsala, Sweden) to exploit any benefits that may accrue by compression for the separation of macromolecular therapeutics by size exclusion.[4]

MATERIALS AND METHODS

Bench-scale setup

Bench-scale experiments were carried out using the ÄKTA Avant 25 (GE Healthcare, Little Chalfont, Buckinghamshire, UK) fast protein liquid chromatography system equipped with pump unit P-903, UV cell (280 nm, 2 mm path length), conductivity cell, and auto sampler A-900. The control software UNICORN 6.0 (GE Healthcare, Little Chalfont, Buckinghamshire, UK) was used. The extra column dead volume was kept to a minimum by using 0.12 mm I.D. capillary tube to connect the column to the injector. An XK16 column (GE Healthcare, Uppsala, Sweden) was used with an inner diameter (I.D.) of 0.016 m (XK16, with adjustable column lengths). All chromatography experiments were performed in triplicate and at room temperature 20 ± 5 °C.

Pilot-scale setup

Pilot-scale experiments were carried out using the ÄKTApilot system (GE Healthcare, Little Chalfont, Buckinghamshire, UK) equipped with pump unit P-907, UV cell (280 nm), conductivity cell, and auto sampler A-950 supplied with the UNICORN 5.11 control software. A BPG-100/500 (GE Healthcare Uppsala, Sweden) was used with an I.D. of 0.1 m with adjustable column lengths. All chromatography experiments were performed in triplicate and at room temperature 20 ± 5 °C.

Stationary phase and loading samples

Studies were carried out using a gel filtration resin; Sepharose CL-6B (GE Healthcare Uppsala, Sweden). It is a 6% cross-linked agarose gel filtration based matrix which may be used to separate samples of diverse molecular weight; $1 \times 10^4 - 1 \times 10^6$ Da. The resin is available in both Sepharose and Sepharose CL forms where the cross-linked form is chemically and physically more resistant, allowing identical selectivity but at increased flow conditions. The spherical resins had a size distribution of 45–165 μm (quoted by the manufacturer). The average bead diameter was determined to be, $d_p = 98\ \mu m \pm 5\ \mu m$ (Malvern Mastersizer 3000 laser sizer; Malvern Instruments, Worcestershire, UK).

All reagents were from a single supplier (Sigma–Aldrich, Poole, Dorset, UK) unless stated otherwise. The loading materials for this study were ovalbumin from chicken, BSA and '- globulin with molecular weights of 44, 67 and 158 kDa. A loading volume of 0.05 CV of 5 mg mL^{-1} of total protein was used. The packing buffer used was a 20 mmol L^{-1} sodium phosphate buffered saline (PBS) with 130 mmol L^{-1} NaCl at pH 7.2. All samples were filtered using 0.22 μm Stericup filter units (Merck & Co., Darmstadt, Germany).

Bed compression procedure

Sepharose CL-6B resin was made up to 80% (w/v) slurry in a 50 mL measuring cylinder. The total slurry volume was calculated based on achieving a desired bed height of 20 cm. Each bed was initially gravity settled overnight before flow packing at a velocity of 30 cm h^{-1} (1.0 mL min^{-1} for bench scale column) for 5 column volumes (CV). Once flow packed at this flow rate, a constant initial bed height of 20 cm ± 0.1 cm was achieved. A linear velocity of 30 cm h^{-1} was applied during HETP and protein separation testing. Subsequently, bed properties were measured by asymmetry and height equivalent of a theoretical plate (HETP) to measure the impact of the methods of compression and the level of compression achieved. Two methods of compression were examined: hydrodynamic and mechanical compression.

Bed compression factor

As a consequence of each incremental increase in compression,bed height reduced. This was captured through the bed compression factor (λ) defined as:

$$\lambda = \frac{V_{co} - V_c}{V_{co}} \quad (1)$$

where V_c is the packed bed volume and V_{co} is the initial settled bed volume. A maximum level of bed compression factor of 0.15 was used. This was well below the maximum pressure drop of 0.045 MPa, provided by the manufacturer. For both methods of compression, three repeats were conducted.

Hydrodynamic compression

For hydrodynamic compression, packing buffer was pumped through the column at the maximum flow rate of 150 cm h^{-1} (5.0 mL min^{-1} - within the pressure drop limit) for bench scale column until the desired compressed bed height was achieved. Once the measured pressure drop (less than 0.036 MPa) remained constant for 1 CV, the top column adapter was immediately lowered to the matrix bed surface to retain the level of compression.

Mechanical compression

For mechanical compression, the top adapter was physically pushed down until the desired bed compression had been achieved. When lowering the top adapter, the O-ring was loosened and the column inlet connector disconnected from the

ÄKTA. This allowed buffer to escape at the top of the column during compression. Once compressed, the column adapter was secured and connected back to the ÄKTA. Care was taken to ensure no air was trapped in the tubing or column.

Methods of compression

Two methods of resin packing were investigated. The first method applied compression in a single step by packing the column from the original packed bed to the compressed state. This is referred to as one step compression.

1. Compression was applied to the bed in a single step until the desired bed compression factorwas achieved by hydrodynamic or mechanical compression, described in the previous two subsections.
2. Compression was applied at four different compression factors (0.02, 0.05, 0.10 and 0.15).
3. Column was repacked for the next compression factor.

The second method went from the original packed bed to the compressed state by applying multiple series of steps. This is referred to as multiple incremental step compression.

1. For hydrodynamic compression, a flow rate of 30 cm h^{-1} was applied and increased to 150 cm h^{-1} until the desired bed compression factor was achieved. Mechanical compression was applied as described in the subsection 'Mechanical compression'.
2. Four different compression factors (0.02, 0.05, 0.10 and 0.15) were applied starting with the lowest compression factor. The next compression factor was carried out without repacking the column.

When no compression was applied (compression factor of 0.00), the column was flow packed at a constant linear velocity of 30 cm h^{-1} for 5 CV for both bench and pilot scale experiments as described in the section 'Bed compression procedure'.

Process description

An equilibration step of 3 CV of PBS at pH 7.2 was used before loading the sample directly onto the column. A loading volume of 0.5 CV of 5 mg mL^{-1} of total protein was used. Eluate fractions were collected until the UV trace returned to the baseline. A wash step of 2 CV was used to remove any remaining traces of sample. Following elution, the column was cleaned with 2 CV of 0.5 mol L^{-1} NaCl and 0.1 mol L^{-1} NaOH solution and then washed with ultrapure water (typically at 18.2 M cm at 25 °C) until neutral pH was reached. Columns were stored in 20% v/v ethanol solution, as per the manufacturer's recommendations. Columns stored in 20% v/v ethanol were washed with 5 CV of packing buffer prior the equilibration step. Columns stored in 20% v/v ethanol were washed with 5 CV of packing buffer prior the equilibration step.

Measurement of column efficiency, intraparticle porosity and protein separation

The data required for estimation of the quality of column packing was recorded using UNICORN 6.0 software. The reduced plate height and asymmetry were based on the axial dispersion of an acetone pulse. Acetone and dextran were used to assess the intraparticle porosity.

Acetone test

Column efficiency was measured by asymmetry and reduced plate height using a 2% CV injection of 2% v/v acetone, applied using a V-7 sample injector with a 100 mL loop for the bench scale column and directly injected using the sample pump for the pilot scale column.

Blue dextran test

The voidage at each compression level was measured by an excluded tracer (blue dextran). Dextran is a glucose polymer with covalently attached reactive blue dye molecules of molecular weight 2×10^3 kDa. The volume in which the dextran elutes represents the void space between the resin particles. The intraparticle porosity was determined by the elution profiles of acetone and blue dextran. The intraparticle porosity, ε_p is defined as:

$$\varepsilon_p = \frac{EV_d - EV_a}{EV_a} \quad (2)$$

where EV_d is the elution volume of dextran and EV_a is the elution volume of acetone.

HPLC-SEC protein mixture

SEC-HPLC was used to determine the purity of the eluting protein mixture, this was performed using an Agilent 1100 HPLC system with ChemStation software and an Agilent ZORBAX GF T-250 column (Agilent Technologies UK Ltd, Berkshire, UK). The total protein concentration was determined using the Bradford method with Brilliant Blue G Protein Assay reagent (Sigma–Aldrich, St. Louis, MO, USA).[14] Gel filtration standards (Bio-Rad Laboratories Ltd, Hertfordshire, UK) were used to calibrate the accuracy of the SEC-HPLC column (data not shown).

Purification factor

Based on the SEC-HPLC data collected from the flowthrough fractions, the separation performance was evaluated based on the purification factor (PF). The impurities in the sample load chosen to be ovalbumin (44 kDa) and ɣ'- globulin (158 kDa), whereas BSA (67 kDa) was selected as the product, to allow for separation of smaller and larger impurities. The PF is described as the ratio between the final purity of BSA after purification to the initial purity of the sample load.[15]

RESULTS AND DISCUSSION

Column efficiency tests

The impact of two different methods of compression, hydrodynamic and mechanical, on reduced plate height and asymmetry were investigated. For each method of compression, four different compression factors (0.02–0.15) were achieved by multiple incremental steps or one step compression as presented in Fig. 1(a)–(d). It has been shown that a highly compacted region near the base of the column forms when hydrodynamic compression is used, where pressure will be the greatest.[5] It appears that Sepharose CL-6B achieved improved asymmetry and reduced plate number at 0.02 compression factor via hydrodynamic multiple incremental compression steps; however, the column efficiency declined as further pressure was applied due to the flow of buffer. This finding is consistent with literature.[3,16–18] The effect of hydrodynamic compression has been shown to cause flow instability and an increase in the reduced plate height, which detrimentally affects column

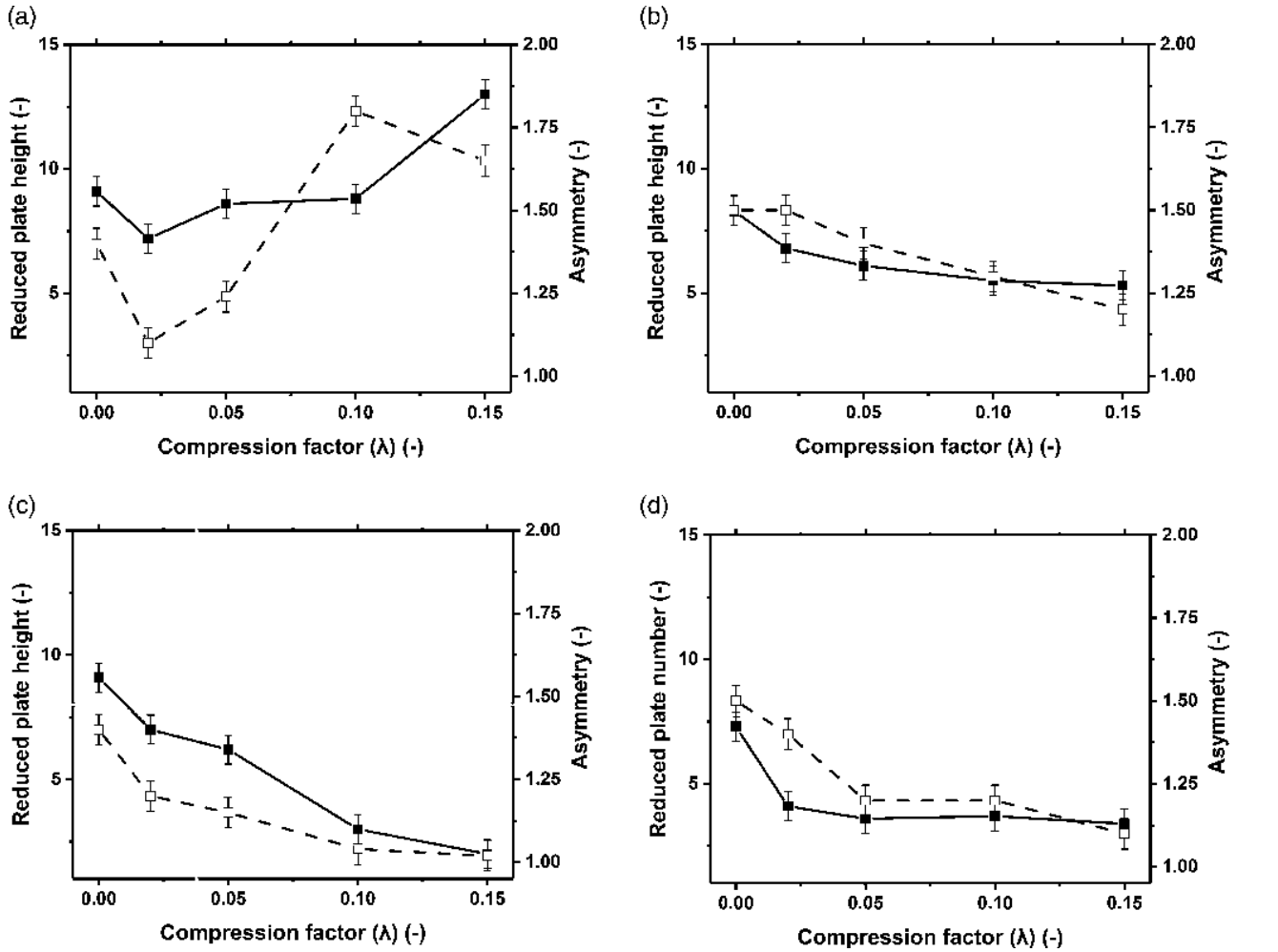

Figure 1. Comparison of reduced plate number and asymmetry for compressed beds achieved by hydrodynamic and mechanical methods. Columns packed with Sepharose CL-6B 0.016 m I.D. 20 cm bed height. (a) Hydrodynamic compression achieved by multiple incremental steps (b) hydrodynamic one step compression. (c) Mechanical compression achieved by multiple incremental steps (d) mechanical one step compression. ( ) Reduced plate height; ( ) asymmetry.

efficiency.[16] Mechanical compression yielded higher column efficiency than did hydrodynamic compression – a 3.5-fold improvement in reduced plate height (Fig. 1(c)–(d)).

Since mechanical compression gave better column efficiency, the impact of mechanical compression on asymmetry and reduced plate height was examined using BSA as a model protein. The impact of mechanical compression defined by multiple incremental steps are presented in Fig. 2(a) and (b). The reduced plate height improved at increased levels of mechanical compression. The improvement doubled as the compression factor increased from 0.0 to 0.15 (Fig. 2). Additional tests were performed to determine how mechanical compression influenced both the intraparticle and interparticle voidage (Table 1).

Mechanical compression led to a decrease in voidage but no discernible effect on intraparticle porosity. The voidage data is consistent with earlier work.[19] It is believed that pore diffusion is enhanced as voidage within the column falls.[20] This allows for greater surface area for diffusion between the resins and analytes to be presented to the molecules.[21,22] The consistent intraparticle porosity even under significant levels of mechanical compression may be explained by considering the elastic properties of the agarose material. Porosity moved from about 0.4 at no compression to 0.3 at a compression factor of 0.15 with mechanical compression. A porosity of 0.4 is expected with randomly packed spheres under gravity settling.[20] When hydrodynamic compression is applied, stress on the stationary phase accumulates in the direction of flow indicating greater compaction at the outlet of the column. In addition, different regions ofvoidage space, particularly at the top of the column, result in uneven flow distribution when hydrodynamic compression is applied. By contrast, under mechanical compression, pressure is applied to the entire cross-section at the top of the bed. This gives an opportunity to compress further the top regions with larger voidage to create a more uniform packed bed along the length of the column. This allows for a more even distribution of pressure along the length of the column when mechanical compression is used compared with hydrodynamic compression. In addition, near-wall packing may be a possible source of poor performance under hydrodynamic compression, since uneven pressure across the cross-section may cause uneven velocity distribution, particularly at higher flow rates.

Others have reported that the void fraction is lower near the column wall than in central and upper regions of the column.[5]

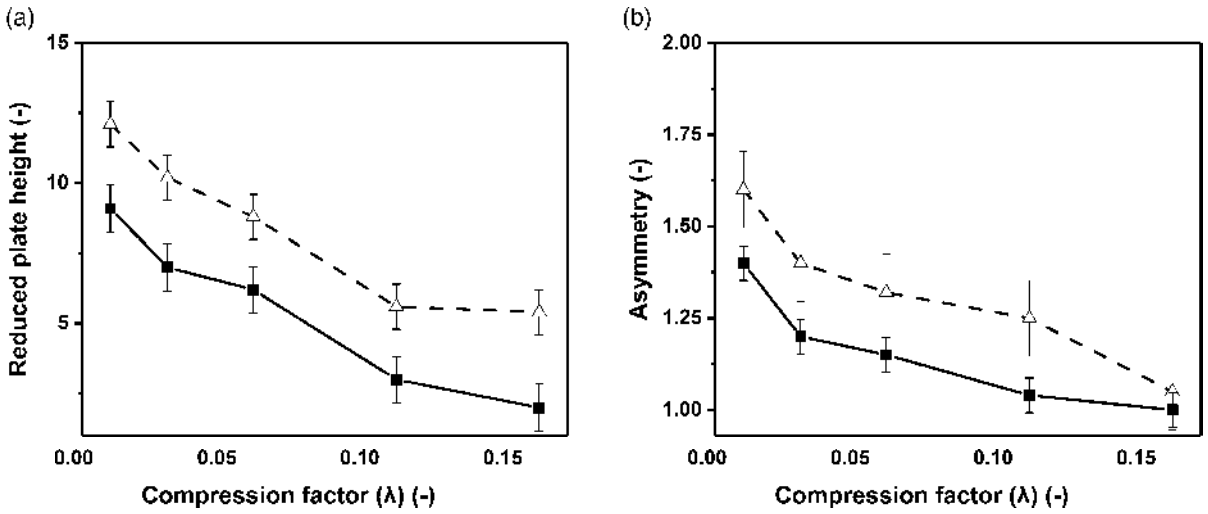

Figure 2. Comparison of reduced plate number and asymmetry achieved by mechanical compression defined by multiple incremental steps. Column was packed with Sepharose CL-6B 0.016 m I.D. 20 cm bed height. Measurements were made using 5 mg mL^{-1} BSA and 2% v/v acetone. (a) Reduced plate height comparison: (▪) acetone; (▲) BSA. (b) Asymmetry comparison: (▪) acetone; (▲) BSA.

These insights were gained using static magnetic resonance imaging (MRI) and were explained by the additional downward force on the upper regions of the column caused by movement of the top adapter which imposed mechanical compression on the bed.[3,5]

Our study suggests that compression achieved by applying pressure through the movement of the top adapter results in a better quality of packing. The fact that the voidage decreases means that interparticle distances are getting smaller and hence mass transfer is expected to rise. The impact of improved mass transfer rates on adsorptive separation was outside the scope of the study but might provide a beneficial impact of column compression by improving separation time and/or the resolution achieved for a given bed.

Effect of mechanical compression on protein separation at bench scale

Table 2 summarises the impact of mechanical compression on the separating performance of the bench scale chromatography system. Figure 3(a) and (b) provide a simple schematic of the separation performance analysed at two extremes; 0.00 and 0.15 compression factor. Mechanical compression beyond a compression factor of 0.10 provided baseline resolution with improvements in both asymmetry and reduced plate height as well as greater peak resolution. These results indicate that for size exclusion separations the performance of a given protein separation can be improved by operating beds under mechanically compressed conditions compared with hydrodynamic compression at 30 cm h^{-1}. This is in contrast to earlier findings based upon hydrodynamic compression and suggests that the mode of compression is closely related to the column efficiency achieved.

Figure 4 displays the purification factor as a function of yield for separating a fixed protein mixture obtained with columns that had undergone mechanical compression. Results show that mechanical compression via multiple incremental steps leads to greater levels of product purity and yields than mechanical compression in one step. The results indicate that performance of protein separation is better the higher the level of mechanical compression achieved, but that compression by multiple incremental step protocols reated separation with significantly higher purification factor (PF) values for all yields. This was especially pronounced for compression levels >0.05. For example, at a typical specification of product yield of 0.9 the PF at 0.15 compression was 1.25 for mechanical compression achieved in one step and 1.75 for mechanical compression in multiple incremental steps. Such increased PF offers the ability to increase purity at a set yield target or to increase yield with no detrimental impact on purity.

Table 1. Impact of mechanical compression achieved by multiple incremental steps on measured intraparticle porosity and bed voidage. Results obtained from the dextran blue and acetone elution profile data with Sepharose CL-6B. Measurements were repeated three times with a relative standard deviation of less than 5% in all measurements

Mechanical incremental steps compression		
Compression factor (λ)	Intraparticle porosity (ε_p)	Voidage space (ε)
0.00	0.63	0.41
0.02	0.60	0.39
0.05	0.63	0.36
0.10	0.62	0.33
0.15	0.60	0.31

Table 2. Impact of mechanical incremental steps compression on the peak resolutions directly measured by absorbance at 280 nm from the resulting ÄKTA chromatogram. Protein mixture of Ovalbumin, BSA and -globulin for Sepharose CL-6B 0.016 m I.D. Measurements were repeated three times with a relative standard deviation of less than 5% in all measurements

Compression factor ()	Bed	Resolution peak 1 and 2	Resolution peak 2 and 3
0.00	20	0.9	0.9
0.02	19.6	1.2	1.1
0.05	19	1.5	1.3
0.10	18	1.6	1.5
0.15	17	1.7	1.8

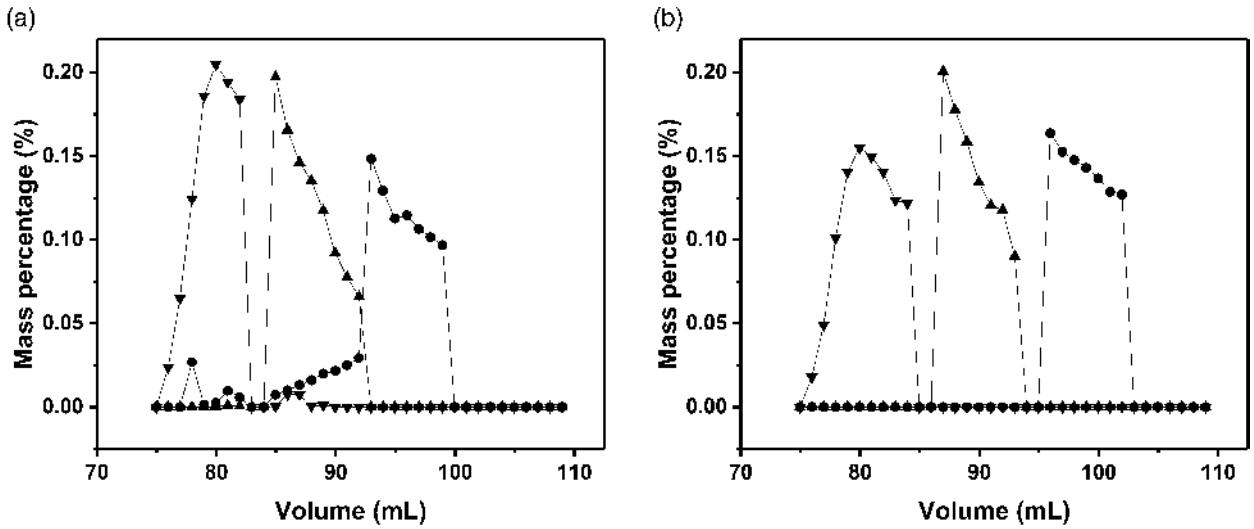

Figure 3. Impact of mechanical compression achieved by multiple incremental steps on the purity of a simple protein mixture. Mass percentage of each fraction based on HPLC-SEC with a protein mixture of ovalbumin, BSA and -globulin. (a) 0.0 mechanical compression; (b) 0.15 mechanical compression. (▼) y-globulin; (▲) BSA; (●) ovalbumin.

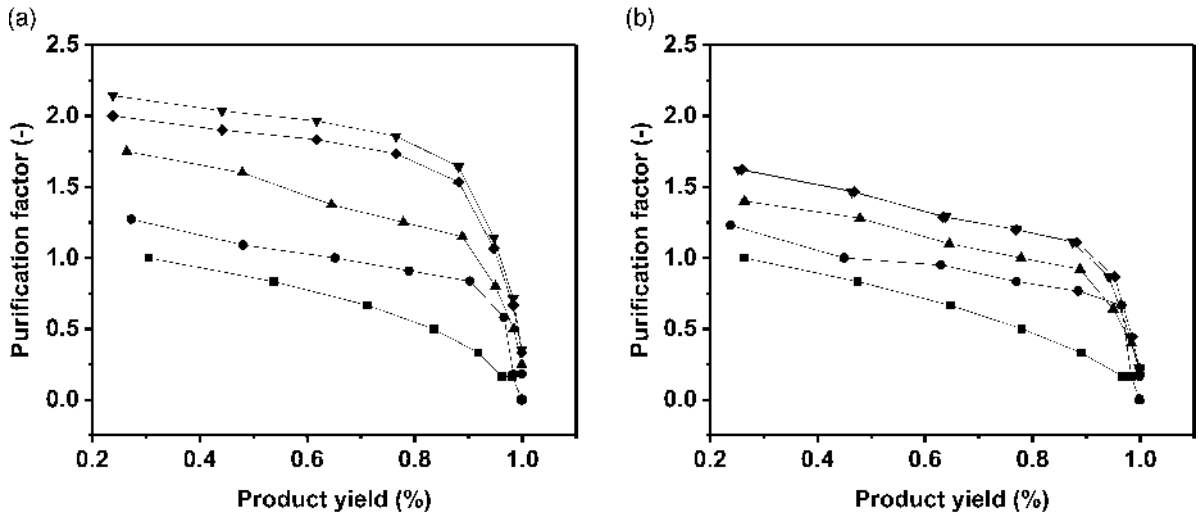

Figure 4. Impact of mechanical compression on separation performance of a fixed protein mixture. Purification factor vs product yield of a protein mixture of 5 mg mL^{-1} with mechanical compression at bench scale. (a) Mechanical incremental steps compression; (b) one step mechanical compression. (▼) 0.0; (▲) 0.02; (▼) 0.05;(◆) 0.10; (▼) 0.15.

Since mechanical compression in multiple incremental steps created separation with significantly higher PF values compared with one step compression, we consequently set out next to examine the impact of multiple incremental steps during scale up.

Scale-up comparison using XK16 and BPG100 with mechanical compression

The impact of mechanical bed compression at bench (XK16) and pilot scales (BPG100) was studied. The results are presented in Fig. 5 where changes in asymmetry at both bench and pilot scales were verified. At pilot scale the asymmetry reduced above a compression factor of 0.10. This was expected, as the bed diameter increases so the extent to which the column wall supports the bed material falls. This allows the longitudinal force down the column to increase.[3] Exceeding a 0.10 compression factor created increasing levels of bed non-uniformity. The degree of compression at the bottom of the column depends on the column diameter. Wider columns allow more compaction (less wall support effect).[7,23–26] This highlights the fact that there can be no one size fits all approach to column packing across columns scales even when utilising the same chromatography matrix. At pilot scale, as the bed reached 0.10 compression factor, optimum asymmetry was achieved when mechanical compression by multiple incremental steps was applied.

CONCLUSIONS

There is a need to understand the effect of the methods by which packed beds are compressed prior to operation. In particular, the impact of mechanical compression on column performance during scale-up is poorly reported. This study aimed to investigate the impact on column efficiency when applying hydrodynamic and mechanical compression to beds formed from Sepharose CL-6B.

Results showed better asymmetry and reduced plate height with increasing levels of mechanical compression, regardless of how this was applied (one step or multiple incremental steps). One step

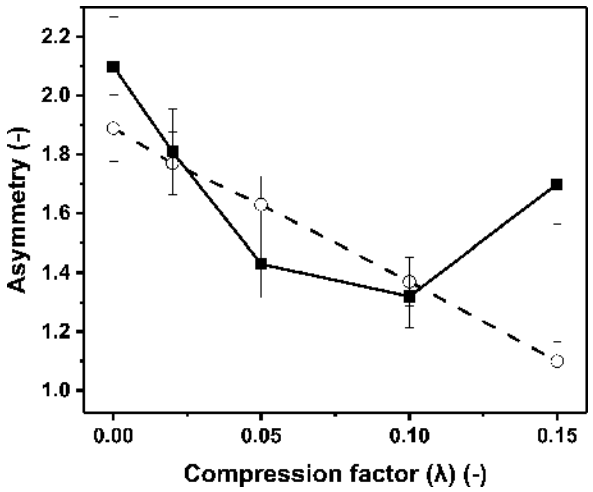

Figure 5. Impact of mechanical compression achieved by multiple incremental steps on asymmetry at bench (XK16) and pilot scale (BPG-100/500) measured with 2% v/v acetone; (▪) BPG 100/500; (●) XK16.

hydrodynamic compression followed a similar trend to mechanical compression with a lower plate height and an asymmetry closer to one. However multi-step hydrodynamic compression caused flow instability, most likely due to the formation of regions of higher compaction towards the bottom of the packed bed which together resulted in poor column efficiency. With mechanical compression, an even distribution of pressure was applied from the top column diameter which gave better column efficiency as measured by both asymmetry and reduced plate height. The voidage decreased with compression, this would translate in smaller interparticle distances and consequently in increased mass transfer.

Mechanical compression by multiple incremental steps resulted in greater levels of product purity and yields than by mechanical compression with one step. The impact of mechanical bed compression during scale up was investigated, exceeding a 0.10 compression factor created increasing levels of bed non-uniformity. Beyond a compression factor of 0.15, no further improvements in bed performance as measured by asymmetry or HETP were recorded for either of the methods of compression investigated.

We have shown column performance to be strongly influenced by the level of bed compression as well as the method by which compression is affected. Investigation of mechanical compression of different resins, such as ion exchange medium during adsorptive separations will form the basis of future work.

ACKNOWLEDGEMENT

The authors gratefully acknowledge The Advanced Centre for Biochemical Engineering (ACBE). Financial support was provided by the Engineering and Physical Sciences Research Council (EPSRC) (EP/L01520X/1) and Ipsen Bioinnovation Ltd. Ipsen Bioinnovation Ltd. reviewed the manuscript for scientific accuracy. The authors declare no financial or commercial conflict of interest.

REFERENCES

1 Carta G, Jungbauer A, Chromatography media, in *Protein Chromatography*.Wiley-VCH Verlag GmbH, Weinheim, pp. 85–124 (2010).
2 Mohammad AW, Stevenson DG and Wankat PC, Pressure drop correlations and scale-up of size exclusion chromatography with compressible packings. *Ind Eng Chem Res* **31**:549–561 (1992).
3 Keener RN, Maneval JE, Östergren KCE and Fernandez EJ, Mechanical deformation of compressible chromatographic columns. *Biotechnol Prog* **18**: (2002).
4 Freitag R, Frey D and Horváth C, Effect of bed compression on high-performance liquid chromatography columns with gigaporous polymeric packings. *J Chromatog A* **686**:165–177 (1994).
5 Yuan QS, Rosenfeld A, Root TW, Klingenberg DJ and Lightfoot EN, Flow distribution in chromatographic columns. *J Chromatogr A* **831**:149–165 (1999).
6 Fishman ML and Barford RA, Increased resolution of polymers through longitudinal compression of agarose gel columns. *J Chromatogr A* **52**:494–496 (1970).
7 Kaltenbrunner O, Jungbauer A and Yamamoto S, Prediction of the preparative chromatography performance with a very small column.*JChromatogrA* **760**:41–53 (1997).
8 Ayazi Shamlou P, Bulk solids flow and handling properties, in *Handling of Bulk Solids – Theory and Practice*. Butterworth & Co., London, pp. 1–13 (1988).
9 Carta G and Jungbauer A, Process development and scale-up, in *Protein Chromatography*.Wiley-VCH Verlag GmbH, Weinheim, pp. 57–125 (2010).
10 Cuatrecasas P, Protein purification by affinity chromatography derivatizations of agarose and polyacrylamide beads. *J Biol Chem* **245**:3059–3065 (1970).
11 Horvath C and Lin H-J, Band spreading in liquid chromatography. *J Chromatogr A* **149**:43–70 (1978).
12 Stickel JJ and Fotopoulos A, Pressure-flow relationships for packed beds of compressible. *Am Inst Chem Eng* **17**:744–751 (2001).
13 Meyer RF and Hartwick RA, Efficient packing of small particle microbore columns. *Analyt Chem* **56**:2211–2214 (1984).
14 Bradford MM, A rapid and sensitive method for the quantitation of microgram quantities of protein utilizing the principle of protein-dye binding. *Analyt Biochem* **72**:248–254 (1976).
15 Ngiam SH, Zhou YH, Turner MK and Titchener-Hooker NJ, Graphical method for the calculation of chromatographic performance in representing the trade-off between purity and recovery. *J Chromatog A* **937**:1–11 (2001).
16 Stickel JJ and Fotopoulos A, Pressure-flow relationships for packed beds of compressible chromatography media at laboratory and production scale. *Biotechnol Prog* **17**:744–751 (2001).
17 Soriano GA, Titchener-Hooker NJ and Shamlou PA, The effects of processing scale on the pressure drop of compressible gel supports in liquid chromatographic columns. *Bioprocess Eng* **17**:115–119 (1997).
18 Edwards VH and Helft JM, Gel chromatography: improved resolution through compressed beds. *J Chromatog A* **47**:490–493 (1970).
19 Davies PA and Bellhouse BJ, Permeability of beds of agarose-based particles. *Chem Eng Sci* **44**:452–455 (1989).
20 De SmetJ, Gzil P, Vervoort N, Verelst H, Baron GV and Desmet G, On the optimisation of the bed porosity and the particle shape of ordered chromatographic separation media. *J Chromatog A* **1073**:43–51 (2005).
21 Chang Y-C, Gerontas Sand Titchener-Hooker NJ, Automated methods for accurate determination of the critical velocity of packed bed chromatography. *Biotechnol Prog* **28**:740–745.
22 Balke ST, Hamielec AE, LeClair BP and Pearce SL, Gel permeation chromatography. *Product R&D* **8**:54–57 (1969).
23 Tran R, Joseph JR, Sinclair A, Bracewell Y D, Zhou Y and Titchener-Hooker NJ, A framework for the prediction of scale-up when using compressible chromatographic packings. *Biotechnol Bioeng* **23**:413–422 (2007).
24 Parker KH, Mehta RV and Caro CG, Steady flow in porous, elastically deformable materials. *J Appl Mech* **54**:794–800 (1987).
25 Janson J-C and Hedman P, Large-scale chromatography of proteins. *Adv Biochem Eng* **25**:43–99 (1982).
26 Ergun S, Fluid flow through packed columns. *Chem Eng Prog* **48**:89–94 (19).